BATTERIES, SECONDARY CELLS

1. Alkaline Cells

Alkaline electrolyte storage battery systems are more suitable than others in applications where high currents are required, because of the high conductivity of the electrolyte. Additionally, in almost all of these battery systems, the electrolyte which is usually an aqueous solution containing 25–40% potassium hydroxide [1310-58-3], KOH, does not enter into the chemical reaction. Thus concentration and cell resistance are invariant with state of discharge and these battery systems give high performance and have long cycle life. The manufacturing value of alkaline storage batteries in 2002 was estimated to be in the range of $4.5–5 billion dollars (worldwide) representing approximately 17% of the value for all secondary batteries. Approximately one half of this production value was in small sealed cells. The remainder was in industrial designs. The latter includes approximately 40,000 nickel-metal hydride (Ni-MH) units for hybrid electric vehicles (HEVs). The annual battery supply for this application was forecasted [100] to increase to over a million units by the year 2008, representing a production value of $1 billion.

Positive electrode active materials have been made from the oxides or hydroxides of nickel, silver, manganese, copper, mercury, and from oxygen. Negative electrode active materials have been fabricated from various geometric forms of cadmium [7440-43-9], Cd, iron [7439-89-6], Fe, and zinc [7440-66-6], Zn, and from hydrogen [1333-74-0]. Two different types of hydrogen electrode designs are common: those used in space, which employ hydrogen as a gas, and those used in consumer batteries, where the hydrogen is used as a metallic hydride. As indicated in Table 1 and Figure 1, nine electrode combinations exist in some scale of commercial production. Five system combinations are in the research/development stage, and two have been abandoned before or after commercial production for reasons such as short life, high cost, low voltage, low energy density, and excessive maintenance.

The annual production value of small-sealed nickel cadmium cells is approximately 1.0×10^9. Environmental considerations relating to cadmium have necessitated changes in the fabrication techniques, as well as recovery of failed cells. Battery system designers have switched to nickel–metal hydride (MH) cells for high power applications. However, the highest discharge/recharge rates are still achieved with nickel–cadmium cells typically in "AA"-size cells, to increase capacity in the same volume and avoid the use of cadmium.

There are many methods of fabricating the electrodes for these cell systems. The earliest commercially successful developments used nickel hydroxide

Table 1. **Rechargeable Alkaline Storage Battery Systems**

System[a]	Historical name	Voltage, V	Production[b]
nickel–cadmium	Jungner	1.30	vl
nickel–iron	Edison	1.37	vs
nickel–zinc	Drumm	1.70	vs
nickel–hydrogen (H_2 or MH)		1.30	vl
silver–cadmium		1.38 and 1.16[c]	vs
silver–iron	Jirsa	1.45 and 1.23[c]	vs
silver–zinc	Andre	1.86 and 1.60[c]	s
silver–hydrogen		1.38 and 1.16[c]	vs
manganese–zinc[d]		1.52	vs
mercury–cadmium		0.92	r
air(oxygen)–zinc		1.60	r
air(oxygen)–iron		1.40	r
air(oxygen)–aluminum			vs
copper–lead		1.20	r
copper–cadmium	Darrieus	0.45	n
copper–zinc	Waddell-Entz, Edison-LeLande Lelande-Chaperon	0.85	n

[a] The substance named first represents the positive electrode; the substance named second is the negative electrode. In all cases except for air(oxygen) systems, the active electrode material is the oxide or the hydroxide of the named species.

[b] vl = $>100 \times 10^6$ A·h/yr product; l = $>25 \times 10^6$ A·h/yr; s = $>5 \times 10^6$ A·h/yr; vs = $<5 \times 10^6$ A·h/yr; r = research and development phase; and n = no longer in production.

[c] Silver oxide electrodes have two voltage plateaus.

[d] Secondary system designs.

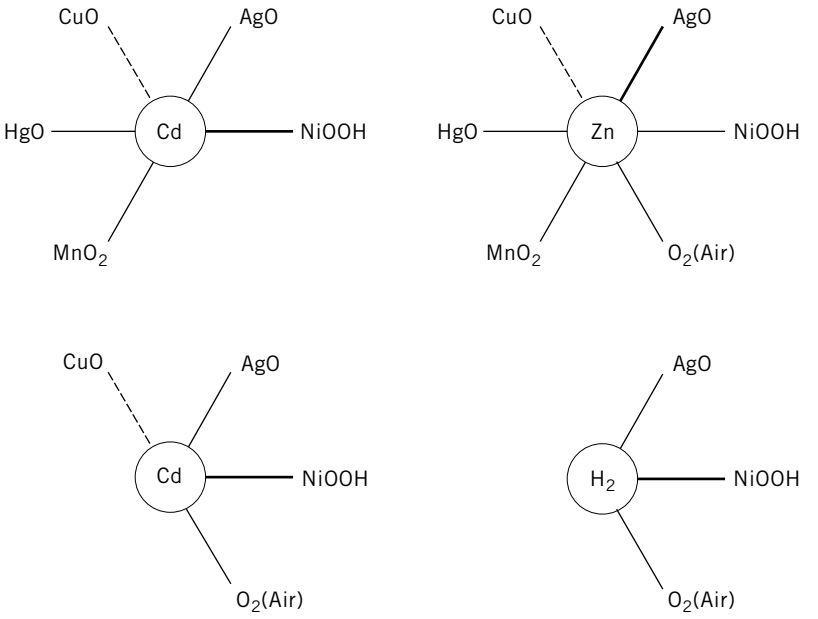

Fig. 1. Electrode combinations for alkaline storage batteries where the substance within the circle comprises the negative electrode and the combinations include (—) commercial products, (—) systems in research and development or limited production, and (- - -) historic system. The air (O_2)–H_2 system is commonly called a fuel cell.

[12054-48-7], $Ni(OH)_2$, positive electrodes. These electrodes are commonly called nickel electrodes, disregarding the actual chemical composition. Alkaline cells using the copper oxide–zinc couple preceeded nickel batteries but the CuO system never functioned well as a secondary battery. It was, however, commercially available for many years as a primary battery (see BATTERIES-PRIMARY CELLS).

The original alkaline battery, designed by Edison around 1900, contained nickel hydroxide mixed with graphite [7782-42-5] in perforated steel pockets as the positive active material and a high surface area iron powder as the negative. Both positive and negative electrodes were "pocket" plates, where the active material was contained in small, rectangular, boxlike pockets formed from finely perforated sheet steel. These plates very closely resembled the pocket plates in use in some current designs of nickel–cadmium batteries.

Because the nickel–iron cell system has a low cell voltage and high cost compared to those of the lead–acid battery, lead–acid became the dominant automotive and industrial battery system except for heavy-duty applications. Renewed interest in the nickel–iron and nickel–cadmium systems, for electric vehicles started in the mid-1980s using other cell geometries. This was supplanted in the 1990s by the use of NiMH batteries in hybrid electric vehicles.

In the early 1930s, production of nickel–cadmium batteries having thinner pocket-type plates and lower internal resistence became available. This grew to be an important design for truck, locomotive, and marine engine starting applications. Very high rate cell designs of nickel–cadmium cells became possible

Table 2. **Technology and Processing Contributions to Alkaline Battery Development**

Year	Procedure	Reference
1948	impregnation procedures for nickel and cadmium electrodes	6
1956	x-ray structure of nickel hydroxide electrode	7
1958	*in situ* x-rays of nickel and cadmium electrodes	8
	slurry-processed nickel-sintered electrode (SAFT)	9
1960	crystal structures of silver oxide	10,11
	structure of nickel hydroxide electrode	12
	in situ study of the nickel electrode	13
1961	microporous plastic-reinforced zinc electrode	14
1962	microporous plastic-bound cadmium electrode	15
1965	solid-state chemistry of nickel hydroxide	16
	crystal structures of nickel hydroxide	17
1966–1970	impregnation procedures for nickel electrodes	18–20
1972	electrochemical impregnation method for nickel electrodes	21
1974	nickel foam substrates	22
1975	plastic-bonded nickel electrodes	23
1978	controlled microgeometry electrodeposited electrodes	24
1980	nickel composite electrode	25
1981	nickel fiber mat substrates	26
1984	nickel felt substrates	27
	production of nickel fiber electrodes	28
1987	rechargeable MnO_2–zinc cell	29
1989	modified manganese dioxide for deep-cycling	30
1990	metal–hydride-type hydrogen electrodes used in commercial nickel–MH cells	31
1995	nickel–MH cells used in hybrid electric vehicles	32

with the development of the sintered nickel substrate in 1928 (2) and then in the late 1940s and early 1950s, the shortcomings of the sealed nickel–cadmium designs were overcome (3). The use of sealed nickel–cadmium cells grew rapidly and beginning in the early 1990s, designs of nickel–hydrogen, the hydrogen as hydride, cells captured a strong commercial and technical interest. Table 2 details the advances in alkaline battery technology from 1948 to 1990.

The nickel–zinc combination has a high cell voltage (about 1.75 V), which results in a very favorable energy density compared to that of nickel–cadmium or lead–acid. Additionally, zinc is relatively inexpensive and, in the absence of mercury additive, is environmentally benign. The nickel–zinc system was discussed as early as 1899 (4). There has been a resurgence of interest in the system for electric vehicles, but the problems of limited cycle life have not been completely overcome.

Silver [7440-22-4], Ag, as an active material in electrodes was first used by Volta, but the first intensive study using silver as a storage battery electrode was reported in 1889 (5) using silver oxide–iron and silver oxide–copper combinations. Work on silver oxide–cadmium followed. In the 1940s, the use of a semipermeable membrane combined with limited electrolyte was introduced by André in the silver oxide–zinc storage battery.

Many of the most recent applications for alkaline storage batteries require higher energy density and lower cost designs than previously available. Materials such as foam and/or fiber nickel [7440-02-0], Ni, mats as substrates, and new

processing techniques including plastic bounded, pasted, or electroplated electrodes, have enabled the alkaline storage battery to meet these new requirements, while reducing environmental problems in the manufacturing plants. In addition, substantial technical efforts have been devoted to the recovery of used batteries. The most recent innovations in materials relate to the development of metal–hydride alloys for the storage and electrochemical utilization of hydrogen. Modifications to the chemical structure and/or the cell design of manganese dioxide [1313-13-9], MnO_2, electrodes have resulted in sufficient improvement to allow the reintroduction of the rechargeable MnO_2–zinc cell to the market as a lower cost, albeit lower performance, alternative to nickel–cadmium consumer size cells. Improvements in materials science and electrical circuits have lead to better separators, seals, welding techniques, feedthroughs, and charging equipment.

1.1. Nickel–Cadmium Cells. *Electrodes.* A number of different types of nickel oxide electrodes have been used. The term nickel oxide is common usage for the active materials that are actually hydrated hydroxides at nickel oxidation state 2+, in the discharged condition, and nickel oxide hydroxide [12026-04-9], NiO·OH, nickel oxidation state 3+, in the charged condition. Nickelous hydroxide [12054-48-7], $Ni(OH)_2$, can be precipitated from acidic solutions of bivalent nickel either by the addition of sodium hydroxide or by cathodic processes to cause an increase in the interfacial pH at the solution–electrode surface (see NICKEL AND NICKEL ALLOYS; NICKEL COMPOUNDS).

Several investigators have used combined approaches, particularly in the *in situ* precipitation of active material in the pores of sintered substrates, using cathodic polarization and caustic precipitation in simultaneous or nearly simultaneous steps. A considerable amount of the reported information on the chemistry, electrochemistry, and crystal structure of the nickel electrode has been obtained on thin films (qv) made by the anodic corrosion of nickel surfaces. However, such films do not necessarily duplicate the chemical and/or crystallographic condition of active material in practical electrodes. In particular, the high surface area, space charge region, and lattice defect structure are different. Some of the higher (3.5+) valence state electrochemical behavior seen in thin films has rarely been reproduced in practical electrodes.

The many varieties of practical nickel electrodes can be divided into two main categories. In the first, the active nickelous hydroxide is prepared in a separate chemical reactor and is subsequently blended, admixed, or layered with an electronically conductive material. This active material mixture is afterwards contained in a confining porous metallic structure or pasted onto a metallic mat or grid. Electrodes for pocket, tubular, pasted, and most button cells are made this way. The porous metallic structures such as the pocket or tube, ensure good particulate contact, prevent shedding, and confine expansion. Less expensive alternatives, those resulting from pasting on expanded metal, foam metal, punched corrugated sheet, or fiber metal nickel mat, do not confine expansion as well or provide the same amount of mechanical strength. Plastic reinforcement to minimize shedding and promote adherence to the substrate is often employed. The plastic mix can be achieved either by milling or extrusion of mixes at plastic flow temperatures or by using plastic–solvent combinations. The latter includes simple gels of water, KOH, and methylcellulose [9004-67-5].

Recent patent literature gives details on preparation of nickel positive electrodes using nickel hydroxide (33–35).

The other type of nickel electrode involves constructions in which the active material is deposited *in situ*. This includes the sintered-type electrode in which nickel hydroxide is chemically or electrochemically deposited in the pores of a 80–90% porous sintered nickel substrate that may also contain a reinforcing grid.

Almost all the methods described for the nickel electrode have been used to fabricate cadmium electrodes. However, because cadmium, cadmium oxide [1306-19-0], CdO, and cadmium hydroxide [21041-95-2], $Cd(OH)_2$, are more electrically conductive than the nickel hydroxides, it is possible to make simple pressed cadmium electrodes using less substrate (see CADMIUM AND CADMIUM ALLOYS; CADMIUM COMPOUNDS). These are commonly used in button cells.

Electrochemistry and Crystal Structure. The solid-state chemistry of the nickel electrode is complex. Nickel hydroxide in the discharged state has a hexagonal layered lattice, where planes of Ni^{2+} ions are sandwiched between planes of OH^-; as shown in Figure 2. This structure, similar to that of cadmium iodide

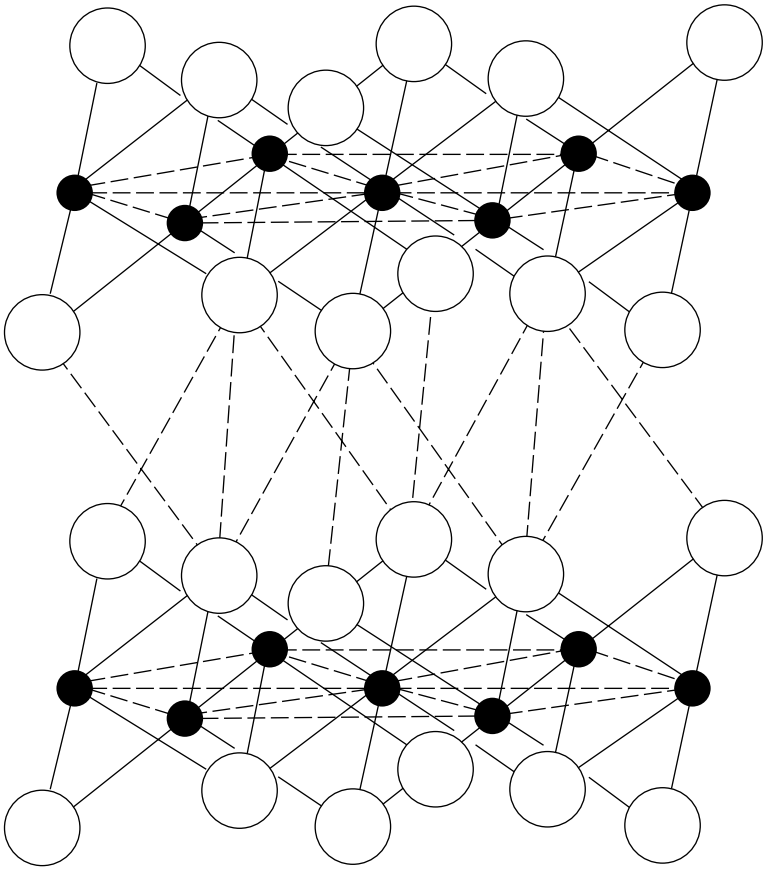

Fig. 2. Nickel hydroxide structure where (●) represents nickel and (○) represents oxygen or hydroxyl.

[7790-80-9], CdI_2, is common to seven metal hydroxides including those of cadmium and cobalt. There are various hydrated and nonhydrated nickel hydroxides that have slightly different crystal habitats and electrochemical potentials. The most common form of charged material observed in batteries is NiOOH, density = 4.6 g/mL. In comparison, $Ni(OH)_2$ has a density of 4.15 g/mL. Thus the theoretical change in density on charge–discharge is less than 10%, and the kinetics involve only a proton transfer. This reaction can be written in simplified form as:

$$2\ \beta\text{–}NiOOH^{*} + Cd + 2\ H_2O \rightleftharpoons 2\ Ni(OH)_2^{*} + Cd(OH)_2$$

where the asterisks represent differing amounts of hydrated or absorbed water and/or electrolyte. It has also been established that species such as Li^+ and K^+ enter the nickel hydroxide structure to form a space–charge region and the actual reaction is believed to be more complicated than that shown. The interlayer separation of planes of nickel ions is increased by insertion of water or ions from the electrolyte. Different preparative and cycling conditions result in variations in defect crystal structures that affect electrochemical activity and the ability to retain charge (36). Additionally, electrode material oxidation states do not range precisely between +2 and +3, and because of hysteresis in the charge–discharge curves, direct measurement of an equilibrium potential is not possible.

The existence of $Ni(OH)_2$ and β-NiOOH as the usual discharged and charged materials was confirmed through x-ray diffraction powder patterns (7,8,37). The presence of other structural forms, in different electrolytes and under unusual cycling conditions, has also been observed. The crystalline-structural variability of $Ni(OH)_2$ has been described as being dependent on preparative procedure (16). Other phases form after prolonged overcharging of β-NiOOH in concentrated sodium hydroxide [1310-73-2], NaOH, or KOH. At elevated temperatures, in lithium hydroxide [1310-65-2], LiOH, electrolytes, $Ni(OH)_2$ is oxidized to a trivalent phase having the lithium nickelate [12031-65-1], $LiNiO_2$, crystalline structure and lithium additions to KOH electrolytes eliminate the formation of α-phase material. The sequence of these electrochemical processes has been summarized as: (*1*) an electrochemical exchange at the solid electrolyte interface involving a set of ionic-electronic lattice imperfections; (*2*) electron transport through the oxidized phase region to the metallic contact; (*3*) mass transport through the oxidized phase to the lower valence phase at the second interface; and (*4*) electrochemical exchange at the second solid-phase interface functioning as a source or sink for the ionic-electronic imperfections necessary to maintain the mass and charge balance.

A sequence of events taking place in the charge process has been described (16) demonstrating that during constant current charge, the surface double-layer region first produces a local interior space–charge field. As the semiconductor charge phase is extended into the interior, a distributed space–charge field is formed that is characterized by a combination of the semiconductor band structure and the mobility of dopant imperfections. When the state of charge increases, the magnitude of the space charge decreases. At the end of charge, there is only an ir (voltage) loss in the solid, and the applied field is mainly at

the solid electrolyte interface. If charging is continued until a steady-state oxygen evolution is attained, the distributed space charge disappears. The semiconductor is characterized by a flat band potential and, if the nickel electrode is left on open circuit, the space charge-field gradually decays through atom movements in the solid phase, approximating a flat band potential condition.

The charge–discharge process cannot be satisfactorily represented by one equation (17). At least two reactions, based on different starting materials as well as different products, can be formulated. Both reactions are heterogeneous. In each of the reaction chains two distinct states exist in the oxidized phase. One of these can only be charged whereas the cathodic current are blocked. The other state, existing at a lower potential, can only be discharged but was blocked in the anodic direction. When the observed potential differences are extrapolated into the region of very low current densities, the difference between the two states is ca 60 mV in one of the reaction chains and ca 100 mV in the other. Thermodynamically this means that neither reaction series can be described by a single, reversible potential as in the manner of the $Cd–Cd(OH)_2$ electrodes. Rather, the semiconductor properties of oxidized nickel hydroxides play some part.

The description of the process is best illustrated as (17):

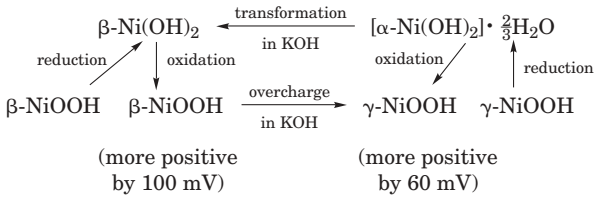

The nickel oxide modification obtained electrochemically in KOH electrolyte contained potassium ion and its nickel oxidation level are higher than that of $NiO_{1.5}$. Conclusions regarding the transitions between the reduced and oxidized products within the two series are that the redox process was not reversible and although the oxidized phases of the β- and the γ-nickel hydroxides differ in energy contents, differences in analyses and x-ray patterns are not significant.

Some γ-NiOOH has been shown to be formed in sintered nickel electrodes (38), and changes in water and KOH concentration during the cycling of nickel electrodes has been studied (12,39–41). Although there is some disagreement on the movement of water, KOH is adsorbed on the nickel electrode when the cell is charged and desorbed from the electrode when the cell is discharged.

The chemistry, electrochemistry, and crystal structure of the cadmium electrode is much simpler than that of the nickel electrode. The overall reaction is generally recognized as:

$$Cd + 2\,OH^- \underset{\text{charge}}{\overset{\text{discharge}}{\rightleftharpoons}} Cd(OH)_2 + 2\,e^-$$

However, there is a strong likelihood of a soluble intermediate in the formation of $Cd(OH)_2$. Cadmium has an appreciable solubility in alkaline solutions: $\sim 2 \times 10^{-4}$ mol/L in 8 *M* potassium hydroxide at room temperature. In general

it is believed that the solution process consists of anodic dissolution of cadmium ions in the form of complex hydroxides (see CADMIUM COMPOUNDS).

In more recent studies involving cyclic line scan voltammetry of the nickel electrode, it was suggested that nickel can exist in the positive 2, 3, and 4 oxidation states (42). The structural parameters (43) using transmission extended x-ray absorption fine structure (exafs) and *in situ* electrodes confirmed earlier x-ray data (7,8), showing that the presence of cobalt [7440-48-4], Co, does not change crystal lattice parameters. The density and compressibility of nickel electrodes have been found to be highly variable (44). Cobalt additions appear to reduce the compressibility of nickel hydroxide, resulting in a firmer attachment of the active material to the substrate. However, a felt metal grid has been shown (45) to reduce shear failures of the electrode structure and minimize the need for stabilizing additives, such as cobalt.

In addition to the normal charge–discharge reaction, properly fabricated sealed nickel–cadmium cells have a mechanism for absorbing infinite amounts of overcharge. The cell must be fabricated with an excess amount of uncharged active material [$Cd(OH)_2$] in the cadmium electrode. When the nickel electrode nears full charge oxygen is evolved. This oxygen diffuses through open areas of the separator and reacts with the charged cadmium species forming cadmium oxide that hydrates to cadmium hydroxide (electrical charge reaction).

$$Cd(OH)_2 + 2\,e^- \longrightarrow Cd + 2\,OH^-$$

Therefore, the cadmium electrode is being electrically charged and chemically discharged at the same rate (chemical discharge reaction).

$$2\,Cd(OH)_2 \longleftarrow 2\,Cd + O_2 + 2\,H_2O$$

Sealed Cells. Most sealed cells are based on the principles appearing in patents of the early 1950s (3) where the virtues of limiting electrolyte, a separator that would absorb and retain electrolyte, and leaving free passage for the oxygen from the positive to the negative plate were described. First, the negative electrode has a surplus of uncharged active material so that the positive plate starts to produce oxygen before the negative plate is fully charged. The oxygen reacts with the negative active material, so that the negative electrode never becomes fully charged and consequently never evolves hydrogen. Second, the amount of electrolyte used is generally lower than can normally be absorbed in the electrodes and separators, facilitating the transfer of oxygen from the positive to the negative plate. Oxygen transport, at least to a certain extent is carried out in the gaseous stage. Third, the separators generally used can pass oxygen to the gaseous state for rapid transfer to the negative plate. Although both pocket and sintered electrodes of the nickel–cadmium type have been used in sealed-cell construction, the preponderant majority of cells in commercial production use sintered positive (nickel) electrodes, and either sintered or pasted negative (cadmium) electrodes.

Although the charged form of the anode is metallic cadmium, some traces of the discharged form always remain in the electrode even at prolonged overcharge. Indeed, as the anode is oxidized (discharged), x-ray diffraction peaks

show lines from both Cd and $Cd(OH)_2$. These lines have sharper peaks than those obtained using the cathodic nickel hydroxides, confirming the more crystalline nature of cadmium.

Cadmium electrodes maintain a flat E° potential throughout discharge, as is true of most electrodes in which the materials of the charged and discharged state form distinct independent crystalline forms. Because the conductivities of cadmium electrodes are high, and no ir drops or films are generated during discharge, they also display a flat working voltage curve.

The nickel–cadmium cell, unlike the lead–acid system, has a negative temperature voltage coefficient that is in the range of $-(0.2 - 0.4)$ mV/°C, depending on design factors and the nature and doping of the nickel active materials. Thus at higher temperatures the cell has a slightly lower open circuit voltage and this, combined with a reduction of internal resistance at higher temperatures, can result in a reduced back emf in charging. Therefore, special precautions must be taken in charging under constant voltage conditions to avoid the so-called runaway condition; ie, an increase in charge current that comes from a reduction in back emf resulting in an increase in temperature and then a new increase in charge current. Cells can be destroyed in this runaway condition unless current limiters are provided in the charge circuit. The runaway condition problem is not limited to the nickel–cadmium battery. However, it is more likely in those systems where the voltage change with temperature is negative and in those designs where there is very low internal resistance.

The capacity utilization of active material depends on cell design, discharge rate, temperature, and charging conditions. High rate ability depends on the degree of conducting support provided for the active material surface that is in contact with electrolyte, separator resistance, and state-of-charge. The maximum capacity that can normally be achieved from nickel active materials is 0.30 A·h/g calculated on the basis of $Ni(OH)_2$. The capacity of negative active material is ca 0.37 A·h/g based on $Cd(OH)_2$. In actual cell use, working capacities range from 60 to 90% of these values, depending on discharge rate and temperature.

Cell Fabrication Methods. Pocket Cells. A view of a pocket electrode nickel–cadmium cell is shown in Figure 3. The essential steps of positive (nickel) electrode construction are (*1*) cold-rolled steel ribbon is cut to proper width and is perforated using either needles or rolls; (*2*) the perforated steel ribbon is nickel-plated and usually annealed in hydrogen. The ribbon is formed into a trough shape, is filled with active material by either a briquetting or a powder-filling technique; (*3*) a second strip is formed into a lid that covers and locks with the filled trough; (*4*) the filled strips are cut to length and are arranged to form an electrode sheet by interleaving. This operation, carried out by means of rollers in a forming roll, is often combined with the pressing of a pattern into the electrode sheet in order to ensure good contact between ribbon and active material and to add mechanical strength to the construction; and (*5*) the electrode sheet is then cut to pieces of appropriate size and side bedding and lugs attached to form a metallic frame. The frame material is usually also cold-rolled steel ribbon.

The pockets are usually arranged horizontally in the electrodes as shown in Figure 3, but in a few cases vertical pockets are used. No significant difference has been observed between the two arrangements.

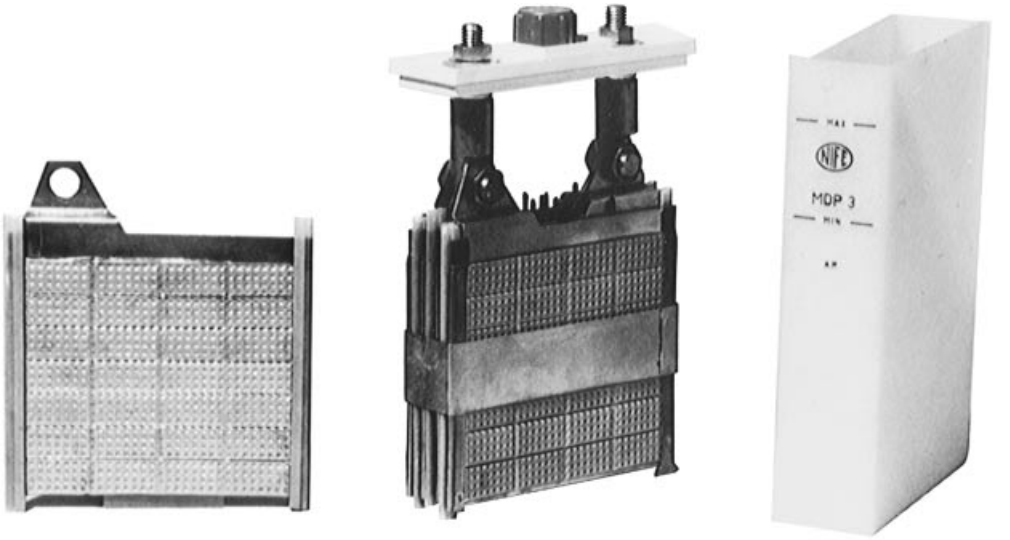

Fig. 3. View of pocket electrode nickel–cadmium cell.

Pocket-type cadmium electrodes are made by a procedure similar to that described for the positive electrode. Because cadmium active material is more dense than nickel active material, and because cadmium has a 2+ valence, cadmium electrodes, when fabricated to equal thicknesses, have almost twice the working capacity of the nickel electrode. A cell having considerably greater negative capacity provides for loss of negative capacity during life and avoids generation of hydrogen during charging. Thus in actual practice plates of equal thickness are used. Some manufacturers prefer to make the electrolyte transfer area larger for the negative electrode by increasing the area of perforation, usually by increasing the hole size. Pocket electrode plates usually have thicknesses of 0.7–6.3 mm.

After the individual pocket electrodes are fabricated, they are assembled into electrode groups. Electrodes of the same polarity are electrically and mechanically connected to each other and to a pole bolt as illustrated in Figure 3. Plates of opposite polarity are interleaved with separators. Ordinarily single-plates are used for each leaf in a plate group, but some manufacturers prefer to use two thin plates back to back to form one leaf in the positive group. Both bolting and welding methods are used in the assembly of electrodes into groups.

To complete the assembly of a cell, the interleaved electrode groups are bolted to a cover and the cover is sealed to a container. Originally, nickel-plated steel was the predominant material for cell containers but, more recently plastic containers have been used for a considerable proportion of pocket nickel-cadmium cells. Polyethylene, high impact polystyrene, and a copolymer of propylene and ethylene have been the most widely used plastics.

Steel containers are mechanically stronger than plastic and easier to fabricate in large sizes. They dissipate heat better and tend to keep the electrodes cooler during high temperature or high rate operations. However, cells

assembled in steel containers must not have contact with each other during assembly to prevent intercell shorts. Plastic containers are the better option for most small and medium-sized cells because they require no protection against corrosion, they permit visual observation of the electrolyte level, they are lighter than steel containers, they can be closely packed into a battery, and small cells can be cemented or taped into batteries, eliminating a tray.

The cells are usually filled with an electrolyte solution of potassium hydroxide of density 1.18–1.23 g/mL, which may also contain lithium hydroxide. A potassium hydroxide solution of 1.20 g/mL freezes at $\sim -27^{\circ}C$. Thus cells intended for climates colder than $-27^{\circ}C$ have an electrolyte density of 1.25 g/mL or greater. In some designs there is a large volume of excess electrolyte above the electrodes in order to reduce the need for rewatering to once every few years. In these cells, the initial electrolyte density is lower than normal because the solution concentrates during operation. Concentrations might be as high as 1.26 g/mL at the time of rewatering (topping up). Lithium hydroxide has been shown to increase the life of positive pocket electrodes in cycling operation. However, the addition also increases the electrolyte resistivity, and is not ordinarily used in high rate starter batteries.

Individual cells are usually precycled before assembling into batteries. These early charge–discharge cycles, often called formation cycles, improve the capacity of the cell by increasing the surface area of the active material and effecting crystal structure changes.

The individual cells are assembled into batteries after a leakage test to check for faulty welding joints in steel containers or cracks and improper seals in the plastic encased cells. Cells that are to be delivered without electrolyte are emptied after the formation cycles. The steel-cased cells have to be separated by mechanical means to prevent intercell shorts and are often assembled into wooden crates. The cells in plastic cases can be cemented together or strapped with tape.

Tubular Cells. Although the tubular nickel electrode invented by Edison is almost always combined with an iron negative electrode, a small quantity of cells is produced in which nickel in the tubular form is used with a pocket cadmium electrode. This type of cell construction is used for low operating temperature environments, where iron electrodes do not perform well or where charging current must be limited.

Sintered Cells. The fabrication of sintered electrode batteries can be divided into five principal operations: preparation of sintering-grade nickel powder; preparation of the sintered nickel plaque; impregnation of the plaque with active material; assembly of the impregnated plaques (often called plates) into electrode groups and into cells; and assembly of cells into batteries.

A good powder for sintering purpose should be very pure (Fe, Cu, and S should be especially avoided) and should have a very low apparent density, in the range of 0.5–0.89 g/mL. An excellent powder for this purpose is made by the decomposition of nickel carbonyl [13463-39-3], $Ni(CO)_4$, (see CARBONYLS). Nickel carbonyl is a poisonous vapor obtained by passing carbon monoxide [630-08-0] over finely divided metallic nickel at about $200^{\circ}C$ in rotary kilns using special gas-tight seals. The gas is condensed and the liquid carbonyl distilled to eliminate impurities. The purified liquid nickel carbonyl is injected

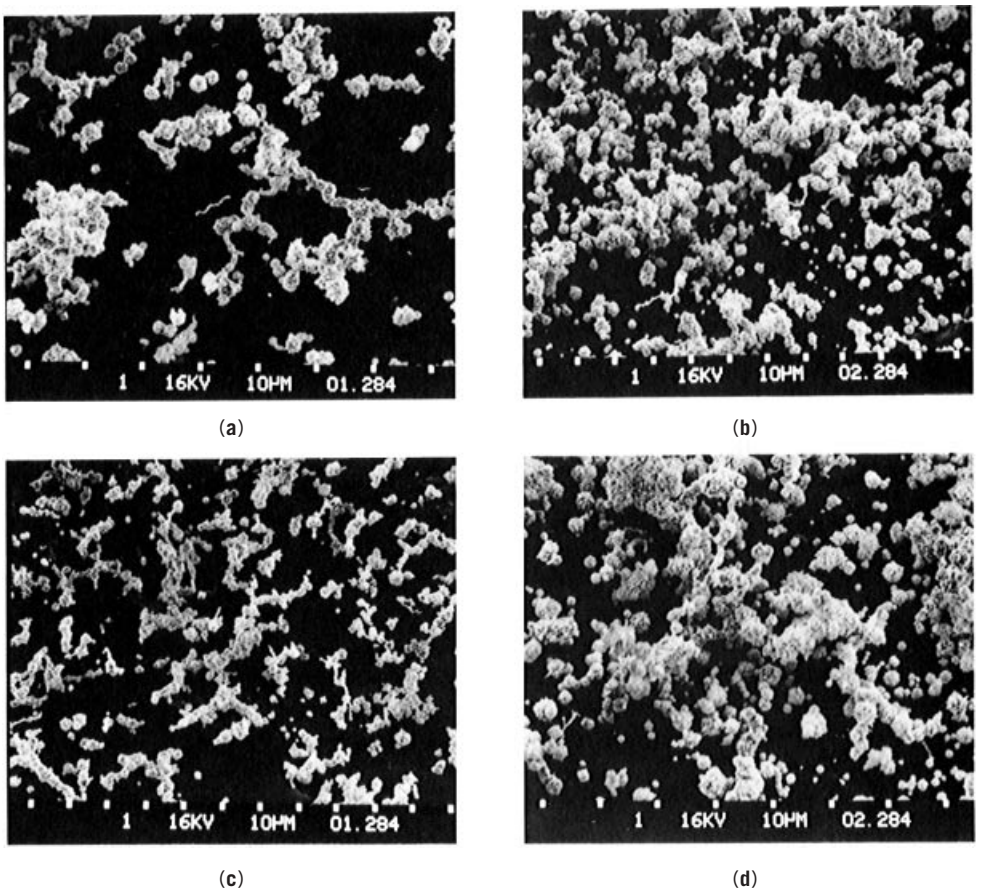

Fig. 4. Microstructure of carbonyl nickel powder at various magnifications (**a**) and (**c**) 1000x, (**b**) and (**d**) 1500x. Courtesy of Inco.

into large decomposers that have heated walls. The nickel carbonyl decomposes into carbon monoxide, which can then be recirculated, and a finely divided nickel powder. The structure of such powders is shown in Figure 4.

Sintering is a thermal process through which a loose mass of particles is transformed to a coherent body. It usually takes place at a temperature equal to two-thirds the melting point, or ca 800–1000°C for nickel. The sintered nickel structure without active material is called a plaque and it can be prepared by either dry or wet processes (see METALLURGY, POWDER).

In the dry process, nickel powders are sifted into ceramic or carbon molds with a reinforcing layer of wire mesh cloth or electroformed nickel. In most production processes part of the powder is sifted into the mold, a grid is inserted, and a second layer of sifted powder is added. The reinforcing grid is provided to reduce shrinkage during the sintering, reduce electrical resistivity, and provide extra mechanical strength. The molds are transferred to a sintering furnace that contains a reducing or inert atmosphere. Usually a reducing atmosphere is maintained by cracking ammonia ($2\ NH_3 \longrightarrow N_2 + 3\ H_2$) or partially dissociating

natural gas. After 5–10 min in a hot zone, the molds are transferred to a cold zone in the furnace. Most furnaces for the dry processes are horizontal and of the moving-belt type.

To reduce labor and other expenses, most sintered nickel plaques are produced by a wet-slurry method. A nickel slurry is prepared by mixing a low density nickel powder with a viscous aqueous solution such as carboxymethylcellulose [9004-42-6] (CMC). Pure nickel gauze, a nickel-plated gauze, or a nickel-plated perforated steel strip is continuously carried through a container filled with the nickel paste and sintering is done in a horizontal furnace. The time of sintering in the furnace is ca 10–20 min.

Usually the plaques produced by either method are coined (compressed) in those areas where subsequent welded tabs are connected or where no active material is desired, eg, at the edges. The uncoined areas usually have a Brunauer-Emmet-Teller (BET) area in the range of 0.25–0.5 m^2/g and a pore volume >80%. The pores of the sintered plaque must be of suitable size and interconnected. The mean pore diameter for good electrochemical efficiency is 6–12 μm, determined by the mercury-intrusion method.

The process by which porous sintered plaques are filled with active material is called impregnation. The plaques are submerged in an aqueous solution, which is sometimes a hot melt in a compound's own water of hydration, consisting of a suitable nickel or cadmium salt and subjected to a chemical, electrochemical, or thermal process to precipitate nickel hydroxide or cadmium hydroxide. The electrochemical (46) and general (47) methods of impregnating nickel plaques have been reviewed.

In the original process for the positive electrode, the plaques were placed in a metal vessel, which was evacuated to <5.3 kPa (40 mm Hg), and a nearly saturated solution of nickel nitrate (density 1.6 g/mL) admitted. After a 5–15 min soaking period, the plaques were transferred at 101 kPa (1 atm) to a polarizing unit where they were cathodically polarized in hot caustic solution. After polarization the plates were washed and dried. These four steps were repeated four or five times until the desired weight gain of active material was achieved.

For the negative electrolyte, cadmium nitrate solution (density 1.8 g/mL) is used in the procedure described above. Because a small (3–4 g/L) amount of free nitric acid is desirable in the impregnation solution, the addition of a corrosion inhibitor prevents excessive contamination of the solution with nickel from the sintered mass (see CORROSION AND CORROSION CONTROL). In most applications for sintered nickel electrodes the optimum positive electrode performance is achieved when 40–60% of the pore volume is filled with active material. The negative electrode optimum has one-half of its pore volume filled with active material.

Other processes have been developed in which the impregnation is accomplished in one or two steps; the most promising is electrodeposition directly from nitrate solutions having pH controlled at 4–5. After electrodeposition, the plaques are either cathodically polarized in sodium hydroxide solution or electrochemically formed in sodium hydroxide to eliminate all traces of nitrate. The latter steps must proceed at low current densities to avoid blistering and shedding of the loaded plaques.

Some manufacturers add a small (10–20% of the positive loading) amount of cadmium to positive plates as an antipolar mass to prevent some of the

problems of reversal in sealed cells. This practice may, however, create as many problems as it solves in that positive capacity is reduced proportionally to the quantity of antipolar mass added.

In most cases, the impregnation process is followed by an electrochemical formation where the plaques are assembled into large temporary cells filled with 20–30% sodium hydroxide solution, subjected to 1–3 charge–discharge cycles, and subsequently washed and dried. This eliminates nitrates and poorly adherent particles. It also increases the effective surface area of the active materials.

Formation also offers a convenient means of regulating the state of charge of the plates prior to cell assembly. This is important in sealed cell manufacture, where cell performance is optimized when 10–15% of the negative active mass is in the charged condition prior to initial cell charging. Some manufacturers have found that elimination of formation is feasible by extensive conversion of the nitrates in the impregnation process, followed by meticulous washing. However, charge retention can suffer to some degree because of traces of nitrate in the finished cells.

Cell Assembly. The methods for cell assembly, starting with the processed plaques depend on whether the cells are to be vented or sealed. For vented cells, processed plaques are usually compressed to 85–90% of their processed thickness allowing sufficient porosity for electrolyte retention and strengthening the plate structure. For sealed cells, sizing of the negative plaques is usually avoided because maximum surface area is important to oxygen recombination.

The next operation is the cutting of plaques into individual plates, usually through the coined areas (Fig. 5). Plate edges are sometimes coated with an

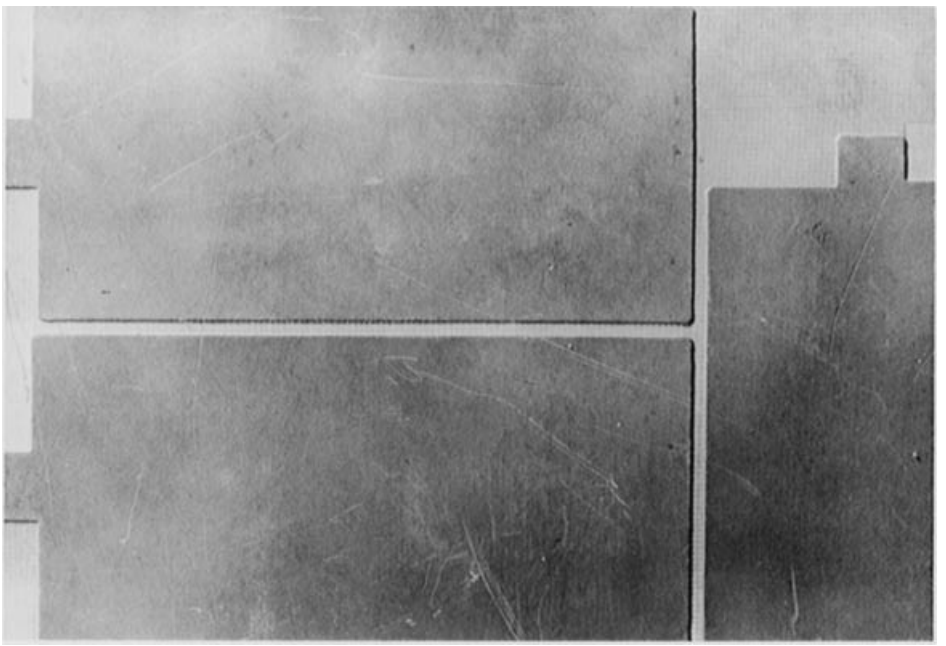

Fig. 5. Coined master plaque.

adherent plastic film to smooth any rough edges that could otherwise penetrate the thin separators used in sintered-plate cells. A tab of nickel or nickel-plated steel is welded to each plate. In some cases, this is accomplished by spot or projection welding at the coined area. For plates provided with perforated sheet grids the tabs are spot welded directly to the sheet at the proper point at the edge of the sheet. For both types of cells most of the requirements of the separators are high electronic resistance and low electrolytic resistance in the usual electrolyte (30% KOH solution). Separators should be as thin as possible and have small and evenly distributed pores. Additionally, they should be resistant to heat, KOH, gases formed on charge, and other components of the system.

The most important separator material property difference for vented and sealed cells is permeability to oxygen. In the charging of the vented cells, it is important to minimize oxygen transport from the positive to the negative plates. In float-charge applications, oxygen recombination at the negative plates results in generation of heat and ultimately to thermal runaway if excessive charge current is drawn with rising temperature. The opposite is required in sealed cells, where oxygen recombination is necessary to prevent an increase of internal pressure. Glycerol-free cellophane is used as part of the separator in the vented cells. Other components in typical vented cell separators are woven nylon, felted nylon, felted nylon–cellulose, felted (vinyl chloride–acrylonitrile) copolymer, microporous polypropylene, and irradiated polyethylene. Most sealed-cell separators are single-layer felted materials, usually nylon or polypropylene, chosen for the ability to retain electrolyte and prepared in such a manner as to allow oxygen permeability, eg, calendering of such materials should be avoided.

Another difference between vented and sealed cell manufacture is found in the ratio of negative to positive active material. Although both types of cells require an excess of negative material, in the vented type a ratio of 1.5 is sufficient for the high rates of discharge and low temperature conditions encountered. In the sealed type a typical ratio is 2, to provide for sufficient sites for the oxygen recombination, to provide for the residual negative capacity mentioned earlier, and to preclude the possibility of the negative plate reaching the fully charged state exemplified by H_2 evolution.

Both vented and sealed cells use the same basic electrolyte (30% KOH), but different amounts are required. The vented cell contains a considerable amount of free electrolyte to allow for decomposition and loss of water on charge and to allow for maximum performance on discharge. The sealed cell contains only enough electrolyte to fill the plate pores and to completely saturate the separator; excess electrolyte inhibits oxygen recombination by reducing the number of sites, ie, oxygen–cadmium–electrolyte interfaces, for oxygen recombination. In certain applications, 15–30 g/L lithium hydroxide is added to the electrolyte. Where elevated temperature operation is encountered, this addition improves charge acceptance, especially in sealed cells. Larger (50 g/L) amounts of lithium hydroxide are used in repeated cycling with constant voltage charging and in float-charge applications (vented cells). This larger amount of lithium hydroxide maintains capacity better than KOH alone but increases electrolyte resistance and adversely affects low temperature performance.

The presence of certain forms of cellulose (qv) in the electrolyte is beneficial for negative electrodes, probably by preventing the formation of large grain sizes

of cadmium on charge. Cellophane in vented cell separators usually provides sufficient cellulose for this effect. Early sealed cells using a single layer of cellulosic filter paper as separator gave excellent performance but had reduced cycle life as a result of the degradation of the cellulose. In later sealed cells, where felted nylon or felted polypropylene was used as separator, the addition of small amounts of cellulose to the electrolyte, improved negative plate performance, but led to early separator degradation.

Assembly of vented cells begins by interleaving the electrodes and separators. A most widely used separator is a sandwich of woven nylon (0.08–0.10 mm), cellophane (0.05 mm), and woven nylon (0.08–0.10 mm) of the proper width, usually 0.6 cm wider than the plate height, and of a length to form a continuous barrier around the edges of all the plates. The electrode tabs of each polarity are brought together and connected to the cell terminals by spot welding or, in a few cases, by bolting. The stack is attached to the cell cover by inserting terminals through holes that are marked for polarity. When threaded terminal posts are used, sealing is accomplished by compressing a neoprene gasket or O-ring between a flat or groove on the horizontal surface of the terminal and the inside surface of the cover, with the proper torque being applied by means of a nut on the outside of the cover. In the case of a smooth terminal post, compression is effected by means of a snap ring and belleville washer arrangement.

The most common cell case and cover materials are nylon, polyolefin, polysulfone, and styrenic (ABS). After inserting the cell element, with cover attached, into the cell case, cover and case are cemented. For nylon, a most satisfactory adhesive is phenol. For styrene copolymers, either a solvent seal or an ultrasonic seal is effective (see ADHESIVES).

The cell filler caps in the covers are designed to prevent spillage and usually contain a venting mechanism to allow for escape of gas during charge and to prevent the carbon dioxide of the air from contacting the electrolyte. Most filler caps are a type of rubber-ring screw vent assembly provided with holes or slits that are sealed by the rubber ring. These are usually made of nylon or polystyrene, but in certain applications they are made of nickel-plated steel.

In filling cells with electrolyte, vacuum techniques are employed for uniformity and for hastening the complete wetting of plates and separator. A properly manufactured cell is ready for use immediately after the first charge following electrolyte fill. The first charge is ideally at the 10-h rate for 20 h. Higher rates can be used but should not exceed the 5-h rate.

Plastic-cased cells are assembled into batteries by placing them a small distance apart or in contact with heat-conducting fins in a specially treated steel container tray. The cell spacing depends on the battery application. For example, in aircraft starting batteries provision is required for circulating cooling air between cells. The steel boxes (battery cases) are previously prepared by coating all surfaces with a tough, insulating plastic (usually epoxy). Excellent results are obtained using a fluidized bed technique of application, which results in a uniformly thick coating. Intercell connectors are normally of nickel-plated copper, but in small sizes connectors are often of nickel or nickel-plated steel.

The prismatic sealed cells are made in a manner similar to the above. Most prismatic sealed cells use a metal case and cover. The most desirable case material is stainless steel, although nickel-plated steel can be used. Terminal

feed-through is effected by ceramic-to-metal or glass-to-metal sealing techniques; and case-to-cover seal, by inert gas welding. Most prismatic sealed cells incorporate a high release, resealable vent in the cover that usually consists of a metallic spring working on an elastomer sealing disk or ring.

The prismatic sealed cells are not self-supporting and are normally used in battery operation where the battery case is used to constrain cell cases because internal cell pressures in the range of 690 kPa (100 psi) are common.

By far the majority of sealed cells are of the small cylindrical self-supporting type in the familiar "AA," "C," and "D" commercial sizes such as that shown in Figure 6. The element for these cells contains only one plate of each polarity; thus the electrodes are relatively long. The plates and the single-layer separator are rolled into a tight spiral, the plates arranged so that the positive tabs protrude from the element in one direction and the negative tabs in the opposite direction. The top and bottom of the element are protected and insulated by circular plastic disks having slits for the protruding tabs.

Elements are then inserted in nickel-plated steel cans, normally with the negative tab bent 90° to make contact with the can bottom. The tab is spot welded to the can bottom employing a long slender electrode that fits through the center hole of the element. The cell cover is welded to the positive tab. The cover

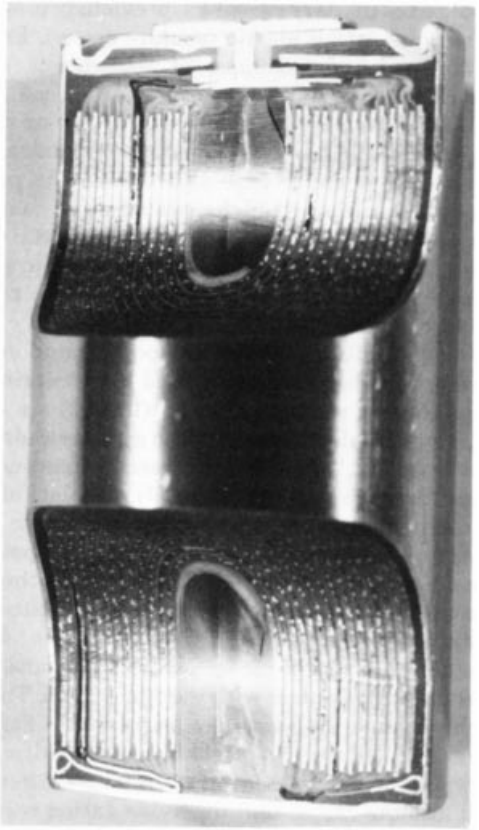

Fig. 6. Partial cutaway of a coiled, sintered-plate, nickel–cadmium cell ("D"-size).

is nickel-plated steel with a nylon gasket around the edges. After adding electrolyte, the cover is pressed into the can so that the nylon gasket rests on a shelf formed into the can well by scoring (after insertion of element). The rim of the can and sometimes the upper part of the gasket is folded over either in a press or by a rolling, rotating tool.

The cover assembly usually contains a safety vent. The most common type consists of a steel or nickel diaphragm built into the cover and a bent point cut from the cover. At a certain internal cell pressure, the diaphragm moves to the bent point and is pierced. Some cylindrical sealed cells use one or more terminal feed-throughs employing glass-to-metal or ceramic-to-metal techniques.

Battery assembly using cylindrical cells varies, and cell-to-cell connections are spot welded after using either flat tabs or cup tabs. Cell-to-cell insulation is effected either by using plastic cell jackets (shrink-on) or by inserting cells in plastic modules with each cell occupying its own cavity.

Other Cells. Other methods to fabricate nickel–cadmium cell electrodes include those for the button cell, used for calculators and other electronic devices. This cell, the construction of which is illustrated in Figure 7, is commonly made using a pressed powder nickel electrode mixed with graphite that is similar to a pocket electrode. The cadmium electrode is made in a similar manner. The active material, graphite blends for the nickel electrode, are almost the same as that used for pocket electrodes, ie, 18% graphite.

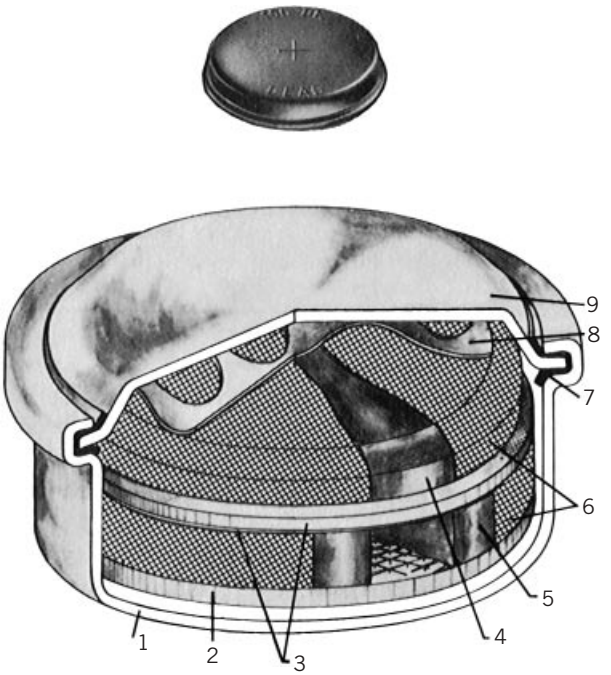

Fig. 7. Section of disk-type cell where: 1, is the cell cup; 2, is the bottom insert; 3, is the separator; 4, is the negative electrode; 5, is the positive electrode; 6, is the nickel wire gauze; 7, is the sealing washer; 8, is the contact spring; and 9, is the cell cover.

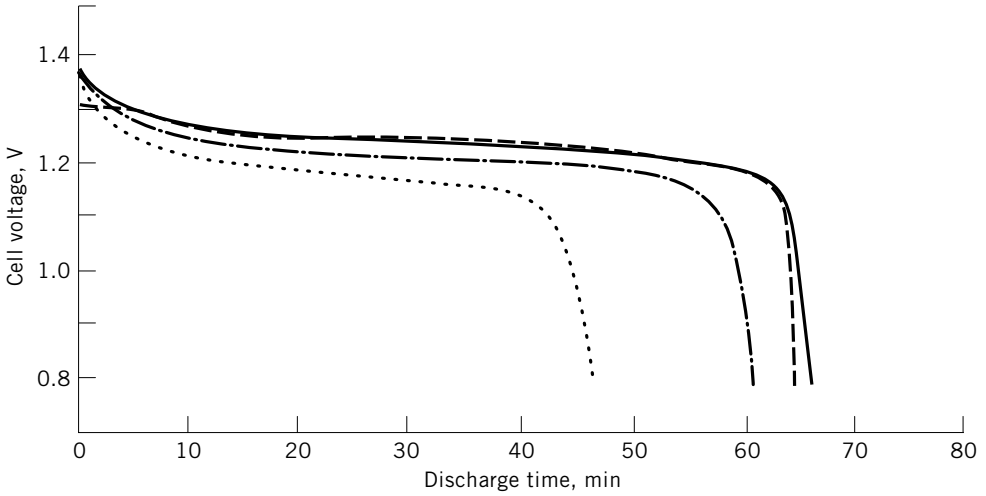

Fig. 8. Discharge capacity of small sealed nickel–cadmium cells where the initial charge is 0.1 C × 16 h at 20°C and the discharge is 1 C at temperatures of (· · ·) −20°C, (– · –) 0°C, (—) 20°C, and (– – –) 60°C. C is the current required to discharge the cell in one hour.

Lower cost and lower weight cylindrical cells have been made using plastic bound or pasted active material pressed into a metal screen. These cells suffer slightly in utilization at high rates compared to a sintered-plate cylindrical cell, but they may be adequate for most applications. The effect of temperature and discharge rate on the capacity of sealed nickel-cadmium cells is illustrated in Figure 8 and Table 3.

Applications. In the U.S., rechargeable NiCd batteries provide power for about three-fourths of most common portable products (48). Uses are divided into three categories: pocket cells are used in emergency lighting, diesel starting, and stationary and traction applications where the reliability, long life, medium-high rate capability, and low temperature performance characteristics warrant the extra cost over lead–acid storage batteries; sintered, vented cells are used in extremely high rate applications, such as jet engine and large diesel engine starting; and sealed cells, both the sintered and button types, are used in computors, phones, cameras, portable tools, electronic devices, calculators, cordless razors, toothbrushes, carving knives, flashguns, and in space applications, where

Table 3. **Nominal Capacities of Consumer Nickel–Cadmium Cells**

	Capacity, A · h	
Size	Normal cells	High capacity cells
"AA"	0.6–0.7	0.9–1.0
"Sub-C"	1.2	1.7
"C"	2.0	2.3
"D"	4.0	5.0
"F"	7.0	

nickel–cadmium is optimum because it can be recharged a great number of cycles and given prolonged trickle overcharge. Cells of this category are generally made in sizes comparable to conventional dry cells, such as "D", "C", "AA", etc. In sizes larger than the "D" cell, sealed lead–acid cells offer a useful economic alternative for applications where the extra weight and space of the lead–acid is not critical.

In order to reduce costs, achieve higher energy density, and minimize environmental problems, a growing percentage of prismatic and cylindrical cells are now made by pasting on substrate. The newer substrates include nickel fiber mat, nickel foam, and nickel-plated graphite fiber. One manufacturer uses a nickel-plated plastic fiber substrate for the fabrication of large nickel–cadmium cells in prismatic configurations (28). These cells are reported to require less maintenance than the older design pocket cells (48). In small industrial sizes, pasted cells are offered as sealed batteries.

Charger Technology. Alkaline storage batteries are commonly charged from rectified d-c equipment, solar panels, or other d-c sources and have fairly good tolerance to ripple and transient pulses. Because the voltage of the nickel electrode is variable, the cutoff voltage is not a good control parameter for nickel–cadmium cells. It is, however, often used in vented cell chargers. For sealed nickel–cadmium cells, and other systems where a combination mechanism exists, a negative voltage slope detector is often incorporated into the charger control circuit. As the charge of a cell or battery progresses there is a slow rise in the unit voltage. When the nickel electrode approaches full charge, the oxygen evolved combines with the cadmium electrode reducing the overpotential on the cadmium electrode. This slight change in cell voltage can be detected by electronic voltage slope detectors and used to reduce the charge current or shut off the charge. A method for charging sterilizable rechargeable batteries has been reported (49).

Nickel–Iron Cells. The original tubular design nickel–iron battery developed by Edison has little commercial application. In the 1980s –1990s there was a renewed interest in a high rate sintered electrode design for electric vehicle applications (50–58). However, when interest shifted to hybrid electric vehicles, in the early 2000s, with lower battery capacity requirements, interest shifted to Ni-MH because of superior performance (at greatly increased cost).

Electrochemistry and Kinetics. The electrochemistry of the nickel–iron battery and the crystal structures of the active materials depends on the method of preparation of the material, degree of discharge, the age (life cycle), concentration of electrolyte, and type and degree of additives, particularly the presence of lithium and cobalt. A simplified equation representing the charge–discharge cycle can be given as:

$$2\,\mathrm{NiOOH}^{*} + \alpha\text{–}\mathrm{Fe} + 2\,\mathrm{H_2O} \rightleftharpoons 2\,\mathrm{Ni(OH)_2^{*}} + \mathrm{Fe(OH)_2}$$

where the asterisks indicate adsorbed water and KOH. However, the discharge can be carried to a lower plateau for the iron electrode, although this is usually undesirable for life cycle, represented by:

$$8\,\mathrm{NiOOH}^{*} + 3\,\mathrm{Fe} + 4\,\mathrm{H_2O} \rightleftharpoons 8\,\mathrm{Ni(OH)_2^{*}} + \mathrm{Fe_3O_4}$$

When discharges are carried out beyond the voltage range of the ferrous hydroxide [18624-44-7], $Fe(OH)_2$, plateau which is ca -0.90 to -0.85 V vs HgO, a second reaction in the voltage range of -0.65 to -0.5 V takes place (59,60).

$$3\ Fe(OH)_2 + 2\ OH^- \rightleftharpoons Fe_3O_4 + 4\ H_2O$$

Discharging to this lower cell voltage usually results in shorter cycle life. Enough excess iron should be provided in the cell design to avoid this problem.

Active iron in the metallic state is slowly attacked by the alkaline electrolyte according to

$$Fe + 2\ H_2O \longrightarrow Fe(OH)_2 + H_2$$

This reaction is accelerated by increased temperature, increased electrolyte concentration, and by the use of sodium hydroxide rather than potassium hydroxide in the electrolyte. It is believed that the presence of lithium and sulfur in the electrode suppress this problem. Generally, if the cell temperature is held below 50°C, the oxidation and/or solubility of iron is not a problem under normal cell operating conditions.

Electrode Structures. The classical iron active material for pocket and pasted iron electrodes was formed by roasting recrystallized ferrous sulfate [7720-78-7], $FeSO_4$, in an oxidizing atmosphere to ferric oxide [1309-37-1], Fe_2O_3, and then reducing the latter in hydrogen. The α-iron formed was then heated to a mixture of Fe_3O_4 and Fe. As such it was pure enough to be used for pharmaceutical purposes. For battery use, a small amount of sulfur, as FeS, was added as were other additives which were believed to increase the cycle life by acting as depassivating agents, ie, helping to reduce the tendency of iron to evolve hydrogen upon standing in alkaline electrolyte. Extensive studies on the stability of iron active material have been reported (61–63). Addition of cadmium and antimony salts have been claimed to decrease hydrogen evolution on stand by 50% (62). However, some blends also reduce electrode capacity. A blend of materials such as mucic acid [526-99-8], $C_6H_{10}O_8$, with indium [7440-74-6], In, increases the iron stability on stand without changing electrode capacity (63). The effects of electrolyte makeup and concentration on iron corrosion have also been studied (64).

A study of sintered iron electrodes claimed advantages of high rate capability, long life, and low hydrogen evolution (52). Fine carbonyl generated iron powder was coated on a nickel screen and sintered in a hydrogen–nitrogen atmosphere. Sintered raw plaques were believed suitable if the porosity was between 50 and 80%. The sinter had to be strong enough to leave a conductive skeleton after part of the iron was corroded to active material. This process is unlike sintered-type nickel electrodes in which active material is deposited directly into the pores of a very porous plaque. Sintered iron electrodes (49) were in pilot production in Sweden and the United States.

Sintered nickel electrodes used in nickel iron cells are usually thicker than those used in Ni/Cd cells. These result in high energy density cells, because very high discharge rates are usually not required.

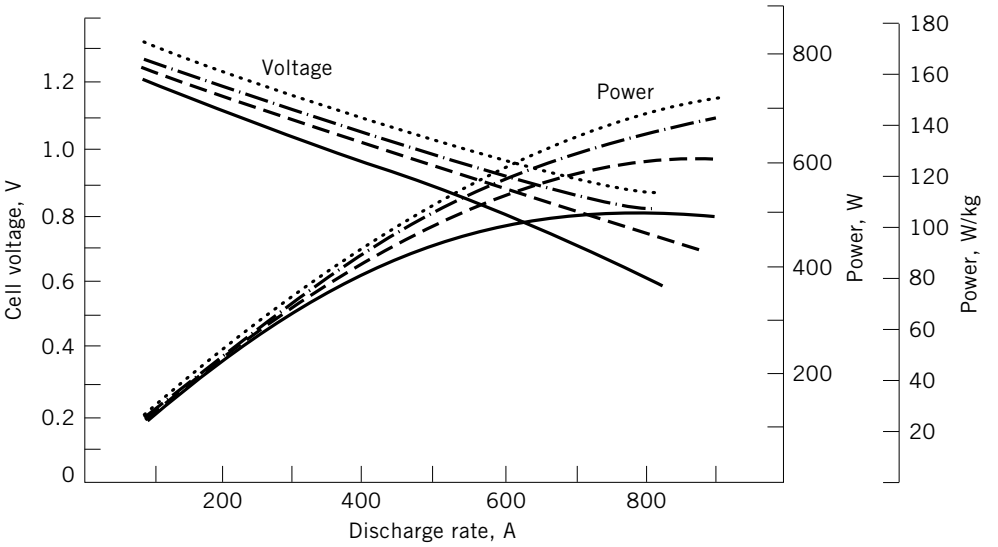

Fig. 9. Power and voltage characteristics of the nickel–iron cell where the internal resistance of the cell, R_i, is 0.70 mΩ, at various states of discharge: (···) 8%; (– · –) 32%; (– – –) 52%; and (—) 72%. Courtesy of Westinghouse Electric Corp.

Performance Characteristics. The sintered nickel-sintered iron design battery has outstanding power characteristics at all states of discharge making them attractive to the design of electric vehicles (EV) which must accelerate with traffic even when almost completely discharged. Although the evolution of hydrogen is a problem preventing sealed cell design, introduction of automatic watering systems have ameliorated the maintenance time requirements. Typical performance curves are given in Figure 9.

1.2. Silver–Zinc Cells. The silver–zinc battery has the highest attainable energy density of any rechargeable system in use except for lithium-ion cells as of this writing. In addition, it has an extremely high rate capability coupled with a very flat voltage discharge characteristic. Its use, in the early 1990s, was limited almost exclusively to the military for various aerospace applications such as satellites and missiles, submarine and torpedo propulsion applications, and some limited portable communications applications. The main drawback of these cells is the rather limited lifetime of the silver–zinc system. Life is normally limited to less than 200 cycles with a total wet-life of no more than about two years. The silver–zinc system also carries a very high cost and applications are justified only where cost is a minor factor. The high cost of silver battery systems is attributable to the cost of the active silver material used in the positive electrodes.

Cellophane or its derivatives have been used as the basic separator for the silver–zinc cell since the 1940s (65,66). Cellophane is hydrated by the caustic electrolyte and expands to approximately three times its dry thickness inside the cell exerting a small internal pressure in the cell. This pressure restrains the zinc anode active material within the plate itself and renders the zinc less available for dissolution during discharge. The cellophane, however, is also the

principal limitation to cell life. Oxidation of the cellophane in the cell environment degrades the separator and within a relatively short time short circuits may occur in the cell. In addition, chemical combination of dissolved silver species in the electrolyte may form a conductive path through the cellophane.

A second lifetime limitation is the zinc anode. In spite of the separator and cell designs, some zinc material is solubilized during the charge–discharge reaction. Over a period of cycling there is a shift of active material, originally distributed evenly over the face of the electrode, to the center and bottom areas of the electrode (50). This shape change limits the life of the cell as exemplified by a fading of the capacity and a build-up of internal pressure that may eventually lead to a short circuit.

Reaction Mechanisms. There is considerable difference of opinion concerning the specific cell reactions that occur in the silver–zinc battery. Equations that are readily acceptable are

$$2\,AgO + Zn + H_2O \rightleftharpoons Ag_2O + \begin{matrix} Zn(OH)_2 \\ (ZnO + H_2O) \end{matrix} \qquad E^\circ = 1.85\ V$$

and

$$Ag_2O + Zn + H_2O \rightleftharpoons 2\,Ag + \begin{matrix} Zn(OH)_2 \\ (ZnO + H_2O) \end{matrix} \qquad E^\circ = 1.59\ V$$

The charge and discharge of silver–zinc cells occurs at two voltage levels, representing the energy levels of AgO (an overall valence 2 silver oxide compound sometimes mislabeled as silver peroxide) and a lower energy level material Ag_2O. The AgO is often represented as Ag_2O_2, since crystallographic data indicates there are two different bond lengths in the structure.

Electrochemistry. Silver–zinc cells have some unusual thermodynamic properties. The equations indicate that the higher valence silver oxide is AgO, silver(II) oxide [1301-96-8]. However, in the crystallographic unit cell, which is monolithic, there are four silver atoms and four oxygen atoms, and none of the Ag–O bonds conforms to a silver(II) bond length. Instead there are two Ag–O bonds of 0.218 nm corresponding to silver(I) and two Ag–O bonds of 0.203 nm corresponding to silver(III) (67). This structure has also been proposed on the basis of magnetic and semiconductor properties (67) and confirmed using neutron diffraction (68,69).

For the Ag–O material a reversible voltage of 1.856 V is obtained and the $(\partial E/\partial T)_P$ is positive, $+5.7 \times 10^{-5}$ V/°C. For the Ag_2O material a reversible voltage of 1.602 V is obtained in 11.6 *N* KOH but the $\partial E/\partial T$ is negative, -16.9×10^{-5} V/°C. This is about one-third the value of nickel–cadmium cells. However, because the negative coefficient compound is not present in the fully charged state, the high risk of thermal runaway described for nickel–cadmium cells does not exist. The high conductivity of the silver active material and the low internal resistance of the remaining components do, however, make thermal runaway a possibility to be considered in charger and system design.

Electrodes. All of the finished silver electrodes have certain common characteristics: the grids or substrates used in the electrodes are usually made

of silver, although in some particular cases silver-plated copper is used. Material can be in the form of expanded silver sheet, silver wire mesh, or perforated silver sheet. In any case, the intent is to provide electronic contact of the external circuit of the battery or cell and the active material of the positive plate. Silver is necessary to avoid any possible oxidation at this junction and the increased resistance that would result.

Finished electrodes need fairly good physical strength so that they can be handled easily during separator wrapping and cell assembly. This is usually accomplished by a sintering process. Finished electrodes should also have a relatively high surface area per unit weight of active material coupled with an apparent porosity of about 50–60% based on the active material. The high surface area of the active material is attained by high surface area starting materials. These can be finely divided powders of metallic silver or either the monovalent or divalent oxides of silver. Silver electrodes can attain coulombic efficiencies of up to 85% of theoretical when manufactured from high surface area active material.

There are three methods of silver electrode fabrication: (*1*) the slurry pasting of monovalent or divalent silver oxide to the grid, drying, reducing by exposure to heat, and then sintering to agglomerate the fine particles into an integral, strong structure; (*2*) the dry processing of fine silver powders by pressing in a mold or by a continuous rolling operation onto a silver grid followed by sintering; and, (*3*) the use of plastic-bonded active material formed by imbedding the active material (fine silver powder) in a plastic vehicle such as polyethylene, which can then be milled into flexible sheets. These sheets are cut to size, pressed in a mold on both sides of a conductive grid, and the pressed electrode subjected to sintering where the plastic material is fired off, leaving the metallic silver. Silver electrodes produced by these processes range from 0.18 to 1.52 mm in thickness. Electrodes prepared by method (*1*) usually cannot be below 0.76 mm in thickness whereas the thinner electrodes can be prepared by methods (*2*) and (*3*).

Silver electrodes prepared by any of the three methods are almost always subjected to a sintering operation prior to cell or battery assembly. Sintering is basically a heating operation at temperatures well below the melting point of pure silver, 960.5°C, during which an agglomeration of the particles occurs, greatly strengthening the electrodes produced. Sintering is normally carried out in electric muffle furnaces, either on an individual batch process or a continuous conveyor belt-type operation. Reducing atmospheres are not necessary for silver electrode sintering because the process is carried out well above the decomposition temperatures of the various silver oxides. Sintering process parameters vary, however, examples are: 537°C for 30 min and 732°C for 3 min. The longer exposure at a somewhat lower temperature is said to produce electrodes that are less susceptible to shedding. Such a procedure, however, requires a furnace with a long heating zone, is more expensive, and is not practical to most manufacturers.

Zinc electrodes for secondary silver–zinc batteries are made by one of three general methods: the dry-powder process, the slurry-pasted process, or the electroformed process. Current-carrying grids for zinc electrodes can be the same regardless of the process of plate manufacture chosen. Expanded metal, screen, or perforated metal is the generally accepted form for these grids. Silver is the material of preference. However, cost considerations often dictate that copper

be used. In these cases silver-plated copper forms are usually employed to avoid the possibility of copper dissolving in the caustic solution during over-discharge of a cell.

The active material used in any of the processes for the manufacture of electrodes is a finely divided zinc oxide powder, USP grade 12. The zinc oxide active material is usually blended with from 1–4% mercuric oxide in the dry state for any of the dry processing procedures. Mercuric oxide is converted to mercury during charge which then amalgamates the zinc formed at the same time. This tends to suppress the evolution of hydrogen on the zinc electrode during charged stand, and is required in most military applications to avoid a hydrogen hazard.

In the dry powder process the active material mix is spread evenly in a mold, the grid and lead assembly inserted, and the entire electrode then pressed in a hydraulic press. Often binder additives such as poly(vinyl alcohol) (PVA) or fine Teflon powder are added to the active material mix to increase the cohesiveness of the finished electrodes. Cellulosic paper liners are also used, and they are inserted into the mold prior to introduction of the active mix and grid. After the active mix and grid are introduced, the paper liner is then folded over the top of the electrode and the electrode pressed as before. Porosities obtained by pressing electrodes in this manner are usually in the range of 50%, although in actual production these figures can range from about 35–60% depending on the rate of discharge required. In the slurry or paste method a paste is prepared by mixing water with the active material mix (zinc oxide plus mercuric oxide). Sometimes a binder such as CMC, or a flock such as short rayon or Dynel fibers is added to the paste to increase the cohesiveness of the pasted electrode. Pasting is usually done on large strips of grid material.

After pasting, the strips are air dried at relatively low heats, individual electrodes are cut from the strip, and the electrodes are pressed to desired thicknesses. The porosities and densities of the active material made by the pasting processes are approximately the same as those indicated for the dry pressed powder processes. One danger in pasting electrodes is the occurrence of sharp grid edges on the electrodes after cutting to size. Often a secondary operation of smoothing or trimming is required to avoid this problem.

The electroforming or deposition of zinc from solution uses a slurry of zinc oxide in strong caustic solution or actual metallic zinc anodes in caustic solution. In the slurry method, the zinc oxide is deposited on silver or copper grids that comprise the grids of the finished electrodes. In the metallic zinc anode method, the solutions are not depleted but rather the anodes are depleted. Both methods utilize large sheets onto which the active zinc material is deposited. Often individual plate leads are welded in position prior to deposition. In other cases active zinc must be scraped from the grid in a secondary operation and the plate leads then welded into position. Zinc plates prepared by these deposition methods usually have the active material in a voluminous, mossy state. After plating, the sheets of deposited material must be washed to completely free them of any traces of caustic solution to avoid fire hazards during production and the subsequent drying operation.

After the plates have been washed and dried thoroughly, they are pressed in a preliminary operation to the desired thickness. Individual electrodes are then cut from the sheets and a secondary pressing operation to final thickness

is done. Often a secondary operation is required to remove sharp edges of electrodeposited zinc electrodes.

Silver–Zinc Separators. The basic separator material is a regenerated cellulose (unplasticized cellophane) which acts as a semipermeable membrane allowing ionic conduction through the separator and preventing the migration of active materials from one electrode to the other. Usually, multiple layers are used in cell fabrication.

A stronger separator is one made of sausage casing material (FSC), a regenerated cellulose similar to cellophane but including some fibrous material. FSC is usually extruded in tubes and electrodes are inserted into each end of the tube. The tube is folded to form the so-called U wrap.

Another method of extending the life of the cellulosic separators has been to incorporate a silver organic compound, eg, silver xanthate [6333-67-1], into the cellulosic separator. This is done by passing the separator material through a hot caustic solution containing a silver salt. The result is a deposition of a silver organic compound within the structure of the cellophane or FSC separator. This type of material resists the degradative effects of oxidation more than the untreated material. In general the positive electrodes are wrapped in the layers of separator. Normally, an absorber is used around each positive electrode to maintain an adequate supply of electrolyte. Absorbers are usually of nonwoven materials, such as polyamide or polypropylex felts. In some cases, nonwoven cellulosic felts are also used, but these tend to degrade more rapidly. The absorber wrapped positive electrodes are usually wrapped in several layers of cellophane or FSC and then folded to form Us. Negative electrodes are alternately stacked forming the cell assembly. Normally ca three or four layers of PUDO (battery-grade) cellophane 0.025 mm thick are used in so-called high rate designs. For lower rate cells where longer life is required the number of layers of cellophane may be as many as ten. Occasionally cells are constructed with the negative electrodes wrapped in the separator material. This is said to reduce the shape change effect on the negative electrodes and increase life of the cell. These so-called reverse-wrap cells are usually reserved for low rate applications only.

Electrolyte. The electrolyte in silver–zinc cells is 30–45% KOH. The lower concentrations in this range have higher conductivities and are preferred for high rate cells. Higher concentrations have a less deleterious effect on cellulosic separators and are preferable for extended life characteristics. The higher concentrations also have a greater capacity for dissolving zinc oxide and accelerate change in shape of the zinc electrode. In most cases, a concentration of about 40% KOH is considered as the optimum. Occasionally, some manufacturers use as electrolyte a saturated zincate solution at the particular concentration desired. This supposedly slows the effect of zinc dissolution. However, in actual use such additives have not been shown to have much beneficial effect. Other additives, such as LiOH, which are used in other alkaline systems, have no beneficial effect on silver–zinc batteries. In practice the electrolyte is added to the cell in the discharged condition, and a period of soaking is allowed for the separators to absorb electrolyte and the electrodes to become thoroughly impregnated with electrolyte.

Cell Hardware. Cell jars are constructed almost exclusively of injection-molded plastics, which are resistant to the strong alkali electrolyte. The most

generally used materials are modified styrenes or copolymers of styrene and acrylonitrile (SAN). Another material that has been found to increase shock resistance of cells is ABS plastic (acrylonitrile–butadiene–styrene). All of these plastics can be injection-molded, are solvent-sealable and, in general, meet operating temperature ranges up to about 70°C. For applications that require greater resistance to temperature, some of the more recent plastics such as polysulfone and poly(phenylene oxide) (PPO) injection-moldable materials able to withstand operating temperatures up to 150°C are used.

Cell terminal connections are usually brought out by two-threaded terminals that protrude through the cell jar cover. They are usually steel, brass, or copper with a hollow construction. The plate leads are soldered in place in the center hollow portion of the terminal to effect an electrical contact and cell seal. The terminal itself is potted into the jar cover using epoxy-type potting compounds. Normally, terminal hardware is silver-plated. However, for corrosion resistance nickel-plating has been used.

Performance. Charging. Charging of silver–zinc cells can be done by one of several methods. The constant-current method which is most common consists of a single rate of current usually equivalent to a full input within the 12–16-h period. A typical two-level constant-current charge curve results as shown in Figure 10. The first 20–30% of the A·h input is attained at slightly above the monovalent silver level of ca 1.65 V. After this input a sharp rise to the divalent level takes place, and the remainder of the charge is completed at a voltage somewhat above the divalent silver level of 1.90–1.95 V. When the silver electrodes have reached full charge, there is a sharp rise to about 2.0–2.05 V; at this point oxygen is liberated at the positive electrode. Normally the charge is terminated to avoid excessive overcharge of the zinc electrodes and further oxygen evolution. If the charge is continued beyond this point, charging voltage remains at approximately a 2.05–2.1 V level until all of the zinc material is fully charged. Then another rise in voltage occurs to ca 2.2–2.3 V, and both hydrogen and oxygen are liberated. Further charging results in electrolysis of the water in the electrolyte.

Other acceptable charging methods that have been used are the two-level charging, modified constant potential, and constant potential methods. The two-level method is one in which a relatively high rate of charge is used until

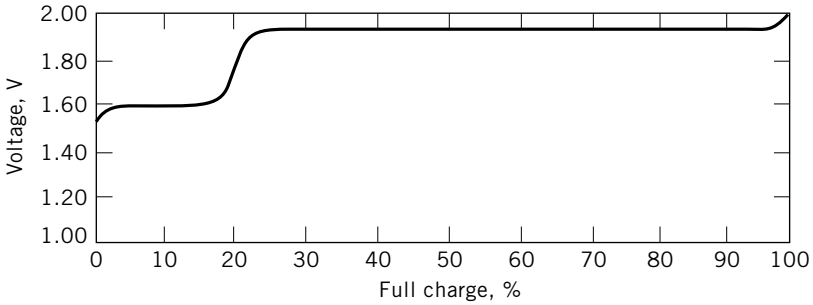

Fig. 10. Constant-current charge curve for a high rate Ag–Zn cell at room temperature. Charging carried out at the 10-h rate.

a specified input is obtained, at which time the charging rate is lowered to a second level until a voltage cut-off is reached. In the modified constant potential method an initial charging rate is set, somewhat higher than would be used for a single-level constant, current charge; and then the charging current is allowed to drift downward as the battery voltage rises during charge. The constant potential systems are usually current-limited to avoid excessive inrush currents, and are essentially similar to modified constant potential methods in that the initial current is a very high value which rapidly decreases and approaches zero during final stages of charge.

Charge acceptance of the silver–zinc system is normally on the order of 95–100% efficient based on coulombic (ampere-hour output over input) values. This is true of any of the charging methods when carried out in the proper manner. Thus overcharge is rarely necessary in charging silver–zinc cells and batteries.

Discharge. Silver–zinc cells have one of the flattest voltage curves of any practical battery system known. However, there are two voltage plateaus. Even at rates as high as 10 minutes a fairly flat characteristic is obtained. The actual level of voltage is, of course, rate dependent. However, because of the high conductivity of the silver electrode, derating of voltage with higher rates is less than other systems. Figure 11 gives typical discharge curves for a high rate silver–zinc cell. At the low rates the initial part of the voltage discharge curve exhibits the higher level or peroxide voltage. After about 20–25% of the A·h capacity has been discharged, this drops to the monovalent level. As the rate increases, the proportion of the discharge capacity at the higher voltage level becomes less, and at very high rates a dip often occurs at the beginning of discharge as in the 10-min curve. The capacity of the silver–zinc cells is also rate dependent, but less derating occurs here than in most other batteries. For example, from Figure 11 it can be seen that even at the 10-min rate a high rate silver–zinc cell provides over 60% of its rated capacity.

Performance of silver–zinc cells is normally considered to be adequate in the temperature range of 10–38°C. If a wider temperature range is desired silver–zinc cells and batteries may be used in the range 0–71°C without any appreciable derating. Lower temperatures result in some reduction of cell voltage capacities at medium to high rates, and higher temperatures curtail life

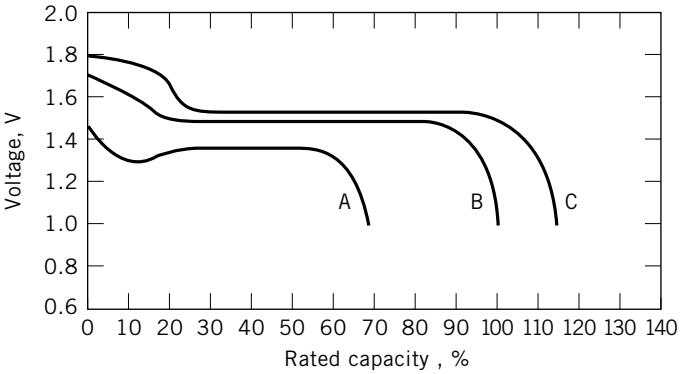

Fig. 11. Silver–zinc cell discharge curves at rates of A, 10 min; B, 1 h; and C, 10 h.

because of deterioration of the separator materials. Operation at temperatures below 0°C results in more serious derating and normally external heat is provided for operation in this range. Long use at temperatures above 71°C seriously curtails life.

Cell Life. Silver–zinc cells are usually manufactured as either low or high rate cells. Low rate cells contain fewer and thicker electrodes and have many layers of separator (up to the equivalent of 10 layers of cellophane). High rate cells, on the other hand, contain many thinner electrodes and have separator systems of the equivalent of three to four layers of cellophane. Approximately 10–30 cycles can be expected for high rate cells depending on the temperature of use, the rate of discharge, and methods of charging. Low rate cells have been satisfactorily used for 100–300 cycles under the proper conditions. In general, the overall life of the silver–zinc cell with the separator systems normally in use is approximately 1–2 yr.

1.3. Other Silver Positive Electrode Systems. *Silver–Cadmium Cells.* The first silver–cadmium batteries were manufactured in 1900 for motor cars. Use of this electrochemical system was quite limited. Then in the late 1950s, there was interest for applications such as appliances, power tools, and scientific satellites when it was hoped that silver–cadmium batteries could offer an energy density close to silver–zinc batteries and a life characteristic approaching that of the nickel–cadmium system. In satellite applications the nonmagnetic property of the silver–cadmium battery was of utmost importance because magnetometers were used on satellites to measure radiation and the effects of magnetic fields of energetic particles. Satellites had to be constructed of nonmagnetic components in sealed batteries.

The overall reactions are

$$2\,AgO + Cd + H_2O \rightleftharpoons Ag_2O + Cd(OH)_2 \qquad E^\circ = 1.38\ V$$

$$Ag_2O + Cd + H_2O \rightleftharpoons 2\,Ag + Cd(OH)_2 \qquad E^\circ = 1.16\ V$$

The silver–cadmium cell exhibits a two-plateau voltage characteristic on charge and discharge. At moderate discharge rates at 25°C, approximately 20% of the A·h capacity is delivered at a nominal 1.2 V; and the remaining capacity is delivered at 1.08–0.9 V. The discharge voltage characteristics are very sensitive to current rates, amount of cycling, charged stand time, float-charging, and temperature. For example, cells that are continuously float-charged exhibit a flat discharge voltage and no loss of capacity. At moderate charge rates, the voltage characteristic consists of two levels, 1.3 V and 1.5 V, nominal. Either constant current or constant potential charging is used. During cycling, A·h efficiencies are >95% and W·h efficiencies are <75%.

The positive plates are sintered silver on a silver grid and the negative plates are fabricated from a mixture of cadmium oxide powder, silver powder, and a binder pressed onto a silver grid. The main separator is four or five layers of cellophane with one or two layers of woven nylon on the positive plate. The electrolyte is aqeous KOH, 50 wt%. In the aerospace applications, the plastic cases were encapsulated in epoxy resins. Most useful cell sizes have ranged from 3 to 15 A·h, but small (0.1 A·h) and large (300 A·h) sizes have been evaluated. Energy densities of sealed batteries are 26–31 W·h/kg.

Silver–cadmium satellite batteries have been used in cyclic periods of five hours or more with discharge times of 30–60 min. Based on nominal capacities, depths of discharge have been 8–30%. The electrical performance of silver–cadmium batteries degrades below 0°C and above 40°C. At low temperatures the main problems are capacity maintenance during cycling and a dip in voltage on initiation of discharge. Operational and test programs have shown cycle life periods of 3 yr at low temperatures. At temperatures of 40°C and 50°C, the cycle life is 1 yr and 0.2 yr, respectively. The cycle life at intermediate temperatures is 1.4–2.0 yr.

Another application for silver–cadmium batteries is propulsion power for submarine simulator-target drones. High current drains are required (average C, pulses up to 6C), and greater recyclability than the silver–zinc counterparts used in torpedo propulsion. Batteries designed for this use utilize vented cells, high temperature plastic cell jars, and cell designs having a large number of thin electrodes to maximize electrode surface area.

Silver–Iron Cells. The silver–iron battery system combines the advantages of the high rate capability of the silver electrode and the cycling characteristics of the iron electrode. Development has been undertaken (70) to solve problems associated with deep cycling of high power batteries for ocean systems operations.

Cells consisted of porous sintered silver electrodes and high rate iron electrodes. The latter were enclosed with a seven-layered, controlled-porosity polypropylene bag which serves as the separator. The electrolyte contains 30% KOH and 1.5% LiOH.

Initial experiments were conducted with 350–A · h cells that maintained capacity over 200 cycles. Conventional silver-zinc cells lose capacity in similar deep-cycle operations. Cell tests conducted under a variety of temperature and pressure conditions revealed no discernable effects up to pressures of 69 MPa (10,000 psi) using a flooded electrolyte system. Tests at 0–25°C showed less than 5% capacity loss resulting from temperature when tested at the 8-h discharge rate. The cells as produced have a discharge voltage of ca 1.1 V. Voltage capacity characteristics of a nominal 140–A · h silver–iron cell are shown in Figure 12. The discharge capacity of a typical cell is 145 – 155 A · h at discharge rates of 80–10 A. A battery of 24 series-connected cells (containing excess electrolyte) weighs 40 kg and provides an energy density of 3.5 kW · h. At the 3-h rate the energy density is 100 W · h/kg, or about three and a half times the energy density of comparable lead–acid batteries.

Applications have been found for these batteries in emergency power applications for telecommunications systems in tethered balloons. Unfortunately, the system is expensive because of the high cost of the silver electrode. Applications are, therefore, generally sought where recovery and reclamation of the raw materials can be made.

Small silver–iron sealed button cells have been produced in Sweden (70) for long-life operation of hearing aids, calculators, and electric razors. These units have energy densities similar to silver–zinc button cells but are reported to be capable of being fully charged and discharged up to five hundred times without leakage or change in performance. Comparable performance silver–zinc cells have limited cycle life of the order of 75–100 cycles.

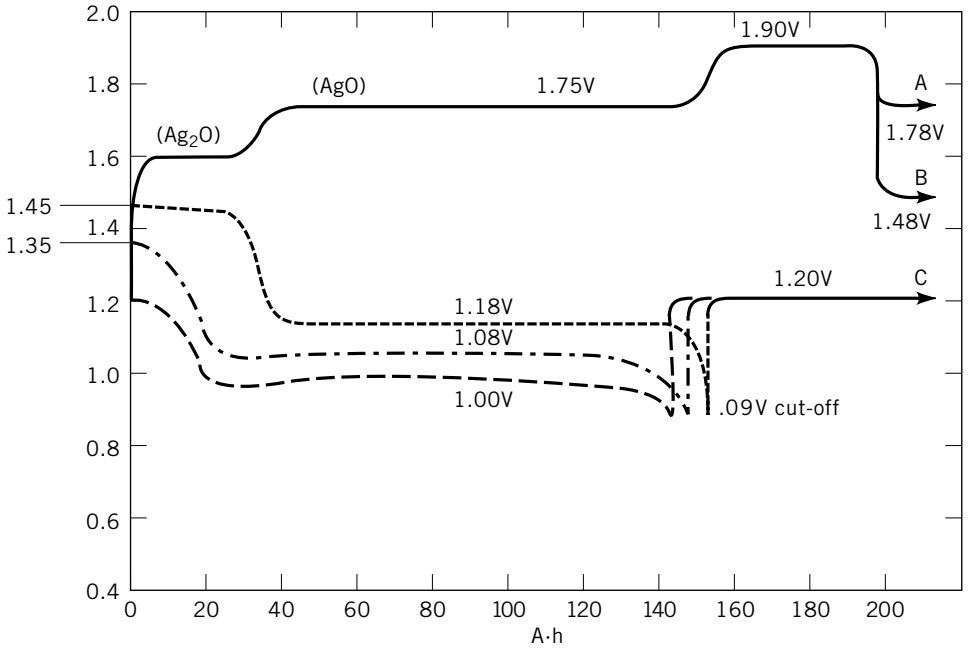

Fig. 12. Charge–discharge characteristics of a nominal 140–A · h silver–iron cell where the charge (—) is at 25 A for 8 h, A represents a 0.25 A float charge; B an open circuit; and the discharge at open circuit after 1 h is shown for (—) 10 A, (– – –) 45 A, and (– – –) 80 A; and C represents the open circuit discharge.

1.4. Nickel–Zinc Cells. Nickel–zinc cells offer some advantages over other rechargeable alkaline systems. The single-level discharge voltage, 1.60–1.65 V/cell is approximately 0.35–0.45 V/cell higher than nickel–cadmium or nickel–iron and approximately equal to that of silver–zinc. In addition, the use of zinc as the negative electrode should result in a higher energy density battery than either nickel–cadmium or nickel–iron and a lower cost than silver–zinc. In fact, nickel–zinc cells having energy densities in the range of 50–60 W · h/kg have been successfully demonstrated.

Work in the 1930s resulted in a rechargeable nickel–zinc railroad battery utilizing standard Edison tubular or Jungner pocket nickel positives and electrodeposited zinc negatives. Cells were constructed utilizing physical separations between the plates and containing a large excess of KOH electrolyte. This Drumm battery exhibited a limited life caused by negative shape change and premature short circuits. Shape change is a phenomenon caused by zinc replating in a nonuniform manner during charge and resulting in a loss of negative capacity. Short circuits resulted from zinc dendrites formed during discharge that grew perpendicular to the face of the negative electrode until electrical contact was made with the positive. In the late 1950s and 1960s interest in the nickel–zinc system was again aroused as a possible substitute for silver–zinc batteries (71–75). By then the technology of nickel and zinc electrodes was well developed and led to a higher energy density nickel–zinc battery having tightly packed

electrodes, barrier separators, and limited electrolyte. Most of this work related to vented batteries for low to medium rate applications, such as portable military communication applications.

Some efforts toward sealed battery development (76) were made. However, a third electrode, an oxygen recombination electrode was required to reduce the cost of the system. High rate applications such as torpedo propulsion were investigated (77) and moderate success achieved using experimental nickel–zinc cells yielding energy densities of 35 $W \cdot h/kg$ at discharge rates of 8 C. A commercial nickel–zinc battery is considered to be a likely candidate for electric bicycle development in China. Activity continues in electric vehicle design in several parts of the world (78,79). If the problems of limited life and high installation cost are solved, a nickel–zinc EV battery could provide twice the driving range for an equal weight lead–acid battery. Work is developmental; there is only limited production of nickel–zinc batteries.

Reaction Mechanism. The overall reactions in the nickel–zinc cell can be represented by

$$2\ NiOOH + Zn + 2\ H_2O \rightleftharpoons 1\,2\ Ni(OH)_2 + Zn(OH)_2 \qquad E^\circ = +1.73\ V$$

Alternatively the discharged state of the zinc electrode is represented as ZnO.

Cell Construction. Nickel–zinc batteries are housed in molded plastic cell jars of styrene, SAN, or ABS material for maximum weight savings. Nickel electrodes can be of the sintered or pocket type, however, these types are not cost effective and several different types of plastic-bonded nickel electrodes (78–80) have been developed.

Nickel hydrate, usually 5–10% cobalt added, serves as the active material and is mixed with a conductive carbon, eg, graphite. The active mass is mixed with an inert organic binder such as polyethylene or poly(tetrafluoroethylene) (TFE). The resultant mass is rolled into sheets on a compounding mill or pressed into electrodes as a dry powder on a nickel grid. The resultant electrodes offer a high energy density and low cost of fabrication. In performance, the plastic-bonded electrodes can support rates up to C/2, discharge capacity in 2 h, at voltages equivalent to those of sintered electrodes, but at higher rates some derating occurs. Life of plastic-bonded electrodes has not been fully evaluated, but a life of 500 cycles appears attainable.

Negative electrodes are fabricated of zinc oxide by any of the methods (pasting, pressing, etc) described. Binders, usually TFE, are used to reduce the solubility of the electrode in KOH. In addition, other techniques such as extended edges, inert extenders, contouring, and variable density have been tried in an effort to reduce shape change of the negative electrode upon cycling. The electrolyte is KOH, usually a 30–35% aqueous solution with the addition of LiOH at a level of 10–25 g/L to enhance nickel capacity throughout life.

Separators are both of the organic and inorganic type. During the 1960s most cells were built using cellophane or FSC (fibrous sausage casing) separators. Developments by NASA (81) and others in the area of inorganic films, consisting of a layered or film structure of a heavy metallic oxide such as zirconia, ZrO_2, or magnesia, MgO, bonded by an inert organic film and often layered with an organic resin-impregnated asbestos mat led to use of these materials as

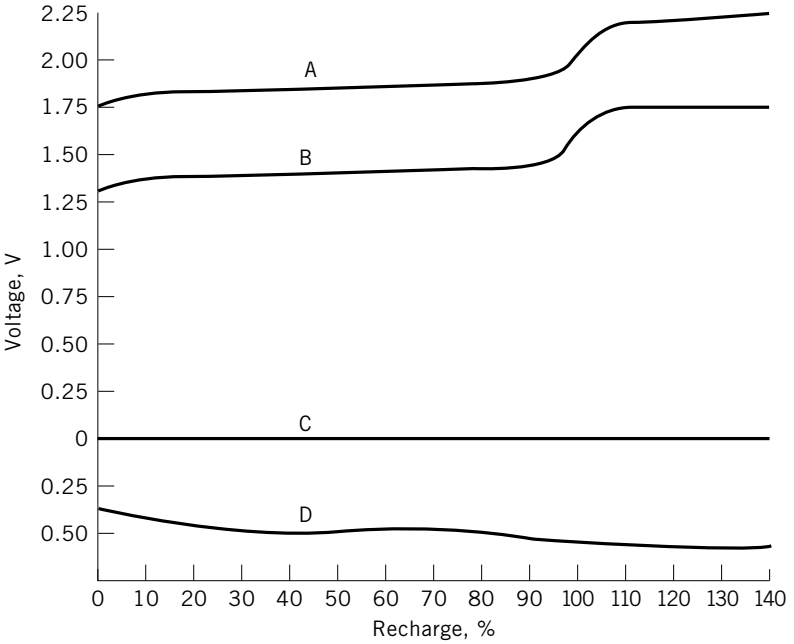

Fig. 13. Nickel–zinc electrode potential on charge A, the Ni–Zn cell; B, the Zn vs Hg ref.; C, the Hg–HgO ref.; and D, the Ni vs Hg ref.

separators. In Ni–Zn electric vehicle batteries (82), over 800 cycles at 50% depth are claimed for these inorganic separators. Drawbacks are the relatively high cost of manufacture and the increased resistance per layer, which in effect limits discharge rate.

Performance. The limited life of nickel–zinc batteries is the principal drawback to widespread use. Normally the nickel cathode is not a factor. Even plastic-bonded nickel electrodes perform for a greater number of cycles than either the zinc counter electrodes or the separator used and to a great extent it is the zinc electrode that limits the life of a nickel–zinc cell. In order to charge nickel electrodes sufficiently, a discreet amount of overcharge is necessary. Unfortunately, overcharge is not desirable for the zinc electrodes, as it promotes dendritic growth which will eventually penetrate the separator and cause short circuits. This can be alleviated somewhat by an overdesign in zinc capacity, but that reduces energy density. Typical cell and electrode voltage curves are shown in Figure 13 and cycle life data as a function of depth of discharge in Figure 14.

Nickel–zinc batteries containing a vibrating zinc anode has been reported (83). In this system zinc oxide active material is added to the electrolyte as a slurry. During charge the anode substrates are vibrated and the zinc is electroplated onto the surface in a uniform manner. The stationary positive electrodes (nickel) are encased in a thin, open plastic netting which constitutes the entire separator system.

The vibration serves a dual purpose. First, a macroturbulence is created which keeps the ZnO uniformly dispersed in the electrolyte. Second, the microturbulence created at the surface of the negative electrode minimizes the zincate

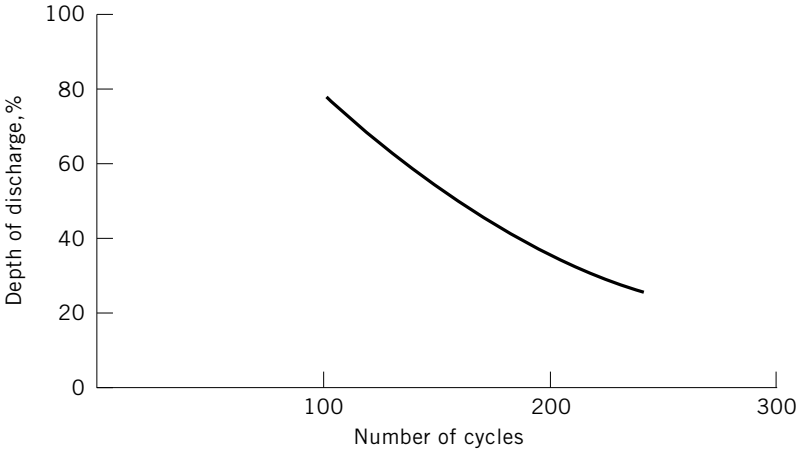

Fig. 14. Cell performance as a function of the number of cell recharge cycles.

concentration gradients, discouraging the formation of zinc dendrites and causing a uniform deposit of zinc. Any zinc dendrites that may form are brushed off against the plastic netting by the vibratory motion. Thus the problems of shape change, dendritic shorting, and separator failure are in theory solved by this system; the zinc electrode dissolves during discharge, replates during charge, and no separator is required. A disadvantage is reduced energy density, especially on a volume basis, as a result of the increased electrode spacing and the quantity of electrolyte required. The vibration hardware imposes an additional 5% weight penalty as well as increased cost. Alternatively, similar benefits have been reported from experiments in which the electrolyte is pulsed.

1.5. Nickel–Hydrogen Cells. There are two types of nickel–hydrogen cells; those that employ a gaseous H_2 electrode and those that utilize a metal hydride, MH.

Gaseous Hydrogen Systems. The nickel–hydrogen cell incorporating a gaseous hydrogen electrode is a hybrid consisting of one gaseous and one solid electrode. The nickel electrode is of the type used in a nickel–cadmium battery and the hydrogen electrode is a gas diffusion electrode of the type used in alkaline fuel cells (qv). These two electrodes are capable of extremely long, stable life. This system was developed to serve as a long life, lightweight battery for satellite applications that would be superior to the aerospace nickel–cadmium batteries (84–86).

The couple has a theoretical energy density of 172 $W \cdot h/kg$ and complete cells are capable of delivering $55 - 66$ $W \cdot h/kg$. The cell reaction is

$$NiOOH + \frac{1}{2} H_2 \rightleftharpoons Ni(OH)_2$$

However, the generation and migration of water in the half-cell reactions must be considered in the cell design. At the nickel electrode:

$$NiOOH + H_2O + e^- \rightleftharpoons Ni(OH)_2 + OH^-$$

and at the hydrogen electrode:

$$\frac{1}{2}\,H_2 + OH^- \rightleftharpoons H_2O + e^-$$

During charge the nickel hydroxide is converted to NiOOH, the charged state of nickel, and on the surface of the hydrogen electrode, hydrogen gas is evolved. By placing the electrode stack in a sealed container, the hydrogen is captured for subsequent reuse. During discharge the same hydrogen is reconsumed on the same electrode surface and the nickel electrode is reduced to provide electric energy.

Another desirable feature of this battery system is its capability of high rate of overcharge. During overcharge oxygen gas is generated on the surface of the nickel electrode. Simultaneously hydrogen continues to be evolved on the surface of the hydrogen electrode. Because there is a large area of catalyzed hydrogen electrode and ready access of the oxygen to diffuse to that surface, the oxygen readily recombines within the cell to form water and the cell pressure remains constant.

The primary packaging arrangements for this chemistry has been single cylindrical cells as shown in Figure 15, where a stack of disk electrodes are placed within a cylindrical outer housing having domed end caps. The housing

Fig. 15. Cutaway view of a typical construction of a nickel–hydrogen cell.

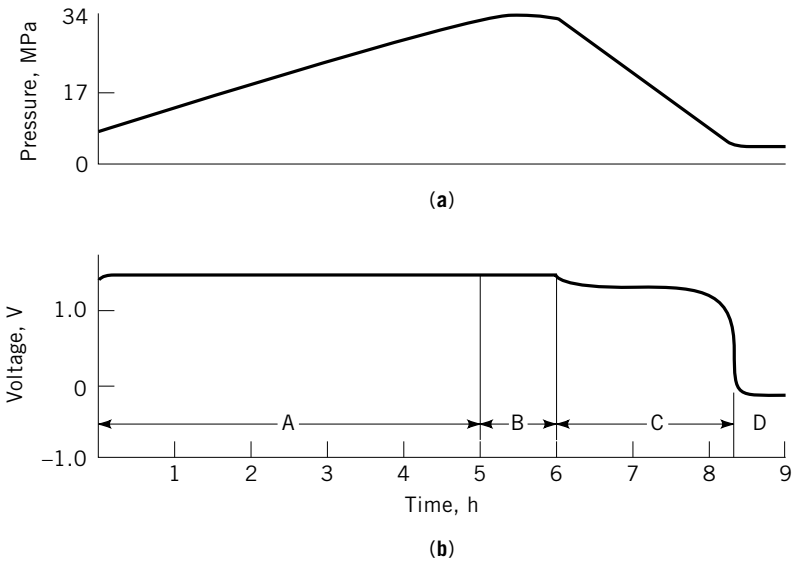

Fig. 16. 50 A·h nickel–hydrogen performance showing (**a**) pressure and (**b**) voltage curves where region A represents charging at 10 A, region B represents overcharge at 10 A, region C represents discharge at 25 A, and region D represents reversal at 25 A. To convert MPa to psi, multiply by 145.

also serves as a lightweight pressure vessel for hydrogen containment with all the free volume inside the housing used for hydrogen storage. Two insulated feed throughs are provided in the cell housing for electric contact to the positive and negative electrodes. The electrode stack is a repeating sequence of sintered nickel, absorber separator, typically asbestos, or other inorganic stable materials, teflon bonded platinum black fuel cell-type electrodes, and gas spacers. The electrolyte is typically 30–35% KOH with a LiOH additive for the nickel electrode.

Figure 16 shows a typical charge–discharge voltage and pressure profile for a50 A·h cell. In this design the cell is precharged at 517 kPa (75 psi) hydrogen and the operating pressure range is from 517 to 4100 kPa (75–600 psi). Monitoring cell pressure, which is typically done with pressure transducers, enables the user to follow the cells state of charge. This is an additional desirable feature of this system. Figure 17 shows cell discharge characteristics as a function of rate, demonstrating the high rate capability of this battery. Figure 18 gives open circuit stand characteristics. This cell exhibits a greater self-discharge than the nickel–cadmium chemistry because of the reaction of pressurized hydrogen with the active nickel material.

Because this battery is only produced for special satellite applications, production quantities are limited. Rigorous quality inspections, expensive light-weight housing and seals, and the use of high loading platinum hydrogen electrodes all make this type of battery very expensive. For typical satellite applications multiple single-cells are connected in series and are packaged in an egg crate mounting. In this arrangement the waste heat generated during discharge

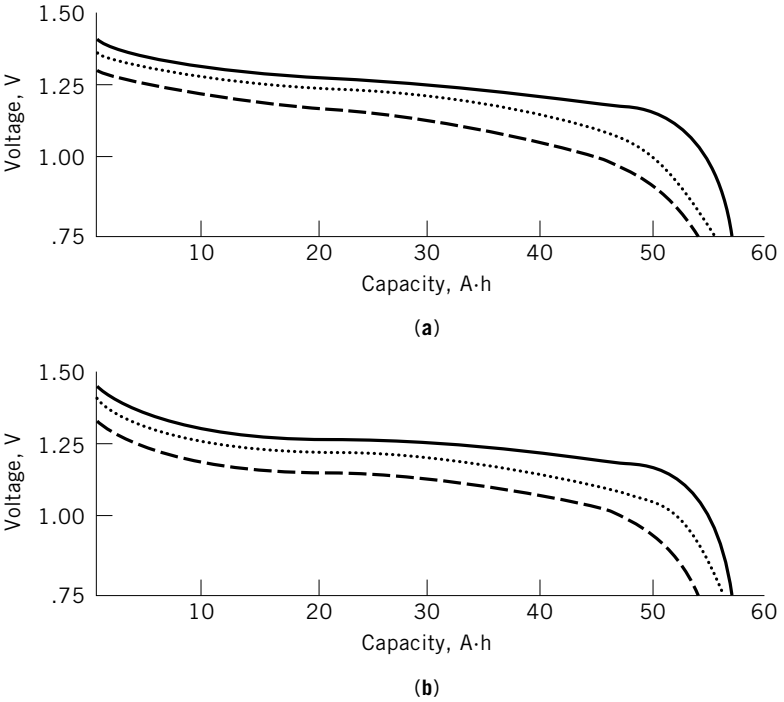

Fig. 17. Discharge characteristics for 50 A · h nickel–hydrogen batteries at (—) 10 A, (· · ·) 25 A, and (– – –) 50 A at (**a**) 20°C and (**b**) 0°C.

and overcharge is conducted from the stack out the cylinder wall through conduction rings to a radiator plate of the satellite.

Limited development efforts have been undertaken to develop a lower cost battery for terrestrial use utilizing reduced catalyst quantities and multicell

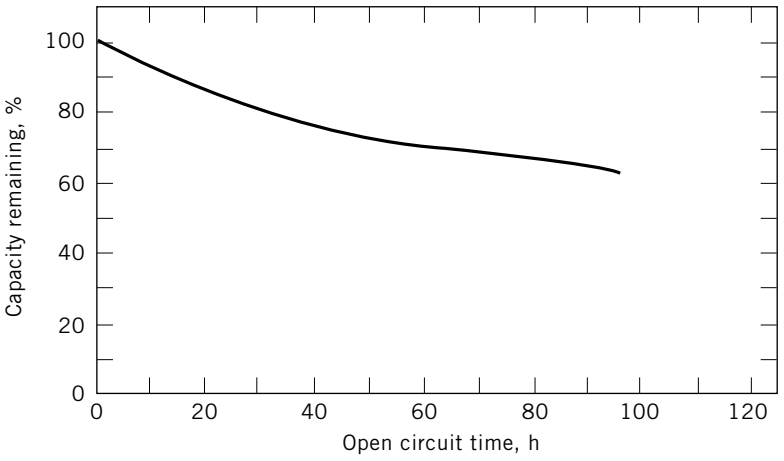

Fig. 18. Self-discharge at ambient temperatures for a 35 A · h cell, NTS-2 prototype Sanyo Electric Co. cell.

packaging. Multicell common pressure vessel arrangements have also been considered for aerospace applications, but these configurations have not found market acceptance.

Metal Hydride Systems. The success of the gaseous nickel–hydrogen system led to the investigation of replacing the gaseous hydrogen with metal hydrides in order to reduce the cell pressure and the volume required for hydrogen storage. A number of metal hydrides were developed for reversible hydrogen storage. Of particular interest were $LaNi_5$ and $MmNi_5$ (Misch metal [8049-20-5]) the isotherms of which are shown in Figures 19 and 20, and FeTi. In the initial efforts these materials were packed into the free volume of standard nickel hydrogen cells using standard catalyzed gas diffusion hydrogen electrodes. The metal hydrides absorb up to one hydrogen atom per metal atom and cells incorporating hydrides could be fabricated that were more compact than gas pressure cells. However these hydrides deactivated upon repeated deep-cycling and

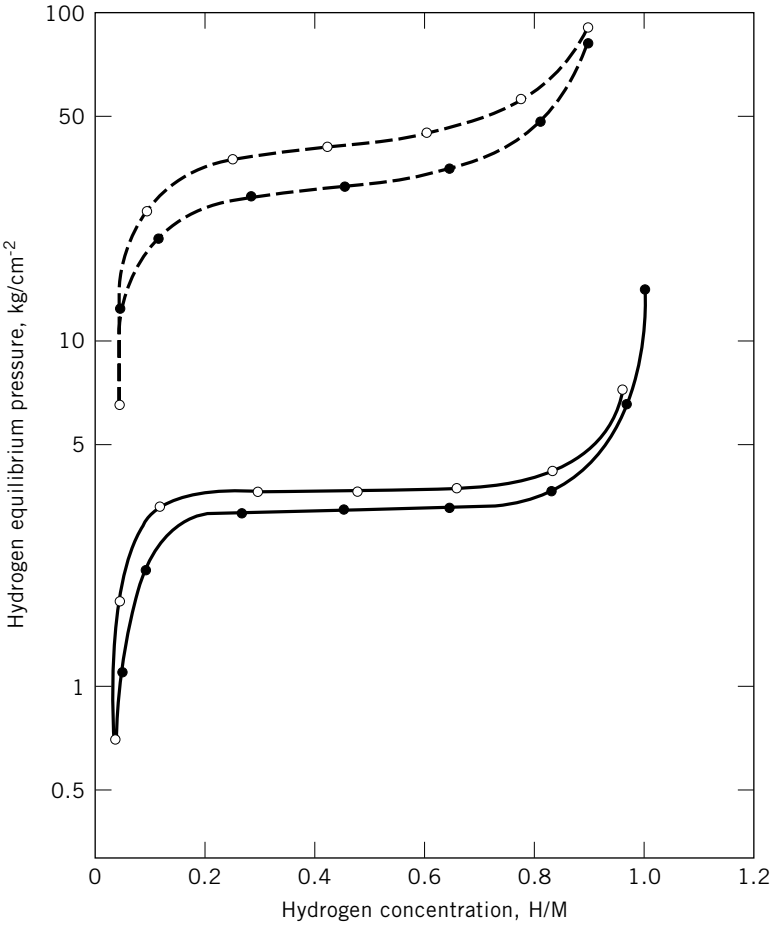

Fig. 19. Pressure concentration curves of $MmNi_5$ (---) and $LaNi_5$ (—) at 45°C where open circles denote absorption and closed circles desorption of hydrogen. H/M represents the ratio in the hydride of the mole fraction of hydrogen to the mole fraction of the metal.

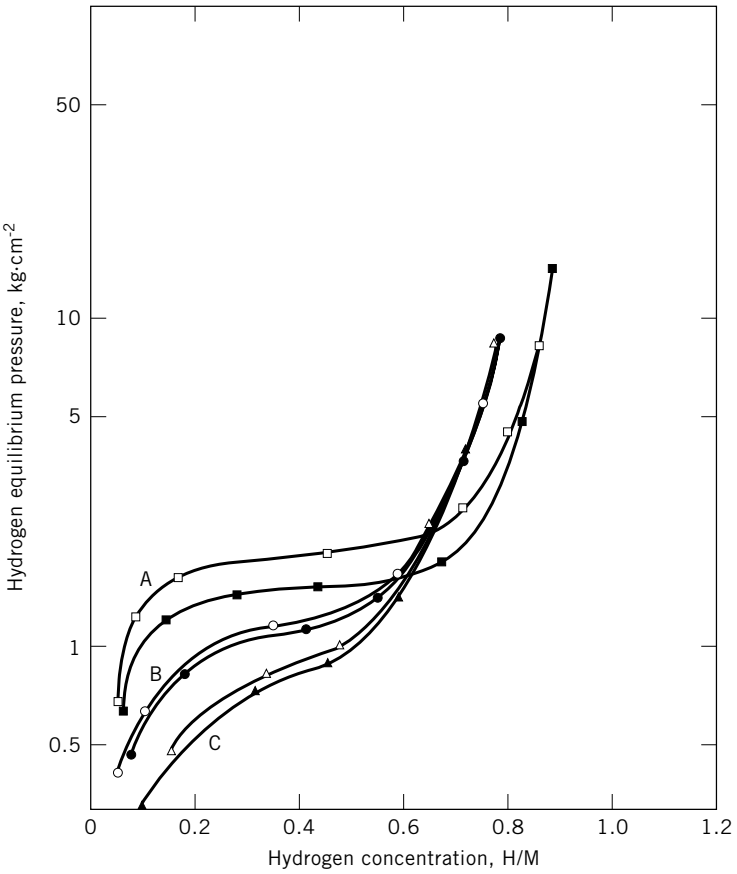

Fig. 20. Pressure constant temperature (PCT) curves of $MmNi_5$ alloy system where open symbols represent absorption and closed symbols represent desorption for A, $MmNi_{4.3}Mn_{0.4}Al_{0.3}$; B, $MmNi_{3.8}Mn_{0.4}Al_{0.3}Co_{0.5}$; and C, $MmNi_{3.5}Mn_{0.4}Al_{0.3}Co_{0.75}$. H/M represents the ratio in the hydride of the mole fraction of hydrogen to the mole fraction of the metal.

gradually lost their hydrogen absorption ability presumably because of attack on the hydrides by water vapor or oxygen gas within the cell environment. Newer, more complex alloys have resolved most of these problems.

An alternative approach utilizes the hydride material as the hydrogen electrode. In this case, as the hydrogen is generated on the hydrogen electrode, it enters the hydride lattice for storage. On discharge the hydrogen leaves the hydride for reaction. The cell reactions are essentially the same as gaseous nickel hydrogen cells.

$$Ni(OH)_2 + OH^- \rightleftharpoons NiOOH + H_2O + e^-$$

$$M + H_2O + e^- \rightleftharpoons MH + OH^-$$

and overall

$$Ni(OH)_2 + M \rightleftharpoons NiOOH + MH$$

The overcharge reactions for the cell are the same as for nickel–cadmium and nickel–hydrogen cells. The oxygen generated on the nickel electrode at the end of charge and overcharge finds its way to the anode and reacts to form water in the Ni–H_2 case and $Cd(OH)_2$ in the Ni–Cd case.

A critical issue is the stability of the hydride electrode in the cell environment. A number of hydride formulations have been developed. Most of these are Misch metal hydrides containing additions of cobalt, aluminum, or manganese. The hydrides are prepared by making melts of the formulations and then grinding to fine powers. The electrodes are prepared by pasting and or pressing the powders into metal screens or felt. The additives are reported to retard the formation of passive oxide films on the hydrides.

A number of manufacturers started commercial production of nickel–MH cells in 1991 (31–35). The initial products are "AA"-size, "Sub-C", and "C"-size cells constructed in a fashion similar to small sealed nickel–cadmium cells. Ovonics also delivered experimental electric vehicle cells, 22 A · h size, for testing. The charge–discharge of "AA" cells produced in Japan (Matsushita) are compared in Figure 21.

From these data, the hydride cells contain approximately 30–50% more capacity than the Ni–Cd cells. The hydride cells exhibit somewhat lower high rate capability and higher rates of self-discharge than nickel–cadmium cells. Life is reported to be 200–500 cycles. Though not yet in full production it has been estimated that these cells should be at a cost parity to nickel–cadmium cells on an energy basis.

Several manufacturers were using nickel-metal hydride batteries to power their gasoline-electric hybrid and pure electric vehicles for 2004 and 2005 models. In the first quarter of 2002, more than 41,300 hybrid automobiles were operating on U.S. highways. An additional 5,200 battery electric automobiles, vans, and

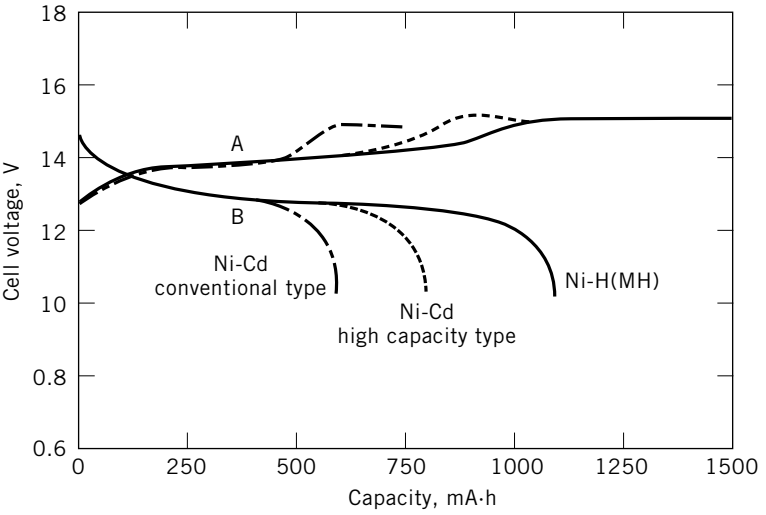

Fig. 21. Charge A and discharge B curves of (—) a Ni–H(MH) cell employing $MmNi_{3.55}Mn_{0.4}Al_{0.3}Co_{0.75}$ alloy compared with those of (——–) conventional and (- - -) high capacity types of Ni–Cd cells (88).

light trucks were leased or sold. One Japanese-based automobile manufacturer was ramping up operations to produce 300,000 hybrid vehicles by 2007 (89).

1.6. Other Cell Systems. *Silver–Hydrogen Cells.* With the development of the nickel–hydrogen system limited attention was directed to the development of a silver–hydrogen cell (89,90). The main characteristics of interest were the potential for a higher gravametric energy density based on the ligher weight of the silver electrode vs that of the nickel. The cell reactions for this couple are

Hydrogen electrode

$$2\,H_2O + 2\,e^- \rightleftharpoons H_2 + 2\,OH^-$$

Silver electrode

$$Ag + OH^- \rightleftharpoons \frac{1}{2}\,Ag_2O + \frac{1}{2}\,H_2O + e^-$$

$$\frac{1}{2}\,Ag_2O + OH^- \rightleftharpoons AgO + \frac{1}{2}\,H_2O + e^-$$

Overall reaction

$$H_2 + AgO \rightleftharpoons Ag + H_2O$$

The packaging approach utilized for this battery is similar to that for nickel–hydrogen single cylindrical cells as shown in Figure 22. The silver electrode is typically the sintered type used in rechargeable silver–zinc cells. The hydrogen electrode is a Teflon-bonded platinum black gas diffusion electrode.

Because the silver oxide electrode is slightly soluble in the potassium hydroxide electrolyte the separator is of a barrier type to minimize silver diffusion to the opposite electrode. Figure 23 shows a charge–discharge profile of a 25 $A \cdot h$ cell that exhibits the two voltage plateaus seen for silver electrodes in the silver–zinc battery system. The silver–hydrogen cell exhibits a lower self-discharge than nickel–hydrogen cells as a result of the slower rate of reaction of hydrogen with silver oxide. The actual cells do not exhibit substantial differences in energy density when compared to those of nickel–hydrogen. Therefore this system is not being actively pursued.

Zinc–Oxygen Cells. On the basis of reactants the zinc–oxygen or air system is the highest energy density system of all the alkaline rechargeable systems with the exception of the $H_2 \cdot O_2$ one. The reactants are cheap and abundant and therefore a number of attempts have been made to develop a practical rechargeable system. The reactions of this system are as follows:

Zinc electrode

$$Zn + 2\,OH^- \rightleftharpoons Zn(OH)_2 + 2\,e^-$$

Oxygen electrode

$$\frac{1}{2}\,O_2 + H_2O + 2\,e^- \rightleftharpoons 2\,OH^-$$

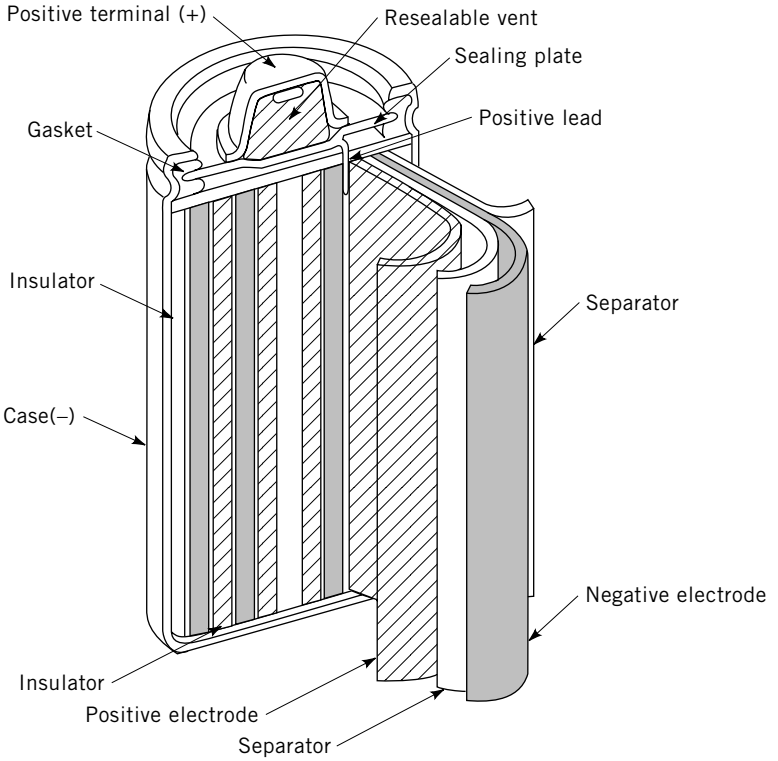

Fig. 22. Schematic diagram of Ni–H(MH) cell (88).

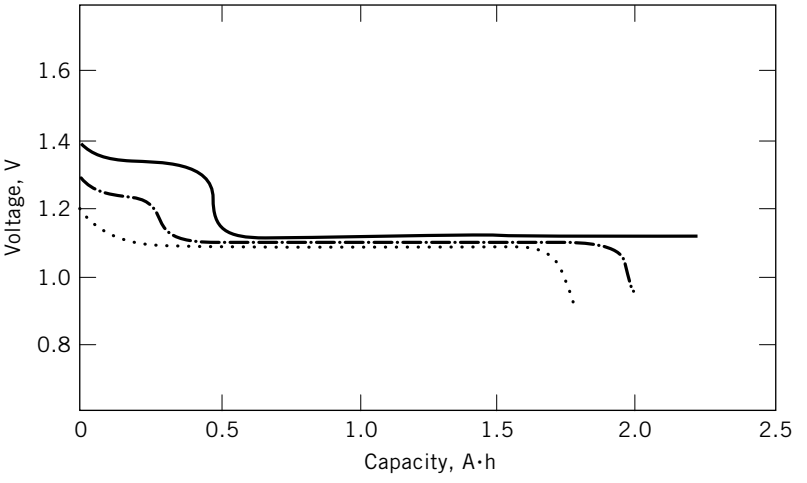

Fig. 23. Silver–hydrogen cell discharge characteristics where (···) represents a 0.5 h rate at 4 A or 80 mA/cm^2; (—·—) represents a 1 h rate at 2 A; and (—) represents a 4 h rate at 0.5 A or 10 mA/cm^2.

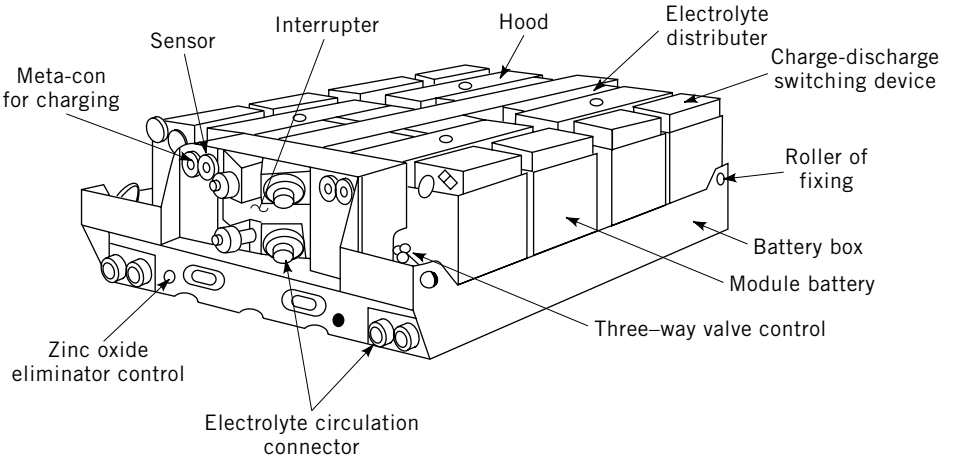

Fig. 24. Zinc–air 124-V battery system. Meta-con is a connector.Courtesy of Sanyo Electric Co.

Overall reaction

$$Zn + H_2O + \frac{1}{2}\,O_2 \rightleftharpoons Zn(OH)_2$$

In open cycle systems the oxygen reactant is released into the surrounding air during charge, and during the subsequent discharge oxygen from the surrounding air is consumed on a fuel cell-type electrode. The oxygen is delivered by forced or free confection depending on the system design. Whereas the zinc–oxygen cell has significant potential, it also has a number of inherent problems. First is the poor rechargeability of the normal zinc electrode; then there is the poor stability of the oxygen electrode when used in a bifunctional, ie, charge and discharge mode, contamination of the electrolyte by carbon dioxide from the air when used as an open cycle system, and poor retention of energy efficiency because of the irreversibility of the oxygen electrode reaction.

The system shown in Figure 24, in which the electrolyte was circulated through a multicell stack to improve the rechargeability of the zinc electrode has been studied by Sanyo Electric. However, such circulating systems are prone to electrolyte leakage and have common manifolds that cause internal self-discharge. Systems in which zinc particles or zinc-coated beads are circulated through the electrode stack and are utilized as a fluidized electrode have also been investigated by many organizations. In these systems the zinc particles contact the anode current collector to undergo reaction. In order to dissolve all the reaction product during discharge, it is necessary to use relatively large quantities of electrolyte so that a zincate solubility of approximately 200 g/L is not exceeded. The CGE (91) (Fig. 25) system utilized a tubular cell and a separate regeneration stack to deposit new zinc particles from the discharged electrolyte, which is saturated with dissolved zincate. By utilizing a separate regeneration stack the stability problem of the bifunctional oxygen electrode is avoided and regeneration can be carried out at any location so that the battery can be refueled

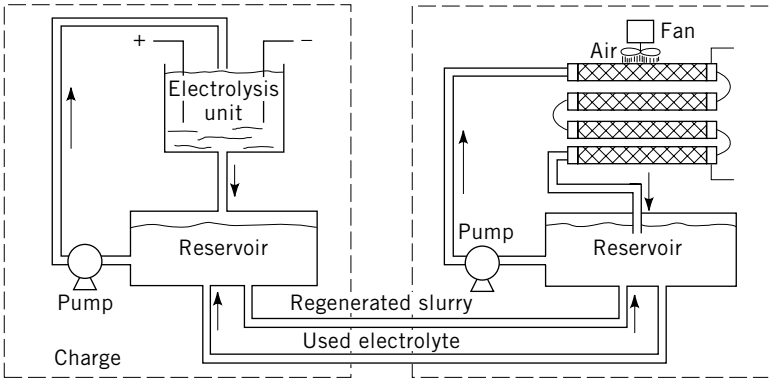

Fig. 25. Schematic diagram of the separate charge and discharge modules of the Générale d'Electricité circulating zinc–air battery (91).

rapidly. A sealed system in a configuration similar to single cylindrical gaseous nickel–hydrogen cells has also been studied (92).

Iron–Air Cells. The iron–air system is a potentially low cost, high energy system being considered mainly for mobile applications. The iron electrode, similar to that employed in the nickel–iron cell, exhibits long life and therefore this system could be more cost effective than the zinc–air cell. Reactions include:

Iron electrode

$$\mathrm{Fe} + 2\ \mathrm{OH}^- \rightleftharpoons \mathrm{Fe(OH)_2} + 2\ e^-$$

Oxygen electrode

$$\frac{1}{2}\ \mathrm{O_2} + \mathrm{H_2O} + e^- \rightleftharpoons 2\ \mathrm{OH}^-$$

Overall reaction

$$\mathrm{Fe} + \frac{1}{2}\ \mathrm{O_2} + \mathrm{H_2O} \rightleftharpoons \mathrm{Fe(OH)_2}$$

In the experimental systems studied the iron electrode has been of the sintered type and the oxygen–air electrodes have been of the bifunctional type.

A system as shown in Figure 26, which incorporates circulating electrolyte for thermal management and removal of gases generated during charge, has been developed (93). The iron electrode has a low hydrogen overvoltage and therefore the electrode evolves hydrogen during charge and to some extent during open circuit stand. A similar system, where the primary emphasis is on the development of a stable bifunctional air electrode is under investigation (94). A Teflon-bonded formulation consisting of a carbon-base, catalyzed with silver and other additives, is reported to be stable for up to 500 cycles. Because of the inefficiency of the iron electrode, and the irreversibility of the oxygen electrode, this system exhibits recharge energy efficiencies of less than 50%.

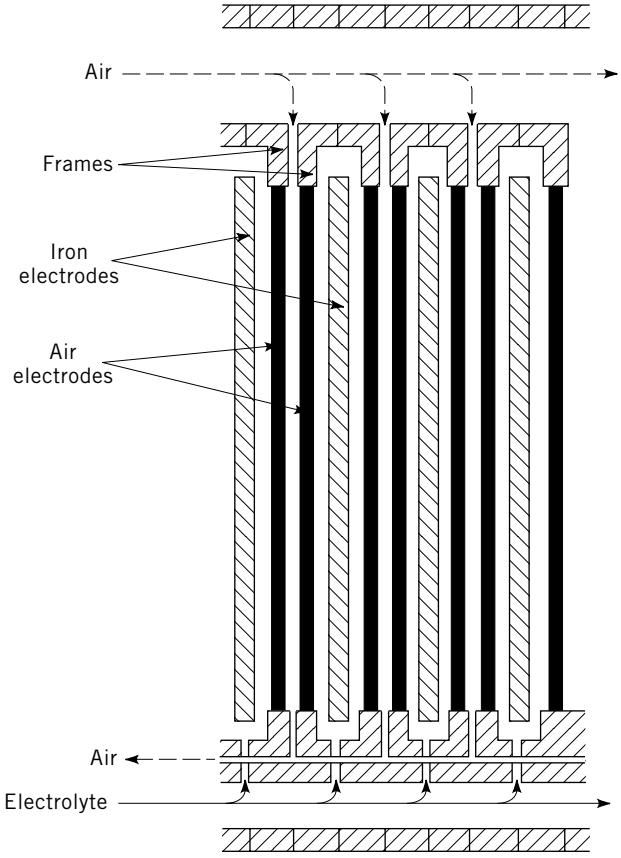

Fig. 26. Cross-section of SNDC iron–air battery pile (93).

Hydrogen–Oxygen Cells. The hydrogen–oxygen cell can be adapted to function as a rechargeable battery, although this system is best known as a primary one (see FUEL CELLS). The electrochemical reactions involve:

Electrodes

$$H_2 + 2\,OH^- \rightleftharpoons 2\,H_2O + 2\,e^-$$

$$\frac{1}{2}\,O_2 + H_2O + 2\,e^- \rightleftharpoons 2\,OH^-$$

Overall

$$H_2 + \frac{1}{2}\,O_2 \rightleftharpoons H_2O$$

During charge, water is electrolyzed to produce hydrogen and oxygen which are stored as pressurized gas. During discharge those gases electrochemically react to produce water. The reactants have a theoretical energy content of 770 $W \cdot h/kg$and the interest that has been directed at this system has been

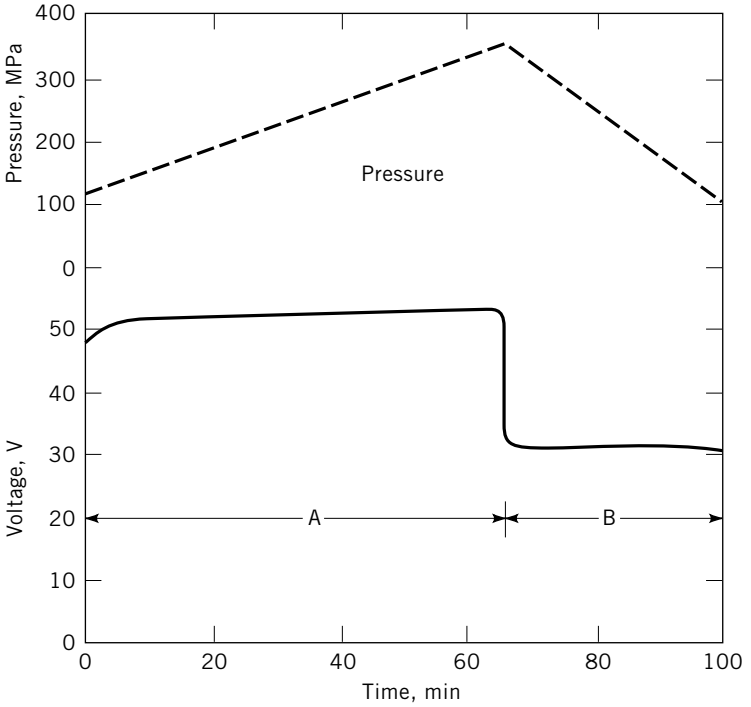

Fig. 27. Cycle of 34-cell regenerative hydrogen–oxygen fuel cell where A represents the charging region at 10 A, B represents discharging at 18.2 A. Both (—) voltage and (- - -) pressure changes are shown. To convert MPa to psig, multiply by 145.

primarily for light batteries for military and/or aerospace applications. In the 1960s a multicell bipolar stack contained inside a cylindrical pressure vessel was studied (95). The stack was internally manifolded to feed hydrogen and oxygen to separate compartments within the pressure vessel at operating pressures that ranged between 0.7 and 2.4 MPa (100–350 psi). Figure 27 shows a charge–discharge profile of the system.

Because of cross-gas leakage and other complexities, a single-cell was developed. In this configuration the electrodes were constructed in the form of a cylinder; the hydrogen gas was stored in the central compartment, and the oxygen gas in the space between the electrode core and the outer pressure vessel. These two compartments were sized in a two to one volume ratio to maintain the two gases at the same pressure as they are generated during charge. A flexible bellows was placed between the two compartments to compensate for slight differences in the compartments' volume and temperature effects. This system was not pursued however; it was dropped in favor of the simpler single-gas nickel–hydrogen system.

As primary alkaline fuel cells were developed for space applications, consideration was given to separate stack rechargeable designs. In these approaches, the product water formed during the discharge of a primary fuel cell is stored, then fed to a separate electrolizer stack during charge. The hydrogen and oxygen gas generated during charge is stored in separate pressure vessels. This

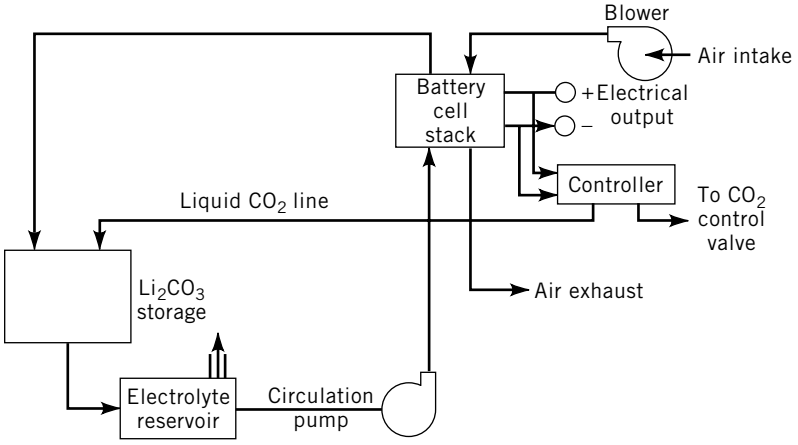

Fig. 28. Schematic of lithium–air automotive propulsion system.

approach overcomes the stability problem of the bifunctional oxygen electrode and the respective stacks can be optimized for their function. This system is still rather complex and bulky and has not yet been applied.

Mechanically Rechargeable Batteries. To avoid the time required for electric recharge, the problems of *in situ* electric recharge, or to utilize anodes that are not electrically rechargeable in aqueous electrolytes, mechanically rechargeable batteries have been studied. These systems are metal–air couples. The anodes that have received attention are zinc, lithium, and aluminum (97–99). Mechanically rechargeable zinc–air batteries were developed for military portable electronic equipment in the 1970s. These batteries were never deployed because of difficulties of leakage, problems of repeatedly replacing the anodes, and the development of lithium primary batteries having superior performance.

Lithium as an anode in alkaline electrolyte has been considered in the battery system shown in Figure 28. Even though lithium reacts directly with water, it was possible to operate the battery because of a protective lithium hydroxide film that forms on the anode. However, the film was not totally protective and units exhibited poor efficiency and were very complex.

The most significant results with these battery types focus on aluminum as the anode. Figure 29 shows an aluminum–air cell being developed for electric vehicle applications. The aluminum hydroxide reaction product would be returned to the factory to be reprocessed into fresh aluminum anodes. One set of anodes could yield up to 500 miles range before replacement. However, the corrosion reaction of the aluminum with the electrolyte is still a problem. Additionally, the system is complex and it is anticipated that replacing the anodes repeatedly will be as problematic as the zinc systems. The system has poor energy efficiency when consideration is given to the full cycle of electric generation, aluminum production, battery efficiency, and reprocessing of the battery reaction product back to aluminum.

1.7. Electrolyte. Potassium hydroxide is the principal electrolyte of choice for the above batteries because of its compatibility with the various electrodes, good conductivity, and low freezing point temperature. Potassium

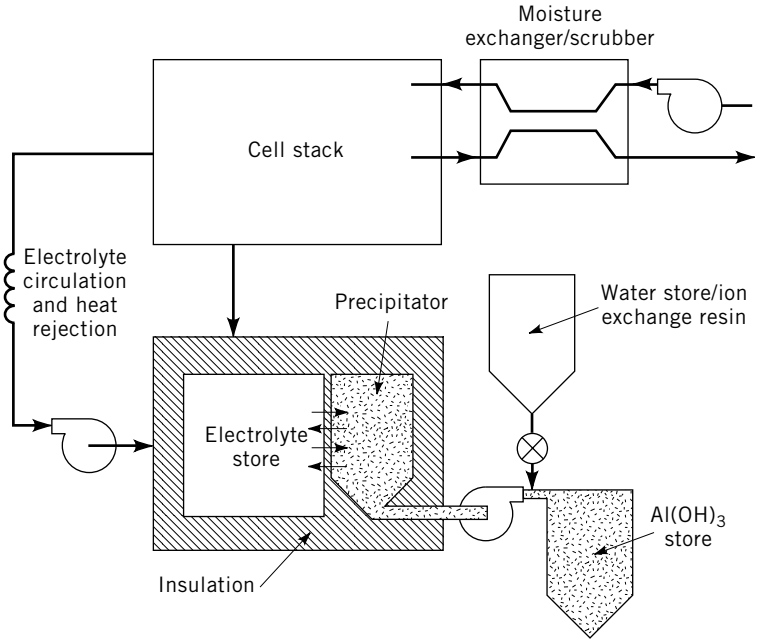

Fig. 29. Aluminum–air power cell system. The design provides for forced convection of air and electrolyte, heat rejection, electrolyte concentration control via $Al(OH)_3$ precipitation, and storage for reactants and products.

hydroxide is a white crystalline substance having a mol wt = 56.10; density = 2.044 g/mL, and mp = 360°C (see POTASSIUM COMPOUNDS). It is hygroscopic and very soluble in water. The most conductive aqueous solution at 25°C is at 27% KOH, but the conductivity characteristics are relatively flat over a broad range of concentrations.

The characteristics for aqueous KOH (97–99) solutions vary somewhat for battery electrolytes when additives are used. Furthermore, potassium hydroxide reacts with many organics and with the carbon dioxide in air to form carbonates. The build-up of carbonates in the electrolyte is to be avoided because carbonates reduce electrolyte conductivity and electrode activity in some cases.

1.8. Health and Safety Factors. The potassium hydroxide electrolyte used in alkaline batteries is a corrosive hazardous chemical. It is a poison and if ingested attacks the throat and stomach linings. Immediate medical attention is required. It slowly attacks skin if not rapidly washed away. Extreme care should be taken to avoid eye contact that can result in severe burns and blindness. Protective clothing and face shields or goggles should be worn when filling cells with water or electrolyte and performing other maintenance on vented batteries.

Alkaline batteries generate hydrogen and oxygen gases under various operating conditions. This can occur during charge, overcharge, open circuit stand, and reversal. In vented batteries free ventilation should be provided to avoid hydrogen accumulations surrounding the battery. A vented battery must never be placed in a sealed container for which it was not designed. As a result of

operation, hydrogen–oxygen mixtures that are flammable or explosive can exist in the cells' head space. Ignition of this mixture, which is rare, can result in blowing off cell lids. This can occur from internal short circuits or external sparks that propagate back into the cell housing.

Alkaline batteries are capable of high current discharges and accidental short circuits should be avoided. Short circuiting can result in significant heat generation, electrolyte boiling, and cell rupture. High voltage cell strings also present an electric shock hazard; therefore tools should be insulated and operators should not wear rings.

Spontaneous low resistance internal short circuits can develop in silver–zinc and nickel–cadmium batteries. In high capacity cells heat generated by such short circuits can result in electrolyte boiling, cell case melting, and cell fires. Therefore cells that exhibit high resistance internal short circuits should not continue to be used. Excessive overcharge that can lead to dry out and short circuits should be avoided.

The European Union is evaluating a proposal to ban all NiCd batteries containing more then 0.002% cadmium by Jan. 1, 2008 and to increase collection rate for all spent industrial and automotive batteries to 95% by weight by Dec. 31, 2003. Some cadmium experts said that the proposal fails to differentiate between the different forms of cadmium with disparate toxicity and does not address the environmental effects of replacements (48).

1.9. Recycling. The most difficult aspect of NiCd battery recycling is collection of spent batteries. Although large industrial batteries, containing 20% cadmium are easy to collect and are recycled at the rate of 80%, the smaller NiCd batteries are usually discarded by the public. Thus, voluntary industry-sponsored collection programs and government agency programs are being devised to improve collection of these smaller batteries.

The most successful recycling program is operated by the Rechargeable Battery Recycling Corp. (RBRC) of Atlanta, Ga. RBRC was supported by more than 285 manufacturers and has a network of 26,000 collection centered across the United States and Canada. The RBRC recycling program contains several key elements that are specified in EPA regulations, Federal law, and in various state laws. These elements include uniform battery labeling, removability from appliances, a national network of collection systems, regulatory relief to facilitate battery collection, and widespread publicity to encourage public participation. Another successful program is run by INMETCO (a subsidiary of International Nickel). INMETCO's has a prepaid container program where companies purchase containers for collection and shipment of spent batteries. Because most of the industrial NiCd batteries are not allowed to be discarded in municipal dumps, they are recycled through collection programs (48,89).

2. Lead Acid Cells

The lead–acid battery is one of the most successful electrochemical systems and the most successful storage battery developed. About 87% of the lead [7439-92-1] (qv), Pb, consumption in the United States was for batteries in 2001.

The lead–acid battery consists of a number of cells in a container. These cells contain positive (PbO_2) and negative (Pb) electrodes or plates, separators to keep the plates apart, and sulfuric acid [7664-93-9], H_2SO_4, electrolyte. The battery reactions are highly reversible, so that the battery can be discharged and charged repeatedly. The number of charge–discharge cycles that can be obtained depends strongly on the use mode and can vary from several hundred to thousands of cycles.

Each cell has a nominal voltage of 2 V and capacities typically vary from 1 to 2000 ampere-hours. Lead–acid cells can be operated with coulombic efficiencies as high as 95% and with energy efficiencies greater than 80%. The many cell designs available for a wide variety of uses can be divided into three main categories: automotive, industrial, and consumer. Shipments of lighting and ignition (SLI) for cranking of internal combustion engines in North America totaled $10^6 \times 10^6$ units in 2001 (100). Industrial batteries are used for heavy-duty application such as motive and standby power. More recently, the use of batteries for utility peak shaving has been increasing. Consumer batteries for emergency lighting, security alarm systems, cordless convenience devices and power tools, and small engine starting is one of the fastest growing markets for the lead–acid battery (100).

In Figure 30, the cutaway view of the automotive battery shows the components used in its construction. An industrial motive power battery, shown in Figure 31 (101), is the type used for lift trucks, trains, and mine haulage. Both types of batteries have the standard free electrolyte systems and operate only in the vertical position. Although a tubular positive lead–acid battery is shown for

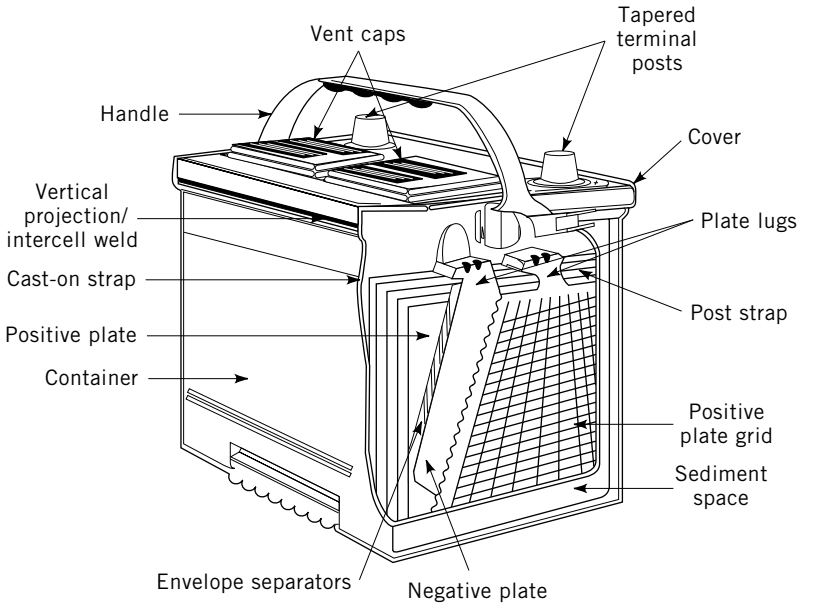

Fig. 30. Cutaway view of an automotive SLI lead–acid battery container and cell element. Courtesy of Johnson Controls, Inc.

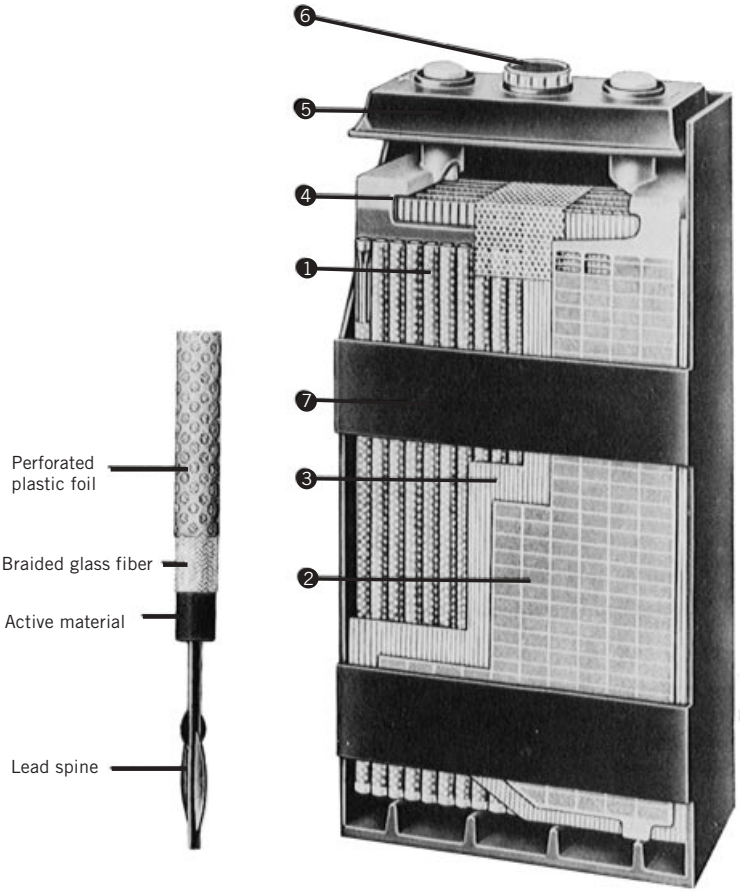

Fig. 31. Cutaway view of a tubular positive lead–acid battery. (1) Positive tubular plate; (2) negative plate; (3) separator; (4) connecting strap; (5) cell cover; (6) cell plug; and (7) cell container. Courtesy of A. B. Tudor, Sweden.

industrial applications, the flat plate battery construction (Fig. 30) is also used in a comparable size.

Two types of batteries having immobilized electrolyte systems are also made. They are most common in consumer applications, but their use in industrial and SLI applications is increasing. Both types have low maintenance requirements and usually can be operated in any position. They are sometimes called valve regulated or recombinant batteries because they are equipped with a one-way pressure relief vent and normally operate in a sealed condition with an oxygen recombination cycle to reduce water loss.

In the gelled electrolyte battery, the sulfuric acid electrolyte has been immobilized by a thixotropic gel. This is made by mixing an inorganic powder such as silicon dioxide [7631-86-9], SiO_2, with the acid (102). Other cells, such as the one shown in Figure 32, use a highly absorbent separator to immobilize the electrolyte (103).

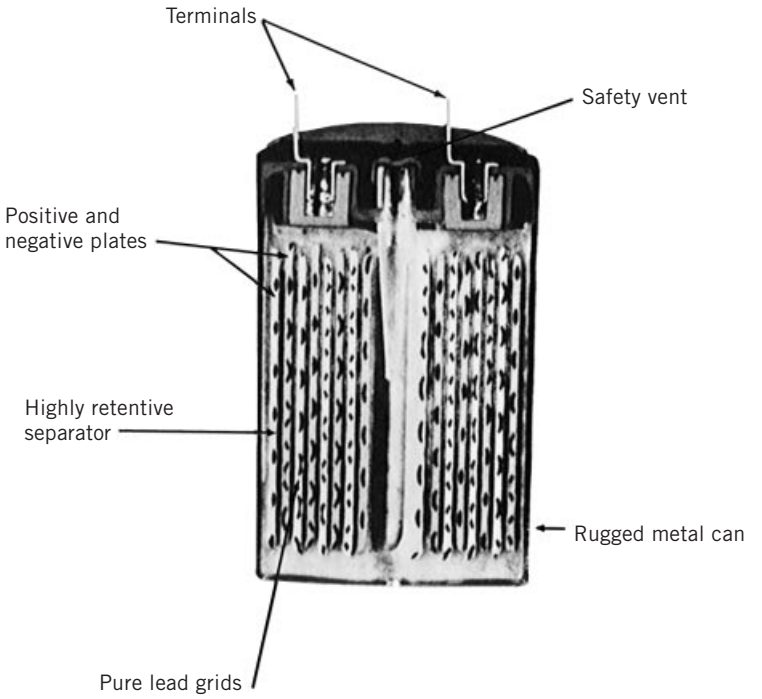

Fig. 32. Sealed cylindrical lead–acid cell.Courtesy of Gates Energy Products, Inc.

2.1. History. Gaston Planté developed the first working model of the lead–acid battery (104) in 1859, but electrochemical energy storage was not practical then because there was no efficient way of recharging a battery. The lead–acid battery generated interest because it could provide higher currents than primary batteries. The use of the system as a capacitor was also of great interest. Between 1860 and 1880, the principal commercial application of the Planté battery was in the telegraphic industry (105).

The first commercial application for a rechargeable energy storage device was electric lighting. Edison had developed a long-lasting incandescent bulb and improved the dynamo in 1879 (106). The invention of pasted plates (107) and the perforated lead current collector (108) in 1881 improved the energy storage capacity of the lead–acid battery and in the 1880s European and American companies were organized to commercialize electric lighting. Lighting provided a strong incentive for improvements in battery technology. Better grids, flat plates, and lead–antimony alloys soon followed (105). Electric vehicles, including boats, submarines, cars, and trams were developed and batteries were an important factor in the development of the power industry. Batteries were first used as transformers in electric power stations and later for load leveling. They provided the flexibility that was necessary for expansion of the industry without excessive capital investment. As power production improved and expanded, however, batteries were phased out because the maintenance costs were too high.

The invention of the self-starter in 1911 impacted heavily on the battery market (109). The battery-started, gasoline-driven vehicle was so successful

that electric vehicles could not compete. Except for submarines and a few delivery trucks, electric vehicles disappeared and automotive starting became the largest market for the lead–acid battery. Indeed, the SLI application has not only grown steadily but it has also financed the majority of lead–acid battery research and development. Over the years, substantial advances have been made by using new materials such as rubber and plastics for battery containers, separators, and other components, to increase the power and energy density of batteries. Maintenance requirements have been reduced substantially, and machine automation has accelerated production rates and lowered costs. Better electronics for charge and discharge control have improved battery performance and life.

In the 1990s, the use of batteries in electric vehicles and for load leveling revived partly for environmental reasons and partly because of scarce energy resources. Improvements in battery performance and life, fewer maintenance requirements, and automatic control systems are making these applications feasible. Research and development is ongoing all over the world to develop improved lead–acid batteries as well as other systems to meet these needs.

2.2. Cell Thermodynamics. The chemical reaction of the lead–acid battery was explained as early as 1882 (110). The double sulfate theory has been confirmed by a number of methods (111–113) as the only reaction consistent with the thermodynamics of the system. The thermodynamics of the lead–acid battery has been reviewed in great detail (114).

At the cathode, or positive electrode, lead dioxide [1309-60-0], PbO_2, reacts with sulfuric acid to form lead sulfate [7446-14-2], $PbSO_4$, and water in the discharging reaction

$$PbO_2 + 3\,H^+ + HSO_4^- + 2e^- \rightleftharpoons PbSO_4 + 2\,H_2O \qquad (1)$$

and the reverse occurs as the battery charges. At the anode, or negative electrode, metallic lead reacts with bisulfate ion to form lead sulfate in the discharging reaction

$$PbSO_4 + H^+ + 2e^- \rightleftharpoons Pb + HSO_4^- \qquad (2)$$

and the reverse occurs as the battery charges. The sum of these two half-cell reactions is called the double sulfate reaction.

$$Pb + PbO_2 + 2\,H_2SO_4 \rightleftharpoons 2\,PbSO_4 + 2\,H_2O \qquad (3)$$

Lead sulfate is formed as the battery discharges, sulfuric acid is regenerated as the battery is charged. The open circuit voltage of the lead–acid battery is a function of the acid concentration and temperature. A review of this subject is available (115). The Nernst equation may be used to calculate the open circuit cell voltage. The battery voltage is then obtained by multiplying the cell voltage by the number of cells.

The Nernst equation for the cell voltage V is

$$V = V^\circ + 2.303(RT/F)\left(\log a_{H_2SO_4} - \log a_{H_2O}\right) \qquad (4)$$

Because Pb, PbO_2, and $PbSO_4$ are all solids having low solubilities, the activities of these substances are unity. At 25°C, the absolute temperature T is 298.15 K. The value of R, the gas constant, used is 8.3144 J/(mol K). F, the Faraday constant, is 96,485 C/mol. The standard cell voltage V° for the double sulfate reaction must be known as well as the activities of sulfuric acid and water at any given concentration or temperature.

The dependence of cell voltage on pressure is small and can be neglected in normal applications. At 25°C and an acid concentration of 3.74 m, $dV/dP = -3.32 \times 10^{-5}$ μV/Pa($-4.81 \times 10^{-3}_{\mu}$V/psi). Tables and equations for the pressure dependence are available (114).

Sulfuric acid dissociates only partially according to the following equilibria.

$$H_2SO_4 \rightleftharpoons H^+ + HSO_4^- K_1 = a_{H^+} a_{HSO_4^-} / a_{H_2SO_4} \quad (5)$$

$$HSO_4^- \rightleftharpoons H^+ + SO_4^{2-} K_2 = a_{H^+} a_{SO_4^{2-}} / a_{HSO_4^-} \quad (6)$$

Here the values of a are the activities of the designated ions in solution, and K_1 and K_2 are the equilibrium constants for the dissociation reactions. K_1 is infinity because dissociation to hydrogen and bisulfate ions is essentially complete. The best value for K_2 is probably 0.0102 (116). Thus sulfuric acid contains a mixture of hydrogen, bisulfate, and sulfate ions where the ratios of these ions vary with concentration and temperature.

The activity of any ion, $a = \gamma m$, where γ is the activity coefficient and m is the molality (mol solute/kg solvent). Because it is not possible to measure individual ionic activities, a mean ionic activity coefficient, $\gamma_\pm$, is used to define the activities of all ions in a solution. The convention used in most of the literature to report the mean ionic activity coefficients for sulfuric acid is based on the assumption that the acid dissociates completely into hydrogen and sulfate ions. This assumption leads to the following formula for the activity of sulfuric acid.

$$a_{H_2SO_4} = (a_{H^+})^2 a_{SO_4^{2-}} = (\gamma_\pm 2m)^2 (\gamma_\pm m) = 4\gamma_\pm^3 m^3 \quad (7)$$

where m is the molality of sulfuric acid (mol acid/kg water).

To adjust the activities of sulfuric acid to the convention which assumes that the acid dissociates only partially into hydrogen and bisulfate ions, the following formula is used:

$$a'_{H_2SO_4} = a_{H_2SO_4} / K_2 \quad (8)$$

The activity coefficient of water is related to the osmotic coefficient by the formula:

$$2.303 \log a_{H_2O} = -3m\phi/55.5 \quad (9)$$

where ϕ is the osmotic coefficient ofsulfuric acid of molality m.

The activity coefficients ofsulfuric acid have been determined independently by measuring three types of physical phenomena: cell potentials, vapor

pressure, and freezing point. A consistent set of activity coefficients has been reported from 0.1 to 8 m at 25°C (113), from 0.1 to 4 m and 5 to 55°C (117), and from 0.001 to 0.02 m at 25°C (118). These values are all based on cell potential measurements. The activity coefficients based on vapor pressure measurements (119) agree with those from potential measurements when they are corrected to the same reference activity coefficient.

To calculate the open circuit voltage of the lead–acid battery, an accurate value for the standard cell potential, which is consistent with the activity coefficients of sulfuric acid, must also be known. The standard cell potential for the double sulfate reaction is 2.048 V at 25°C. This value is calculated from the standard electrode potentials: for the (Pt)$H_2|H_2SO_4(m)|PbSO_4|PbO_2$(Pt) electrode 1.690 V (113), for the Pb(Hg)$|PbSO_4|H_2SO_4(m)|H_2$(Pt) electrode 0.3526 V(19), and for the $Pb|Pb^{2+}|$Pb(Hg) 0.0057 V (120).

Table 4 gives the calculated open circuit voltages of the lead–acid cell at 25°C at the sulfuric acid molalities shown. The corrected activities of sulfuric acid from vapor pressure data (119) are also given.

The temperature dependence of the open circuit voltage has been accurately determined (121) from heat capacity measurements (122). The temperature coefficients E_T are given in Table 5. The accuracy of these temperature coefficients does not depend on the accuracy of the open circuit voltages at 25°C shown in Table 4. Using the data in Tables 4 and 5, the open circuit voltage can be calculated from 0 to 60°C at concentrations of sulfuric acid from 0.1 to 13.877 m.

The mercurous sulfate [7783-36-0], Hg_2SO_4, mercury reference electrode, (Pt)$H_2|H_2SO_4(m)|Hg_2SO_4$(Hg), is used to accurately measure the half-cell potentials of the lead–acid battery. The standard potential of the mercury reference electrode is 0.6125 V (113). The potentials of the lead dioxide, lead sulfate, and mercurous sulfate, mercury electrodes versus a hydrogen electrode have been measured (123,124). These data may be used to calculate accurate half-cell potentials for the lead dioxide, lead sulfate positive electrode from temperatures of 0 to 55°C and acid concentrations of from 0.1 to 8 m.

2.3. Lead Grid Corrosion. The corrosion of the lead grid at thelead dioxide electrode is one of the primary causes of lead–acid battery failure. Grid corrosion is complex for several reasons. First, the acid concentration and voltage at the lead dioxide electrode vary widely during battery operation. Second, the voltage, pH, and other ionic concentrations vary across the corrosion film. Different conditions across the film favor different reactions. Changing conditions mean multiple corrosion products form includinglead sulfate, basic lead sulfates, and lead oxides (125). Third, the lead oxides form a nonstoichiometric series which can be represented by the general formula, PbO_n, where $1 < n < 2$. Two polymorphs have been identified in lead corrosion films for both lead(II) oxide [1317-36-8], PbO, orthorhombic and tetragonal, and PbO_2, rhombic and tetragonal. PbO_2 may also be amorphous. A variety of intermediates, such as the intermediate lead oxide [1314-41-6], Pb_3O_4, and lead(III) oxide [1314-27-8], Pb_2O_3, have also been found.

The mechanisms of lead corrosion in sulfuric acid have been studied and good reviews of the literature are available (126–129). The main techniques used in lead corrosion studies have been electrochemical measurements, x-ray diffraction, and electron microscopy. Laser Raman spectroscopy and photoelec-

Table 4. **Thermodynamic Values for the Lead-Acid Cell at 25°C**

Molality, m	$\gamma_{\pm}$	αH_2O^a	$\alpha H_2SO_4 a$	V
0.1	0.245	9.963×10^{-1}	5.882×10^{-5}	1.798
0.2	0.193	9.928×10^{-1}	2.296×10^{-4}	1.833
0.3	0.169	9.892×10^{-1}	5.167×10^{-4}	1.854
0.5	0.144	9.819×10^{-1}	1.483×10^{-3}	1.881
0.7	0.131	9.743×10^{-1}	3.067×10^{-3}	1.900
1.0	0.121	9.618×10^{-1}	7.164×10^{-3}	1.922
1.5	0.117	9.387×10^{-1}	2.137×10^{-2}	1.951
2.0	0.118	9.126×10^{-1}	5.224×10^{-2}	1.975
2.5	0.123	8.836×10^{-1}	1.158×10^{-1}	1.996
3.0	0.131	8.516×10^{-1}	2.440×10^{-1}	2.016
3.5	0.143	8.166×10^{-1}	4.989×10^{-1}	2.035
4.0	0.157	7.799×10^{-1}	9.883×10^{-1}	2.054
4.5	0.173	7.422×10^{-1}	1.888×10	2.072
5.0	0.192	7.032×10^{-1}	3.541×10	2.090
5.5	0.213	6.643×10^{-1}	6.463×10	2.106
6.0	0.237	6.259×10^{-1}	1.148×10^{1}	2.123
6.5	0.263	5.879×10^{-1}	2.002×10^{1}	2.139
7.0	0.292	5.509×10^{-1}	3.421×10^{1}	2.154
7.5	0.323	5.152×10^{-1}	5.685×10^{1}	2.169
8.0	0.356	4.814×10^{-1}	9.255×10^{1}	2.183
8.5	0.393	4.488×10^{-1}	1.492×10^{2}	2.197
9.0	0.431	4.180×10^{-1}	2.334×10^{2}	2.211
9.5	0.472	3.886×10^{-1}	3.617×10^{2}	2.224
10.0	0.516	3.612×10^{-1}	5.490×10^{2}	2.236
11.0	0.610	3.111×10^{-1}	1.208×10^{3}	2.260
12.0	0.711	2.681×10^{-1}	2.480×10^{3}	2.283
13.0	0.819	2.306×10^{-1}	4.835×10^{3}	2.304
14.0	0.938	1.980×10^{-1}	9.072×10^{3}	2.324
15.0	1.065	1.698×10^{-1}	1.630×10^{4}	2.343
16.0	1.200	1.456×10^{-1}	2.828×10^{4}	2.361
17.0	1.338	1.252×10^{-1}	4.708×10^{4}	2.378
18.0	1.484	1.076×10^{-1}	7.621×10^{4}	2.394
19.0	1.634	9.250×10^{-2}	1.198×10^{5}	2.410
20.0	1.790	7.960×10^{-2}	1.836×10^{5}	2.424
21.0	1.951	6.860×10^{-2}	2.750×10^{5}	2.439
22.0	2.122	5.890×10^{-2}	4.072×10^{5}	2.453
23.0	2.302	5.060×10^{-2}	5.940×10^{5}	2.466
24.0	2.460	4.410×10^{-2}	8.233×10^{5}	2.478
26.0	2.805	3.310×10^{-2}	1.552×10^{6}	2.502
28.0	3.159	2.500×10^{-2}	2.767×10^{6}	2.524
30.0	3.499	1.910×10^{-2}	4.627×10^{6}	2.544

[a] From Ref. 119.

trochemistry have been used to gain new insight into the corrosion process (129,130).

2.4. Charge–Discharge Processes. An excellent review covers the charge and discharge processes in detail (129) and ongoing research on lead–acid batteries may be found in two symposia proceedings (131,132). Detailed studies of the kinetics and mechanisms of lead–acid battery reactions are published continually (133). Although many questions concerning the exact nature of the

Table 5. **Temperature Coefficients of the Lead–Acid Cell, E_T[a], mV**

Concentration, m	Temperature, °C									
	0	5	10	15	20	30	35	40	45	50
0.1	−6.102	−4.713	−3.410	−2.191	−1.055	0.975	1.871	2.689	3.431	4.098
0.2	−3.872	−2.943	−2.092	−1.319	−0.622	0.548	1.024	1.428	1.762	2.026
0.3	−2.414	−1.785	−1.231	−0.749	−0.339	0.270	0.472	0.607	0.676	0.681
0.4	−1.317	−0.914	−0.581	−0.319	−0.126	0.059	0.053	−0.017	−0.151	−0.347
0.5	−0.400	−0.193	−0.050	0.029	0.045	−0.106	−0.271	−0.495	−0.776	−1.115
0.6	0.351	0.399	0.387	0.316	0.187	−0.243	−0.542	−0.894	−1.301	−1.760
0.7	1.005	0.913	0.766	0.564	0.308	−0.360	−0.772	−1.233	−1.744	−2.304
0.8	1.606	1.385	1.113	0.791	0.420	−0.468	−0.982	−1.543	−2.150	−2.801
0.9	2.135	1.801	1.421	0.993	0.519	−0.563	−1.171	−1.821	−2.513	−3.248
1.0	2.620	2.180	1.698	1.173	0.607	−0.647	−1.334	−2.059	−2.823	−3.624
1.110	3.063	2.528	1.953	1.339	0.688	−0.725	−1.485	−2.281	−3.112	−3.977
1.388	4.020	3.280	2.508	1.704	0.867	−0.898	−1.826	−2.784	−3.771	−4.787
1.850	5.175	4.194	3.185	2.150	1.088	−1.113	−2.251	−3.414	−4.601	−5.812
2.220	5.702	4.612	3.496	2.355	1.189	−1.213	−2.449	−3.709	−4.990	−6.294
2.775	6.081	4.912	3.720	2.503	1.263	−1.286	−2.593	−3.923	−5.274	−6.647
3.172	6.168	4.982	3.771	2.537	1.280	−1.302	−2.627	−3.973	−5.341	−6.729
3.700	6.002	4.854	3.679	2.478	1.252	−1.276	−2.577	−3.901	−5.249	−6.620
4.626	5.256	4.270	3.250	2.199	1.115	−1.146	−2.322	−3.527	−4.762	−6.026
5.551	4.134	3.437	2.674	1.846	0.954	−1.016	−2.092	−3.228	−4.423	−5.675
6.167	3.651	3.056	2.393	1.661	0.863	−0.928	−1.919	−2.972	−4.087	−5.262
6.938	3.171	2.674	2.107	1.472	0.769	−0.834	−1.732	−2.693	−3.717	−4.801
7.929	2.760	2.340	1.854	1.301	0.682	−0.745	−1.553	−2.422	−3.350	−4.338
8.539	2.641	2.238	1.772	1.242	0.651	−0.711	−1.481	−2.308	−3.192	−4.131
9.291	2.602	2.192	1.725	1.201	0.628	−0.681	−1.413	−2.195	−3.028	−3.909
10.092	2.647	2.207	1.721	1.191	0.617	−0.659	−1.360	−2.102	−2.884	−3.706
11.101	2.725	2.249	1.737	1.192	0.612	−0.645	−1.322	−2.030	−2.769	−3.539
12.335	2.797	2.290	1.756	1.197	0.611	−0.636	−1.296	−1.981	−2.689	−3.421
13.877	2.843	2.313	1.764	1.195	0.607	−0.626	−1.269	−1.931	−2.611	−3.308

[a] $E = E_{25°C} - E_T$ (mV) of the lead storage cell from the third law of thermodynamics.

reactions remain unanswered, the experimental data on the lead–acid cell are more complete than for most other electrochemical systems.

Significant progress is also being made in simulating battery charge and discharge processes using electrochemical models. Models of the lead–acid cell based on porous electrode theory have been developed (134–138). Discharge behavior can be predicted within 10% accuracy over a wide range of discharge rates. Recharge behavior has also been simulated (139); a detailed model of the changes in acid concentration resulting from convection in free electrolyte cells has been presented (140); a model for distribution of acid immobilized in a porous separator has been developed (141); and a model of the effect of lead sulfate supersaturation on battery behavior has been published (142). Such models can be used to predict the performance of large batteries from data on small cells, develop improved battery designs, and simulate the performance of any design in a new application. Battery development is therefore accelerated by reducing the time required to build and test battery prototypes.

At high discharge rates, such as those required for starting an engine, the voltage drops sharply primarily because of the resistance of the lead current collectors. This voltage drop increases with the cell height and becomes significant even at moderate discharge rates in large industrial cells. Researchers have measured this effect in industrial cells and have developed a model which has been used to improve grid designs for automotive batteries (143,144).

Self-Discharge Processes. The shelf life of the lead–acid battery is limited by self-discharge reactions, first reported in 1882 (145), which proceed slowly at room temperature. High temperatures reduce shelf life significantly. The reactions which can occur are well defined (146) and self-discharge rates in lead–acid batteries having immobilized electrolyte (147) and limited acid volumes (148) have been measured.

The lead current collector in the positive lead–dioxide plate corrodes and the compounds which form are a function of the acid concentration and positive electrode voltage. Other reactions which take place at the positive electrode are shown.

Oxygen evolution

$$PbO_2 + H_2SO_4 \rightleftharpoons PbSO_4 + H_2O\,\frac{1}{2}\,O_2 \qquad (10)$$

Oxidation of organics, R,

$$2\,PbO_2 + R + 2\,H_2SO_4 \rightleftharpoons 2\,PbSO_4 + 2\,H_2O + CO_2 + R' \qquad (11)$$

Sulfation of PbO (in new cells)

$$PbO + H_2SO_4 \rightleftharpoons PbSO_4 + H_2O \qquad (12)$$

Oxidation of additives such as antimony, in the grid alloy:

$$5\,PbO_2 + 2\,Sb + 6\,H_2SO_4 \rightleftharpoons (SbO_2)_2SO_4 + 5\,PbSO_4 + 6\,H_2O \qquad (13)$$

Similar reactions can be written for other metallic additives. At the negative electrode two more reactions can occur.

Hydrogen evolution

$$Pb + H_2SO_4 \rightleftharpoons PbSO_4 + H_2 \quad (14)$$

Oxygen recombination

$$Pb + H_2SO_4 + \frac{1}{2} O_2 \rightleftharpoons PbSO_4 + H_2SO \quad (15)$$

The rate of the oxygen recombination reactions is very fast depending only on the rate at which the oxygen is transported to the lead in the negative electrode. If the cell electrode stack is fully saturated with acid, the oxygen recombination reaction proceeds very slowly. The rate depends on the solubility of oxygen in sulfuric acid. However, in batteries which are stored with limited acid volume, oxygen can recombine very rapidly. A small leak in the cell container results in rapid self-discharge of the negative electrode by atmospheric oxygen. Although hydrogen recombination at the positive electrode has been proposed, its rate appears to be insignificant (149).

The rates of the other self-discharge reactions are primarily determined by the acid concentration (147,148). High acid concentrations accelerate the gas evolution reactions at both electrodes. In contrast, grid corrosion appears to be faster at low acid concentrations and voltages. Sulfation of unconverted lead oxide is so rapid that it generally occurs before the battery is shipped from the factory. Batteries are sometimes recharged just before shipment to complete the conversion of lead oxide to lead dioxide in the positive plate. Organics are necessary additives to the separator and negative plate but are kept to a minimum to avoid excessive self-discharge and grid corrosion.

Overcharge Reactions. Water electrolysis during overcharge is an irreversible process. Oxygen forms at the positive electrode:

$$H_2O \rightleftharpoons 2\,H^+ + \frac{1}{2} O_2(g) + 2e^- \quad (16)$$

At the negative electrode, hydrogen ions react to form hydrogen gas:

$$2\,H^+ + 2e^- \rightleftharpoons H_2(g) \quad (17)$$

The net reaction being

$$H_2O \rightleftharpoons H_2(g) + \frac{1}{2} O_2(g) \quad (18)$$

Theoretically, water should decompose at a voltage below the voltage required to recharge a lead–acid battery. However, the rate of water electrolysis is much slower than the rate of the recharge reaction. Thus the lead–acid battery can operate with as little as 5% excess charge to compensate for water electrolysis. Use of lead–antimony alloys for the current collectors in lead–acid batteries increases water loss. Some of these batteries need regular maintenance by addition of water to replace the water lost on overcharge. Many newer designs, however, use either lower concentrations of antimony in the alloy or lead–calcium

alloys to reduce water loss (see LEAD ALLOYS). This is the basis for the maintenance-free batteries.

Some battery designs have a one-way valve for pressure relief and operate on an oxygen cycle. In these systems the oxygen gas formed at the positive electrode is transported to the negative electrode where it reacts to reform water. Hydrogen evolution at the negative electrode is normally suppressed by this reaction. The extent to which this process occurs in these valve regulated lead–acid batteries is called the recombination-efficiency. These processes are reviewed in the literature (149–151).

The oxygen cycle is often described by equation 16 at the positive electrode, and the reverse of equation 16 at the negative electrode,

$$\frac{1}{2}\,O_2 + 2\,H^+ + 2e^- \rightleftharpoons H_2O \qquad (19)$$

When these half-reactions are summed, there is no net reaction. Thus the material balance of the cell is not altered by overcharge. At open circuit, equation 19 at the negative electrode is the sum of a two-step process, represented by equation 15 and

$$PbSO_4 + 2\,H^+ + 2e^- \rightleftharpoons Pb + H_2SO_4 \qquad (20)$$

These equations are based on the thermodynamically stable species. Further research is needed to clarify the actual intermediate formed during overcharge. In reality, the oxygen cycle can not be fully balanced because of other side reactions, that include grid corrosion, formation of residual lead oxides in the positive electrode, and oxidation of organic materials in the cell. As a result, some gases, primarily hydrogen and carbon dioxide (152), are vented.

2.5. Material Fabrication and Manufacturing Processes. The lead–acid battery is comprised of three primary components: the element, the container, and the electrolyte. The element consists of positive and negative plates connected in parallel and electrically insulating separators between them. The container is the package which holds the electrochemically active ingredients and houses the external connections or terminals of the battery. The electrolyte, which is the liquid active material and ionic conductor, is an aqueous solution of sulfuric acid.

Element. The process of fabricating lead–acid battery elements as depicted in Figure 33 involves numerous chemical and electrochemical reactions and several mechanical assembly operations. All of the processes involved must be carefully controlled to ensure the quality and reliability of the product.

Plates. Plates are the part of the cell that ultimately become the battery electrodes. The plates consist of an electrically conductive grid pasted with a lead oxide–lead sulfate paste which is the precursor to the electrode active materials which participate in the electrochemical charge–discharge reactions.

Lead is the basic raw material for the two components, both the active material and grid, of both the positive and negative plates or electrodes. A finely divided mixture of lead monoxide powder and metallic lead particles is the key ingredient in preparing positive and negative active material. The physical and

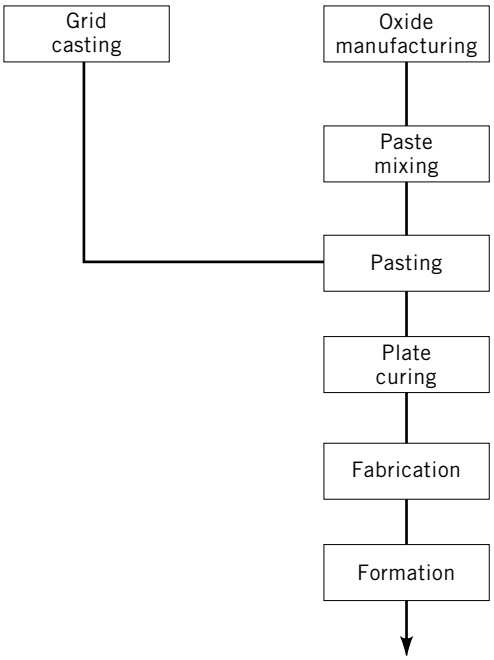

Fig. 33. Flow sheet of plate processing and battery manufacturing.

chemical characteristics of this leady litharge, battery oxide, or grey oxide as it is called, have a profound impact on the performance and life expectancy of the battery. Battery oxide is manufactured from primary or secondary (recycled) lead of extremely high purity using either the Barton or ball mill process.

In the Barton (153) process, molten lead is metered into a reactor or a Barton pot where it impinges on a rotating paddle. The resulting droplets of lead are oxidized and conveyed out in an airstream. The ball mill process converts solid lead pieces directly into oxide through attrition by causing them to rub against each other within a rotating reactor or ball mill. The lead in the ball mill is the grinding media as well as a reactant. The particles or agglomerates produced by the molten lead Barton process are droplike or spherical whereas those produced by the solid state ball mill grinding process are flat or flakelike. The oxidation reaction in either process is controlled such that approximately 75% of the product is oxidized to lead monoxide, leaving about 25% as finely divided metallic lead to be oxidized in subsequent processes. In addition to chemical composition, particle size or reactivity of the material is measured and controlled. Process control variables include reactor temperature, air flow, and lead feed rate.

The oxide exiting either the Barton or ball mill reactor is conveyed by an air stream to separating equipment, ie, settling tank, cyclone, and baghouse, after which it is stored in large hoppers or drummed for use in paste mixing. Purity of the lead feed stock is extremely critical because minute quantities of some impurities can either accelerate or slow the oxidation reaction markedly. Detailed discussions of the oxide-making process and product are contained in

references (154–156). A lightweight low resistance electrode plate for lead–acid batteries has been described (157).

Paste Mixing. The active materials for both positive and negative plates are made from the identical base materials. Lead oxide, fibers, water, and a dilute solution of sulfuric acid are combined in an agitated batch mixer or reactor to form a pastelike mixture of lead sulfates, the normal, tribasic, and tetrabasic sulfates, plus PbO, water, and free lead. The positive and negative pastes differ only in additives to the base mixture. Organic expanders, barium sulfate [7727-43-7], $BaSO_4$, carbon, and occasionally mineral oil are added to the negative paste. Red lead [1314-41-6] or minium, Pb_3O_4, is sometimes added to the positive mix. The paste for both electrodes is characterized by cube weight or density, penetration, and raw plate density.

Additives, ie, carbon or Pb_3O_4, are used to improve pasted plate conductivity and formed or charged plate characteristics. The expander used in the negative paste keeps it porous or spongelike throughout its life, rather than becoming a dense, tightly packed sheet (158,159). The barium sulfate in the negative paste is believed to act to stimulate the formation of fine seed crystals of $PbSO_4$ during discharge of the electrode (160–162). The physical characteristics of the paste are controlled by the mixing process (163,164). The amounts and order of constituent addition also play a role in the makeup of the finished paste.

During the paste mixing process the lead oxides are partially converted to basic lead sulfate (165). Some of these compounds are monobasic lead sulfate [12036-76-9], $PbO \cdot PbSO_4$, dibasic lead sulfate [65589-92-6], $2PbO \cdot PbSO_4$, predominantly tribasic lead sulfate [12202-17-4], $3PbO \cdot PbSO_4$, and, if high temperatures are encountered during the mixing step, tetrabasic lead sulfate [12065-90-6], $4PbO \cdot PbSO_4$. These compounds, because of their crystal morphology, bind tightly together on the grid, and facilitate plate processing and battery cycling. It is the degradation of this binding property resulting from an increased crystal growth (166) that causes failure of the positive plate by shedding of the active material. This active material drops through the separator ribs and collects in the sediment space (Fig. 30). This material is lost during electrochemical conversion and, subsequently, performance of the positive plate deteriorates over repeated cycling. The use of antimony [7440-36-0], Sb, in the positive grid increases the paste adhesion and cohesion. Some designs use tubular positive plates or separator-glass mat combinations to retard shedding.

The water added during the mixing operation functions as a lubricant and bulking agent to produce a paste of the proper consistency. During the plate drying operation, the evaporation of water gives the desired plate porosity. In addition to forming the binding material, the sulfuric acid expands the paste and thus gives it greater porosity.

During the acid addition step of the paste mixing process, considerable heat is generated because of the exothermic reaction of lead oxide and sulfuric acid. Care must be taken to prevent excessive loss of water before the paste can be applied to the grids. The mixer is usually cooled by water or air. After the paste has reached the desired uniformity and consistency for applying to the grid, the mixing is terminated. The paste density range is generally 3.7–4.0 g/mL for high initial capacity battery designs and for long cycle life product it may be as high as 4.3–4.6 g/mL. Muller or plough type mixers are used and a typical

batch size is approximately 1100 kg. An excellent discussion of paste preparation and curing processes is available (167) and comprehensive review (168) describes the morphological features of the compounds used or evolved in the initial paste material.

Grids. The grid in a battery plate performs two vital functions. It acts as the mechanical support framework of the plate during manufacturing, and provides uniform, efficient current flow to and from the plate during formation and use. Grids are designed to have a lug or current collection point, current carrying arms, structural frame, and usually feet (Fig. 34).

The grid must possess sufficient stiffness to prevent damage or distortion during the casting, plate pasting, and battery assembly operations. During the life of the battery the grid must bear significant loads such as active material weight, its own weight, and stresses resulting from corrosion and volumetric changes caused by the sulfation of lead and lead dioxide. The most severe environment for the grid is in the positive plate. The positive active material operates in a potential range where lead is thermodynamically unstable. Thus the lead

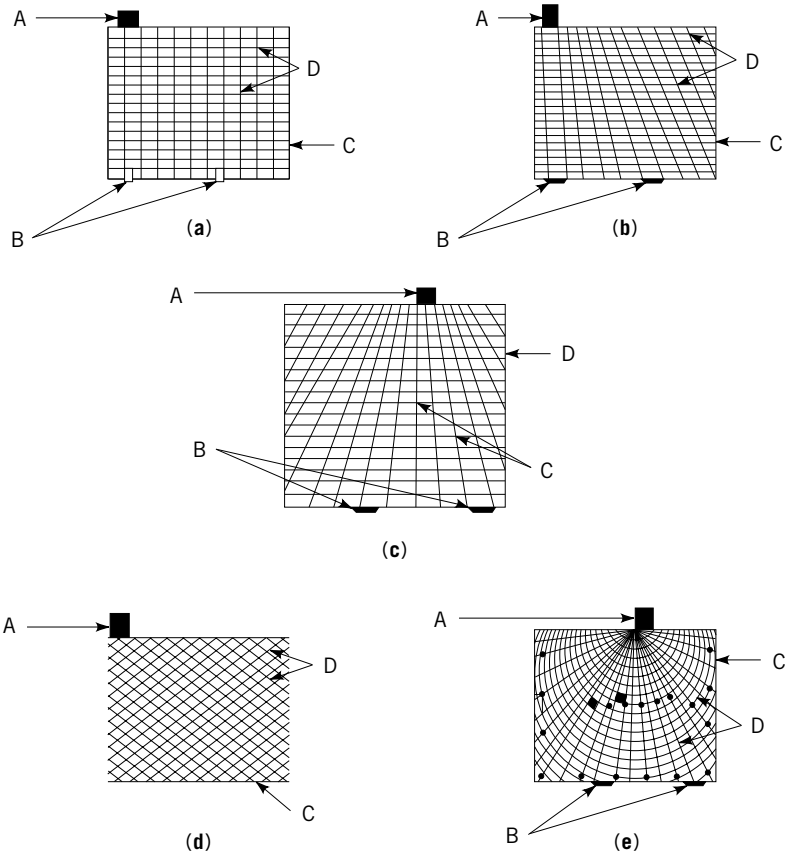

Fig. 34. Lead–acid battery grid design variations showing A lugs, B feet, C frames, and D current carrying wire for (**a**) rectilinear design, (**b**) corner lug radial, (**c**) center lug radial, (**d**) corner lug expanded metal, and (**e**) plastic/lead composite.

grid is continuously oxidizing to PbO and PbO_2 which affects the grid by reducing its strength and conductivity, and sometimes causing elongation of its members, commonly called grid growth.

Most grids are cast or mechanically expanded from cast or wrought strip. Historically, negative and positive grids have been the same; however, with the advent of specialized batteries and extreme performance demands, this is less likely. However if these plates are different, it is generally in configuration, alloy, and/or thickness.

The conductivity of the grid plays a substantial role in a battery's ability to meet high current demands. The importance of grid conductivity for lead–acid batteries has been discussed (100,169). Composition and configuration are important design factors impacting grid conductivity.

Potential distribution in grids (169–172) has been evaluated and the results put into practice (173). Innovative grid structures which incorporate element members positioned to optimize current flow patterns have been proposed (169,174,175) as well as economical lightweight grids for the negative plate made from plastics coated or woven with lead (176,177), or with plastic strengthening members and metallic conductors (178). All incorporate lead terminal connectors in their design for easily soldering to one another, or to current collectors.

Grid Material. Pure lead has low tensile and creep strength, and thus is easily deformed at room temperature. Because the grid supplies plate strength during manufacturing and life, it must be durable. This is accomplished by alloying lead with other elements. The primary alloying ingredients are antimony, calcium [7440-70-2], and tin [7440-31-5]. Numerous other elements, eg, arsenic [7440-38-2], selenium [7782-49-2], etc can and are being used in lesser amounts.

High antimony (2–12%) content lead alloys have been used widely in the manufacture of grids where antimony increases the structural integrity of the resulting grid. Antimony not only improves its manufacturability, but also retards positive grid growth and stress deformation caused by corrosion and active material sulfation. Antimony migrates into, and alters the morphology of, the positive active mass which improves the PbO_2 adhesion and cyclability (179).

Antimony from the grid also diffuses into the electrolyte and migrates to the negative electrode and plates out. This plating or poisoning increases the self-discharge rate of the negative plate. It also reduces the negative plate's hydrogen gassing overpotential, which increases charge inefficiency and water loss resulting from gas generation. These adverse effects have been minimized by using low antimony (1–2%) content alloys (180,181). Such alloys use low percentages of other additives, eg, selenium, tin, sulfur [7704-34-9], and arsenic (182) to improve their strength. The low antimony content alloy reduces the detrimental gassing effects of its high antimony counterpart. It also has improved castability and enhanced corrosion resistance.

Lead alloy containing calcium (0.075–0.1%) as its stiffening agent is used in some maintenance-free batteries. This alloy is more difficult to cast than antimonial–lead alloys. The grids formed from this alloy have somewhat lower self-discharge and water loss than lead–antimony alloy grids, but batteries containing lead–calcium alloy positive grids do not give as much cycle service as those made

with lead–antimony alloy positive grids (181). However, this difference is nullified if the battery is in float (constant voltage) or limited cycling applications (183).

Other alloying ingredients in lead, eg, arsenic (0.5–0.7%) and silver [7440-22-4] (0.1–0.15%), inhibit grid growth on overcharge and reduce positive grid corrosion. Tin added to a lead alloy produces well-defined castings that are readily adapted to mass production techniques (184).

The proper selection of the lead alloy depends on the intended use and the economics of the lead–acid battery application. The metallurgical and electrochemical aspects of the lead are discussed in the literature in a comprehensive manner (181,185–187) as are trends of lead alloy use for manufacture of battery grids (188).

Grid Casting. The grid casting machine consists of a center parting grid, or book mold, trimming mechanism, and melting pots. The grid mold consists of two cast iron parts, each having a grid design for a face. The mold design can also be a single grid or multiple grid configuration. The grid mold is heated to 135–180°C to prevent premature solidification of the lead alloy and holes in the mold release trapped air while the mold is being filled with the molten metal.

The melting pot is heated either electrically or by gas to 427–524°C. The pot capacity is typically over 100 kg of lead alloy, and periodically the top of the molten metal must be skimmed to remove the dross. The pot fumes must be removed by adequate ventilation (forced suction). When the molten metal has reached the proper temperature and flow characteristics, it is transported by pump to the grid mold.

Prior to casting, the grid mold halves are sprayed using a mold-release agent. The releasing agent also serves to control grid thickness and weight during casting. After filling with a slight excess of molten lead alloy, the mold is cooled for several seconds before opening. The cast grid is trimmed to remove rough edges, gates, and minor imperfections before stacking for use in the plate processing operation.

Another common manufacturing technique is expanding cast or wrought lead strip. The strip is typically a calcium alloy of lead, although antimonial alloys have been used. The process consists of casting or rolling a continuous strip and coiling it into large rolls which are subsequently expanded. The expanding process is a multistage process in which the strip is perforated with a cutting tool and progressively stretched apart to form a diamond pattern grid, punched to form lugs, and trimmed to form the singular grids (Fig. 34), before or after pasting.

The advent of higher compression, more powerful engines in compact engine compartments and more electrical loads has precipitated the need for smaller, more powerful batteries. This has driven battery manufacturers to look at thinner plate technology. Grid designs and materials are being reevaluated to establish components to meet future demands. Technologies such as dual material (169), bipolar (189), and folded plate designs (155) are broadening the role of the grid and what it is expected to do.

Plate Pasting. Two types of machines are commonly used to apply paste to grids. They are the belt type and the fixed orifice type. Each of these types of pasters has a paste hopper that supplies paste to the machine and is fed by the

paste mixer. The belt paster presses paste into the grid which is being transported by a belt into the paste stream. A fixed orifice paster squeezes the paste into the grid and then pushes the grid and paste through an orifice to smooth both plate surfaces. In both instances the pasted plate is flash dried and/or papered to remove surface moisture, allowing the plates to be stacked and transported to a curing area. In flash drying the plate passes quickly through a high temperature oven which effectively dries only the surface of the plate. When paper is used, a thin film is applied to both surfaces of the plate directly after pasting. Moisture content of the paste in plates after flash drying is typically 10%.

The tubular positive plate uses rigid, porous fiber glass tubes covered with a perforated plastic foil as the active material retainer (Fig. 31). Dry lead oxide, PbO, and red lead, Pb_3O_4, are typically shaken into the tubes which are threaded over the grid spines. The open end is then sealed by a polyethylene bar. Patents describe a procedure for making a type of tube for the tubular positive plate (190) and a method for filling tubular plates of lead–acid batteries (191). Tubular positive plates are pickled by soaking in a sulfate solution and are then cured. Some proceed directly to formation and do not require the curing procedure.

Plate Curing. Curing strengthens or hardens and dries the paste and establishes a cohesive paste–grid bond. It is a critical process in battery fabrication because it increases the plate's structural integrity and creates the electrode's active material morphology. A typical curing process consists of placing pasted plates in an elevated temperature, high humidity environment for some extended period of time such as from 16 to 48 hours. There, the plate is subjected to a controlled drying scenario. Unreacted lead particles oxidize in an exothermic reaction, creating heat that slowly drives off plate moisture. The rate of reaction of lead to lead oxide is dependent on the moisture content of the paste and the manner in which this happens affects the formation of the lead sulfate–lead oxide crystal structure (192). A normal curing environment results in small crystals of tribasic lead sulfate, $3PbO{\cdot}PbSO_4 \cdot H_2O$. If the temperature is elevated to $>57^{\circ}C$, the result is coarse tetrabasic lead sulfate, $4PbO \cdot PbSO_4$, crystals. This is especially critical for the positive electrode where tribasic sulfate converts readily to PbO_2 during battery formation but tetrabasic sulfate does not (193).

After curing, the plates are allowed to finish the drying process in ambient or elevated temperature air. The moisture and metallic lead content of the cured plates should be substantially reduced to less than 2%.

Separators. The separator's purpose is to isolate the positive and negative electrodes electronically while allowing ionic exchange between the two. This is accomplished using a microporous, electronically nonconductive material. Separators are generally designed with a backweb that has ribs on one side. The microporous backweb is kept thin to reduce resistance to ionic diffusion and migration. The ribs, which are normally placed on the positive electrode side, act as standoffs, allowing a reservoir of electrolyte to exist between the plates.

The separator must be structurally sound to withstand the rigors of battery manufacturing, and chemically inert to the lead–acid cell environment. Numerous materials have been used for separators ranging from wood, paper, and rubber to glass and plastic. Glass fibers are included in this list (194). The majority

of separators used are either nonwoven–bound glass or microporous plastic such as PVC or polyethylene.

Separator containing efficiency improving additions to lead–acid batteries have been patented (195). Separator manufacturing procedures and materials are discussed in the literature (196,197) and separator test procedures are also available (198).

Strap. Plates of similar polarity within a cell, whether positive or negative, are connected in parallel by a strap. Most batteries use either a burned-on or a cast-on strap (COS). In the case of COS, a stacked element is aligned and the lugs are placed in a mold where molten lead is cast around them to form a strap and vertical projection. When burning is used, the lugs are placed into a precast comblike strap and fused by melting the lugs and comb together. The strap has a large vertical projection on one end (Fig. 30) that is used to connect the elements in series once inside the container.

Container. The battery container is made up of a cover, vent caps, lead bushings, and case. Cost and application are the two primary factors used to select the materials of construction for container components. The container must be fabricated from materials that can withstand the abusive environment the battery is subjected to in its application. It must also be inert to the corrosive environment of the electrolyte and solid active materials, and weather, vibration, shock, and thermal gradients while maintaining its liquid seal.

The case is the largest portion of the container. The case is divided into compartments which hold the cell elements. The cores normally have a mud-rest area used to collect shed solids from the battery plates and supply support to the element. Typical materials of construction for the battery container are polypropylene, polycarbonate, SAN, ABS, and to a much lesser extent, hard rubber. The material used in fabrication depends on the battery's application. Typical material selections include a polypropylene–ethylene copolymer for SLI batteries; polystyrene for stationary batteries; polycarbonate for large, single cell standby power batteries; and ABS for certain sealed lead–acid batteries.

Covers for the battery designs in Figures 30 and 31 are typically molded from materials identical to that of the respective case, and vent plugs are frequently made of molded polypropylene. Other combinations are possible, eg, containers molded of polyethylene or polypropylene may be mated with covers of high impact rubber for use in industrial batteries. After the cover is fitted over the terminal post, it is sealed onto the case. The cover is heat bonded to the case, if it is plastic; it is sealed with an epoxy resin or other adhesive, if it is vulcanized rubber. Vent caps are usually inserted into the cover's acid fill holes to facilitate water addition and safety vent gasses, except for nonaccessible maintenance-free or recombinant batteries. In nonaccessible batteries, the vent is fabricated as part of the cover.

2.6. Electrolyte. *Sulfuric Acid.* Sulfuric acid is a primary active material of the battery. It must be present to provide sufficient sulfate ions during discharge and to retain suitable conductivity. Lead–acid batteries generally use an aqueous solution of acid in either a free-flowing or in an immobilized state.

Sulfuric acid solutions are quantified by density or specific gravity. Concentrated sulfuric acid has a density $\approx$1.840 g/mL, sp gr = 1.840 at room tempera-

ture; water is 1.000 g/mL, at room temperature; mixtures vary between these values. The temperature of the electrolyte affects its specific gravity, thus temperature should be noted and correction factors applied when measurements are made. At room temperature a common range of specific gravities for lead–acid batteries is 1.210 to 1.300. The electrolyte's specific gravity changes as the battery is charged and discharged. This specific gravity change occurs as sulfate ions transfer from liquid H_2SO_4 to solid $PbSO_4$. Thus the specific gravity of the electrolyte is often used as a means of approximating battery condition or state of charge.

When acid is used in the immobilized state, it is either absorbed into a high void-volume separator, or it is gelled. Electrolyte is gelled using one of several procedures (199–201). Materials such as silicon dioxide and sodium silicate [1344-09-8], Na_2SiO_4, are used as gelling agents. The components are mixed and poured into the battery cell where the gel is allowed to set for some preset time. In this case the battery has normally been formed and its liquid electrolyte removed, after which the gelled electrolyte is added.

When a battery is designed with absorbed electrolyte, it is built with dry separators, filled with acid and formed (Fig. 32). Excess electrolyte may then be removed.

2.7. Battery Assembly. The cell element (Fig. 30) is normally constructed from groupings of positive and negative plates. The number and size of plates of each type is determined by the desired performance level for the battery. Positive and negative plates are alternately stacked using separators in between to form the proper plate count. When the element is assembled, this piece moves to the final assembly.

The elements are inserted into containers such as that shown in Figure 30. The voltage of each charged cell is approximately 2 V, thus three elements are connected in series in 6 V batteries, six in 12 V batteries, and so forth. Once in the container, the strap vertical projections are fused together in a series arrangement to produce an unformed battery. Normal fusing techniques include resistance welding, burning, or lead extrusion. When the fusing operation is complete, the cover is sealed to the container. Most batteries use heat sealing, although adhesives, friction welding, and other methods have application.

The assembled unit is then subjected to a pressure test to ensure leak-free seals around the periphery and between the cells. Finally, positive and negative external terminations (located in the two end cells) are fused to the cover bushings. The battery is filled with electrolyte by immersing it in a bath of diluted sulfuric acid or by pouring electrolyte into the cells. After filling, the battery is placed on charge as quickly as possible to retard the conversion of tribasic lead sulfate to normal lead sulfate. These neutralization reactions cause undesired heat buildup and create products that are difficult to form. The reactions also dilute the acid, increasing the solubility of expanders, allowing them to leach out. This is detrimental to finished battery performance.

Formation. During formation the cured plate material is electrochemically converted into electrode active material, ie, spongy lead in the negative, PbO_2 in the positive, utilizing current supplied by power sources. Formation reactions create heat which, when coupled with ohmic heat and heat of neutralization, can harm electrode active materials. Thus formation is often done using

evaporative coolers, water baths, or air tables. The efficiency of formation is highly dependent on the precursor cured plate morphology (196), temperature, formation current, and acid concentration (156). These processes are explained in great detail (160,193,202–204) for the positive and negative plate active materials. Normally between 110% and 130% of the battery's capacity ($A \cdot h$), dependent on the formation current, is required to form it and formation times range from eight hours to beyond 48 hours.

The majority of batteries manufactured are supplied as wet, ie, acid in the formed battery, battery products, and thus utilize in-container formation. Some dry charged product where plates are washed and dried after formation, and moist, dumped and/or centrifuged, batteries are produced for some applications and markets (205).

Testing. The finished battery may be tested for voltage, capacity, charge rate acceptance, cycle life, accelerated life, storage stability, overcharge, normal temperature discharge operation, low temperature cranking, shock and vibration, and gas generation (206). The detailed test procedures for automotive battery testing are contained in the specifications of the Battery Council International (BCI) (198) and the Society of Automotive Engineers (SAE) (207). Other battery test procedures are indicative of a specialized application or general all-around use. After completion of testing, the test specimens are frequently disassembled and critically examined by chemical, physical, and metallurgical means to manufacturing methods. The SAE (208) has produced a different test procedure for battery powered vehicles. Method for determining the state of lead–acid rechargeable batteries has been described (209).

2.8. Economic Aspects. Lead–acid batteries including starting-lighting ignition (SLI) and industrial types continue to be the dominant use for lead (87% of total consumption) SLI battery shipments totaled 106×10^6 units in 2001. This total included original equipment and replacement automative-type batteries (100).

In 2001, there was slower growth in demand for industrial-type sealed lead–acid batteries in backup power systems. Industrial-type batteries include stationary batteries, such as those used in uninterruptible power-supply equipment for hospitals, computer and telecommunications networks, and load leveling equipment for commercial electric power systems and traction batteries (ie, forklifts, airline ground equipment, mining vehicles). Telecommunications companies scaled down investment plans and there was also a decline in seasonally related battery failure.

Value regulated lead–acid batteries for use in hybrid-electric vehicles were displayed at the first Automotive Battery Conference in Las Vegas, Nevada in Feb. 2001. They will be marketed soon and will supply sufficient power for automobile idle step and regenerative power recovery and in car luxuries systems features such as electrically conductive oxide coatings for heating windshields, and powere steering. Potential use in mild hybrid vehicles (cars capable of operating in electric assist mode) is also noted (100).

The market for higher voltage batteries is expected to grow significantly in order to handle greater automotive electric demands. The Absorbent Glass Mat lead–acid battery uses a quantity of lead similar to conventional batteries, but is designed to last twice as long. Its sealed design allows use in a variety of

positions without danger of electrolyte spillage and it also permits recombination of hydrogen and oxygen gas to form water resulting in a maintenance-free battery.

Lead–acid batteries are expected to dominate demand for lead. In 2002, North American shipment of SLI batteries were expected to decline 3% to 19.8×10^6 units of automotive original equipment and by 5% to 81.4×10^6 units in the automotive replacement sector (210). Demand for industrial type lead-acid batteries were expected to decline by 2% in the motive power sector and by 5% in the stationary power sector.

The U.S. industrial battery market has grown over a 10-year period rate of 6–8% to posting a 15% drop in demand in 2001. However, for the period 2003–2006 the demand is expected to grow at the rate of 6–8% (211).

2.9. Recycling. Battery Council International reported that the U.S. battery industry recycled 93.3% of the available lead scrap from spent lead-acid batteries during the year 1995–1999 (100). The high rate is the result of a successful collaboration among members of the battery industry, retailers, and consumers.

Law are now in place in 42 states that prohibit the disposal of spent lead–acid batteries and require collection through consumer return procedure when a replacement battery is purchased (212).

3. Other Cells

3.1. Introduction. The proliferation of portable electronic devices has fueled rapid market growth for the rechargeable battery industry. Miniaturization of electronics coupled with consumer demand for lightweight batteries providing ever longer run times continues to spur interest in advanced battery systems. Interest also continues to run strong in electric vehicles (EVs) and the large auto manufacturers continue to develop prototype EVs. It is clear that advances in battery technology are required for a widely acceptable EV. Advanced batteries continue to play a strong role in other applications such as load leveling for the electric utility industry and satellite power systems for aerospace.

The goal of advanced battery research is to develop batteries that supply a high number of watt · hours in a small volume (volumetric energy density) and at low weight (gravimetric energy density). Obviously this increase in energy density must be achieved in a manner that is manufacturable, safe, and of acceptable cost. There has been a significant growth in the number of advanced battery systems in development and several systems are either nearing commercial viability or have been introduced as commercial products in specific applications.

3.2. Ambient Temperature Lithium Systems. Traditionally, secondary battery systems have been based on aqueous electrolytes. Whereas these systems have excellent performance, the use of water imposes a fundamental limitation on battery voltage because of the electrolysis of water, either to hydrogen at cathodic potentials or to oxygen at anodic potentials. The application of nonaqueous electrolytes affords a significant advantage in terms of achievable battery voltages. By far the most actively researched field in nonaqueous battery systems has been the development of practical rechargeable lithium batteries

(213). These are systems that are based on the use of lithium [7439-93-2] metal, Li, or a lithium alloy, as the negative electrode (see LITHIUM AND LITHIUM COMPOUNDS).

The use of lithium as a negative electrode for secondary batteries offers a number of advantages (214). Lithium has the lowest equivalent weight of any metal and affords very negative electrode potentials when in equilibrium with solvated lithium ions resulting in very high theoretical energy densities for battery couples. These high theoretical energy densities have prompted a wealth of research activity in a wide variety of experimental battery systems. However, realization of the technology to commercialize these systems has been slow.

A key technical problem in developing practical lithium batteries has been poor cycle life attributable to the lithium electrode (215). The highly reactive nature of freshly plated lithium leads to reactions with electrolyte and impurities to form passivating films that electrically isolate the lithium metal (216). This isolation results in less than 100% current efficiency for cycling of the lithium electrode, hence limiting cycle life (217). A goal of research for practical rechargeable lithium systems has been to improve the cycling efficiency of the lithium electrode in aprotic electrolytes. Improved cathodes are mentioned in the patent literature. See Refs 218–220 for examples.

The choice of battery electrolyte is of paramount importance to achieving acceptable cycle life because of the high reducing power of the metallic lithium. The formation of surface films on the lithium electrode (221) imparts the apparent stability of the electrolyte to the electrode. It is critical to determining lithium cycling efficiency. In addition to providing a stable film in the presence of lithium, the electrolyte must satisfy additional requirements including good conductivity, being in the liquid range over the battery operating temperature, and electrochemical stability over a wide voltage range. Solubility of the electrolyte salt in the solvent system is important in achieving good conductivity (222). In order to satisfy the various electrolyte system requirements, the use of mixed solvent electrolytes has become common in practical cells. Examples are tetrahydrofuran [109-99-9], C_4H_8O, -based electrolytes (223) or ethylene carbonate [96-49-1], $C_2H_4O_3$, –propylene carbonate [108-32-7], $C_4H_6O_3$, mixed solvent systems (224). Typical electrolyte salts include lithium perchlorate [7791-03-9], $LiClO_4$, lithium hexafluoroarsenate [29935-35-1], $LiAsF_6$, or lithium tetrafluoroborate [14283-07-9], $LiBF_4$ (225). The progress in the development of liquid electrolyte systems that provide near 100% current efficiencies for cycling of lithium has played a critical role in the emergence of rechargeable lithium as a commercially viable technology.

A second class of important electrolytes for rechargeable lithium batteries are *solid* electrolytes. Of particular importance is the class known as solid polymer electrolytes (SPEs). SPEs are polymers capable of forming complexes with lithium salts to yield ionic conductivity. The best known of the SPEs are the lithium salt complexes of poly(ethylene oxide) [25322-68-3] (PEO), $-(CH_2CH_2O)_n-$, and poly(propylene oxide) [25322-69-4] (PPO) (226–228). Whereas a number of experimental battery systems have been constructed using PEO and PPO electrolytes, these systems have not exhibited suitable conductivities at or near room temperature. A new heteroatomic polymer for more efficient solid polymer electrolytes for lithium batteries has been patented. These

Table 6. **Theoretical Energy Densities for Rechargeable Lithium Systems**

Battery couple	Operating voltage range, V	Energy density	
		W · h/kg	W · h/L
Li–CoO_2	4.4–2.5	766	2700
Li–MnO_2	3.5–2.0	415	553
Li–V_2O_5	3.5–2.0	541	1304
Li–TiS_2	2.6–1.6	473	1187
Li–$NbSe_3$	2.1–1.5	436	1600
Li–MoS_2	2.3–1.3	233	882

polyalkyl or polyfluoroalkyl heteroatomic polymers are superior to similar solid polymer electrolytes composed of polyethylene oxide (229).

The lithium or lithium alloy negative electrode systems employing a liquid electrolyte can be categorized as having either a solid positive electrode or a liquid positive electrode. Systems employing a solid electrolyte employ solid positive electrodes to provide a solid-state cell. Another class of lithium batteries are those based on conducting polymer electrodes. Several of these systems have reached advanced stages of development or initial commercialization such as the Seiko Bridgestone lithium polymer coin cell.

The most important rechargeable lithium batteries are those using a solid positive electrode within which the lithium ion is capable of intercalating. These intercalation, or insertion, electrodes function by allowing the interstitial introduction of the Li^+ ion into a host lattice (230,231). The general reaction can be represented by the equation:

$$x\,Li^+ + x\,e^- + MY_n \rightleftharpoons Li_xMY_n$$

where MY_n represents a layered compound. A large number of inorganic compounds have been investigated for their ability to function as a reversible positive electrode in a lithium battery. Intercalation electrodes have found wide application in systems employing both liquid or solid electrolytes. The theoretical electrochemical characteristics of the most advanced of these electrode systems are described in Table 6.

Solid Electrolyte Systems. Whereas there has been considerable research into the development of solid electrolyte batteries (232–235), development of practical batteries has been slow because of problems relating to the low conductivity of the solid electrolyte. The development of an all solid-state battery would offer significant advantages. Such a battery would overcome problems of electrolyte leakage, dendrite formation, and corrosion that can be encountered with liquid electrolytes.

The general configuration of one system that has reached an advanced stage of development (236) is shown in Figure 35. The negative electrode consists of thin lithium foil. The composite cathode is composed of vanadium oxide [12037-42-2], V_6O_{13}, mixed with polymer electrolyte. Demonstration batteries have been constructed having energy densities of 320 W · h/L. A key to the technology is a unique radiation cross-linked polymer electrolyte which shows good conductivity at ambient temperatures (237).

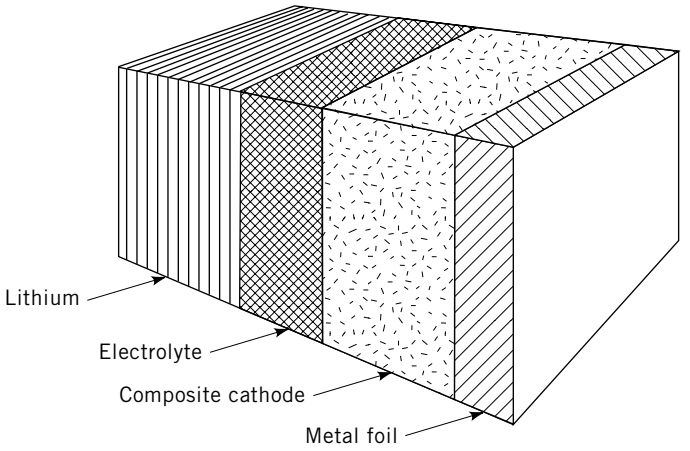

Fig. 35. Configuration for a solid polymer electrolyte rechargeable lithium cell where the total thickness is 100 μm. Courtesy of Mead Corp.

A new all solid-state lithium battery employing a positive electrode comprised of organosulfur polymers, $-(SRS)_n-$, has been reported (238). During discharge of the battery, current is produced by cleavage of the sulfur–sulfur bonds in the polymer, depolymerizing the polymer. On charge, the process is reversed and the disulfides are polymerized back to their original form. This use of a polymerization–depolymerization reaction for a battery electrode is unique and this electrode is expected to offer significantly improved rate capability over intercalation electrodes. The organosulfur electrodes provide excellent stability and reversibility, which should result in long cycle life. Cells constructed to date have employed a PEO electrolyte and hence require operation at elevated temperature (239).

Coin and Button Cell Commercial Systems. Initial commercialization of rechargeable lithium technology has been through the introduction of coin or button cells. The earliest of these systems was the Li–C system commercialized by Matsushita Electric Industries (MEI) in 1985 (240,241). The negative electrode consists of a lithium alloy and the positive electrode consists of activated carbon [7440-44-0], carbon black, and binder. The discharge curve is not flat, but rather slopes from about 3 V to 1.5 V in a manner similar to a capacitor. Use of lithium alloy circumvents problems with cycle life, dendrite formation, and safety. However, the system suffers from generally low energy density.

A commercial introduction of a rechargeable Li–V_2O_5 coin cell having significantly higher energy density than the previous Li–C cell has been announced (242). This system employs a Li–Al alloy negative electrode coupled with a vanadium pentoxide [1314-62-1], V_2O_5, positive electrode. The cell voltage on discharge is 3 V. This cell is claimed to have twice the energy density of a conventional Ni–Cd cell (243).

A rechargeable coin cell that employs a lithium salt electrolyte but avoids the use of a metallic lithium negative electrode has been commercially introduced by Toshiba. This cell employs a material called linear-graphite hybrid (LGH) in lieu of a lithium electrode to avoid formation of lithium dendrites.

LGH is synthesized by carbonizing organic aromatic polymers. The LGH electrode is coupled with an amorphous V_2O_5 positive electrode to give a battery with a working voltage of 3 V to 1.5 V (244). A similar system employing pyrolytic carbon as a negative electrode has also been reported (245).

A significant development in commercial acceptance of rechargeable lithium was the introduction by Sanyo of rechargeable Li–MnO_2 coin and button batteries (246,247). Manganese dioxide [1313-13-9] is an attractive positive electrode system because of its relatively high and flat discharge voltage and the low cost of MnO_2. The widespread use of Li–MnO_2 primary batteries demonstrates the utility of this system. However, the rechargeability of the MnO_2 conventionally employed in primary cells was not sufficient to yield practical secondary cells. The breakthrough came in the modification of the crystal structure of the MnO_2 to improve rechargeability by a lithiation reaction (248). This modified MnO_2, referred to as composite dimensional manganese oxide (CMDO), is coupled with a Li–Al alloy having special additives to give excellent cycle life and stress resistance to prevent cracking and blistering of the alloy during cycling (249). Lithium batteries with new manganese oxide materials as lithium intercalation hosts have been patented (250). These batteries show significant improvement in cycling performance.

Advanced Systems. Applications for the coin and button secondary lithium cells is limited. However, researchers are working to develop practical "AA"-sized and larger cells. Several systems have reached advanced stages of development.

The first commercially available lithium "AA" cell was introduced in the early 1980s by Moli Energy Ltd. This cell, known as the Molicel, employs a molybdenum disulfide [1317-33-5], MoS_2, positive electrode coupled with a pure Li negative one (251). The cell is constructed in a spirally wound configuration using a microporous separator (Fig. 36). The cells have an open circuit voltage of about 2.3 V when fully charged. The discharge curve slopes, with a midpoint voltage of 1.2 V when discharged. The sloping discharge curve allows indication of state of charge (252). Cell capacity is about 600 mA for "AA" cells. Cycle life was found to be strongly dependent on operating conditions including depth of discharge, recharge and discharge currents, and voltage limits on charge and discharge. However, cycle lives of 300 cycles or more were achieved under normal cycling conditions (253).

One of the most widely studied intercalation electrode materials is titanium disulfide [12039-13-3], TiS_2. A number of factors make TiS_2 attractive for secondary lithium cells including good rate capability, high theoretical energy density, and a highly reversible intercalation reaction (254). Very high cycle lives have been demonstrated for TiS_2 electrodes (255). One of the earliest efforts to develop commercial lithium cells employed TiS_2 (256).

The development of "AA" Li–TiS_2 cells combines the excellent properties of TiS_2 and a proprietary method for preparing polymer bonded electrodes (257) to give a flexible, high capacity bonded electrode. Using this technology, "AA" cells have been constructed giving 1.05 A · h capacity at a voltage of 2.3 V to 1.6 V on discharge. Using excess Li for the negative electrode, cycle lives of 200 cycles are claimed for this cell. Other advantages are a good high rate capability (up to C rate), good gravimetric energy density, and very low self-discharge (258).

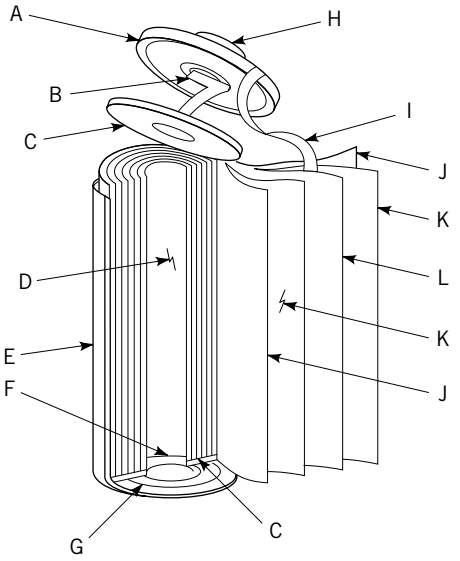

Fig. 36. Configuration for spirally wound rechargeable lithium cell. A, Cap; B, cathode tab; C, insulating disk (2); D, mandrel; E, can; F, ball; G, safety vent; H, glass-to-metal seal (with center pin); I, anode tab; J, cathode; K, separator; L, anode. Courtesy of Moli Energy Ltd.

A rechargeable lithium "AA" cell employing niobium triselenide [12034-78-5], $NbSe_3$, as the positive electrode material has been developed (259,260). The key to this system was a method for thermally growing $NbSe_3$ fibers that can then be pressed onto a current collector to provide a very high energy density electrode. No binder or additional conductive material is required. The excellent properties of this electrode also allow for higher discharge currents than those typically available for rechargeable lithium systems. Discharge rates in excess of C rate have been demonstrated. "AA" cells employing this technology give capacities of 1.1 $A \cdot h$ when cycled between 2.4 and 1.4 V. Cycle lives of over 250 cycles have been demonstrated for this cell (261).

An "AA" Li–MnO_2 cell was announced in the late 1980s, (262,263). This cell is claimed to offer considerable advantages over the conventional Ni–Cd system, offering higher energy density, high operating voltage, high rate capability, and excellent cycle life. A comparison of the parameters of these cells is shown in Table 7 (262).

An advanced Li–MnO_2 battery under the trade name Molicel^2 has been developed by Moli Energy Ltd. (264). The cell has a nominal voltage of 3 V, allowing replacement of two NiCd cells with one Molicel^2, hence significantly reducing battery pack size and volume. Production "AA" cells demonstrate a nominal capacity of 600 $mA \cdot h$ for an energy density of 100 $W \cdot h/kg$. Cycle life for this cell is reported to be typically 200 cycles (265).

Other solid cathode systems that have been widely investigated include those containing lithium cobalt oxide [12190-79-3], $LiCoO_2$ (266), vanadium pentoxide [1314-62-1], V_2O_5, and higher vanadium oxides, eg, V_6O_{13} (267,268).

Table 7. **Comparison of "AA"-Size Li–MnO_2 and NiCd Cells**

Parameter	Cell system		Parameter ratio
	Li–MnO_2	Ni–Cd	Li–MnO_2/Ni–Cd
cell weight, g	16.0	25.0	0.65
operating voltage, V	2.8[a]	1.2[b]	2.3
cutoff voltage, V	2.0	1.0	
energy at 0.8 W discharge, W · h	2.03	0.85	2.4
self-discharge after 1 mo	1%	25%	0.04
cycles (% DOD[c])			
at 0.85 W · h/cycle	1000 (40%)	500 (100%)	2
at 1.3 W · h/cycle	400 (64%)		
at 1.7 W · h/cycle	200 (84%)		

[a] Average voltage.
[b] Nominal voltage.
[c] DOD = depth of discharge

In addition to cells employing solid positive electrodes, a rechargeable lithium cell employing sulfur dioxide [7446-09-5], SO_2, as a liquid electrode has been developed (269). The widespread use of primary Li–SO_2 batteries, particularly by the U.S. military, led to a strong interest in developing a rechargeable version. The cell electrolyte for this system consists of liquidsulfur dioxide andlithium tetrachloroaluminate[14024-11-4], $LiAlCl_4$, salt. The overall cell chemistry of the rechargeable system involves the reduction and oxidation of a complex which forms between $LiAlCl_4$, SO_2, and the carbon that is employed as the current collector for the positive electrode. Specifications for a prototype Li–SO_2 "C"-sized cell are shown in Table 8 (269). Advantages for this system include very high energy densities, a flat running voltage, and the ability to sustain limited overcharge. The principal drawback has been safety concerns over potential cell ruptures on cycling resulting from internal short circuits.

Table 8. **Specifications for a Prototype Li–SO_2 "C" Cell**[a]

Parameter	Value
open circuit voltage, V	3.2
operating voltage, at C/6,[b] V	3.0
energy, W · h	5.4
volumetric energy density, W · h/L	220
gravimetric energy density, W · h/kg	134
operating temperature, °C	−30 to 40
cycle life, cycles	50
discharge rate	C/1.8[b,c]
charge rate	C/18[b,d]
charge retention after 9 mo	100%

[a] Where the nominal capacity is1.8 A · h to 2 V.
[b] Where C is the current required to discharge the cell in 1 hour.
[c] C/1.8 = 1 A.
[d] C/18 = 0.1 A.

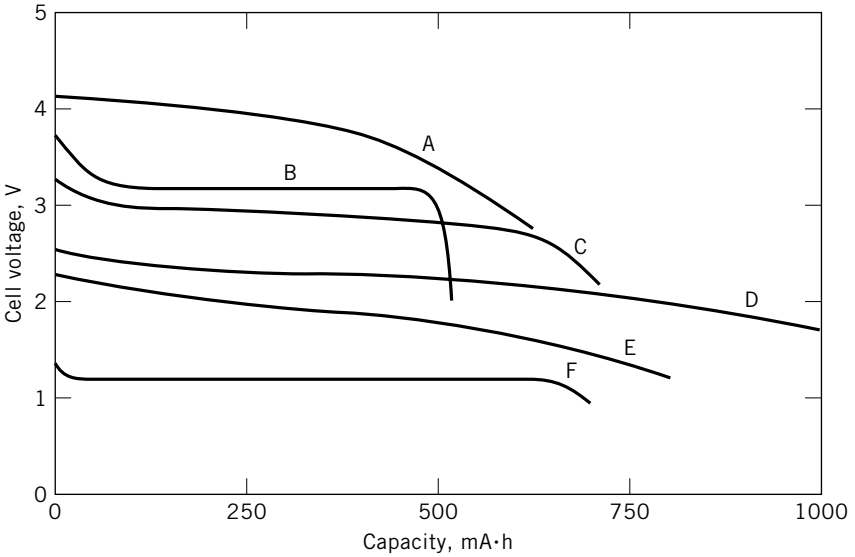

Fig. 37. Cell voltage profiles as a function of discharge capacity for rechargeable "AA" cells: A, Li ion; B, Li–SO_2; C, Li–MnO_2; D, Li–TiS_2; E, Li–MoS_2; F, Ni–Cd.

A related system employs a copper(II) chloride [7447-39-4], $CuCl_2$, electrode in a sulfur dioxide electrolyte (270). "AA" cells of nominal capacity of 500 mA · h at a discharge voltage of 3.4–3.0 V were constructed. Cycle life for this cell is claimed to be 200 cycles. The high voltage of this system offers a significant energy density advantage over conventional Ni–Cd systems.

The discharge performance characteristics of advanced rechargeable lithium "AA" cells and the Ni–Cd cell are illustrated in Figure 37. Whereas it is clear that a number of lithium systems offer energy capacities of significant improvement over conventional Ni–Cd cells, several critical issues remain for cell development before lithium technology gains widespread application. Cycle life continues to be a limitation to most technologies. Unlike Ni–Cd, there is no overcharge or overdischarge protection for the rechargeable lithium cells which generally must be recharged only within closely defined voltage limits. This presents a problem particularly in the design of multicell battery packs. Experiments using electrolyte additives to provide overcharge protection have been carried out (271), but this concept has not been demonstrated in advanced cell designs. Additionally, the high reactivity of lithium metal continues to pose serious safety concerns among battery manufacturers and users. Incidences of lithium cells exploding and/or igniting or venting with flame during use have highlighted the need for extensive safety testing of lithium-containing batteries prior to the widescale commercialization of this technology.

A lithium ion rechargeable cell has apparently been developed in response to safety concerns over the Li–MnO_2 cell. This technology is expected to be used for camcorder battery packs. The technical details of this battery have not been reported, but it is understood that the negative electrode consists of a carbon material capable of undergoing an insertion reaction with Li^+ ion (272). This

electrode is coupled with an insertion positive electrode such as lithium cobalt oxide (273). The resulting cell has a nominal operating voltage of 3.6 V, three times that of NiCd, providing a significant advantage in energy density (see Fig. 37) for multicell battery packs. The cell is claimed to be capable of rapid charge, discharge rates up to 2C, and 1200 cycles (274).

3.3. High Temperature Systems. *Lithium–Aluminum/Metal Sulfide Batteries.* The use of high temperature lithium cells for electric vehicle applications has been under development since the 1970s. Advances in the development of lithium alloy–metal sulfide batteries have led to the Li–Al/FeS system, where the following cell reaction occurs.

$$2\ \mathrm{LiAl}_x + \mathrm{FeS} \rightleftharpoons \mathrm{Fe} + \mathrm{Li_2S} + 2x\ \mathrm{Al}$$

The cell voltage is 1.33 V to give a theoretical energy density of458 $\mathrm{W \cdot h/kg}$ (275). The cell employs a molten salt electrolyte, most commonly a lithium chloride [7447-41-8]/potassium chloride [7447-40-7], LiCl–KCl eutectic mixture. The cell is generally operated at 400–500°C. The negative electrode is composed of lithium–aluminum alloy, which operates at about 300 mV positive of pure lithium. The positive electrode is composed of iron sulfide [1317-37-9] mixed with a conductive agent such as carbon or graphite. Electrodes are constructed by cold pressing powder onto current collectors (276).

Development of practical and low cost separators has been an active area of cell development. Cell separators must be compatible with molten lithium, restricting the choice to ceramic materials. Early work employed boron nitride [10043-11-5], BN, but a more desirable separator has been developed using magnesium oxide [1309-48-4], MgO, or a composite of MgO powder–BN fibers. Corrosion studies have shown that low carbon steel or stainless steel are suitable for the cell housing as well as for internal parts such as current collectors (277).

Li–Al/FeS cells have demonstrated good performance under EV driving profiles and have delivered a specific energy of 115 $\mathrm{W \cdot h/kg}$ for advanced cell designs. Cycle life expectancy for these cells is projected to be about 400 deep discharge cycles (278). This system shows considerable promise for use as a practical EV battery.

A similar system under development employs iron disulfide [12068-85-8], $\mathrm{FeS_2}$, as the positive electrode. Whereas this system offers a higher theoretical energy density than does Li–Al/FeS, the $\mathrm{FeS_2}$ cell is at a lower stage of development (279,280).

Sodium–Sulfur. The best known of the high temperature batteries is the sodium [7440-23-5]–sulfur [7704-34-9], Na–S, battery (281). The cell reaction is best represented by the equation:

$$2\ \mathrm{Na} + 3\ \mathrm{S} \rightleftharpoons \mathrm{Na_2S_3}$$

occurring at a cell voltage of 1.74 V, to give a specific energy of 760 $\mathrm{W \cdot h/kg}$. The cell is constructed using a solid electrolyte typically consisting of β-alumina [1344-28-1], $\beta\text{-}\mathrm{Al_2O_3}$, ceramic, although borate glass fibers have also been used. These materials have high conductivities for the sodium ion. The negative electrode consists of molten sodium metal and the positive electrode of molten sulfur.

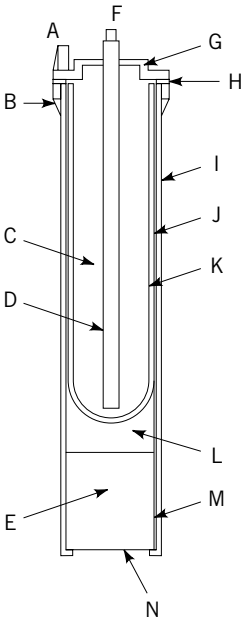

Fig. 38. Construction of a sodium–sulfur battery. A, Negative terminal; B, springs plus graphite felt; C, sulfur; D, carbon; E, sodium reservoir; F, positive terminal; G, insulator; H, aluminum sealing gaskets; I, steel case; J, film of sodium; K, β-alumina tube; L, carbon felt; M, wick; N, aluminum can (282).

Because sulfur is not conductive, a current collection network of graphite is required. The cell is operated at about 350°C. A typical cell design is shown in Figure 38. The outer cell case is constructed from mild steel. The β-alumina separator tube fits inside the cell case with a small gap in between. The positive electrode of molten sulfur is placed inside the alumina tube with a carbon current collector. The molten sodium is stored below the cell and is wicked into the space between the separator and outer cell casing. The mild steel case acts as the negative electrode current collector (282).

The Na–S battery couple is a strong candidate for applications in both EVs and aerospace. Projected performance for a sodium–sulfur-powered EV van is shown in Table 9 for batteries having three different energies (283). The advantages gained from using a Na–S system rather than the conventional sealed lead–acid batteries are evident.

Table 9. **Electric Vehicle Battery Performance**

	Battery			
Parameter	Lead–acid	Sodium–sulfur		
battery energy, kW · h	40.0	40.0	60.0	85.0
range, km	84.0	113.0	169.0	242.0
max payload, t	0.9	1.7	1.6	1.6
battery weight, kg	1250.0	330.0	424.0	580.0

The Na–S system is expected to provide significant increases in energy density for satellite battery systems (284). In-house testing of Na–S cells designed to simulate midaltitude (MAO) and geosynchronous orbits (GEO) demonstrated over 6450 and over 1400 cycles, respectively.

Difficulties with the Na–S system arise in part from the ceramic nature of the alumina separator: the specific β-alumina is expensive to prepare; and the material is brittle and quite fragile. Separator failure is the leading cause of early cell failure. Cell failure may also be related to performance problems caused by polarization at the sodium/solid electrolyte interface. Lastly, seal leakage can be a determinant of cycle life. In spite of these problems, however, the safety and reliability of the Na–S system has progressed to the point where pilot plant production of these batteries is anticipated for EV and aerospace applications.

A battery system closely related to Na–S is the Na–metal chloride cell (285). The cell design is similar to Na–S; however, in addition to the β-alumina electrolyte, the cell also employs a sodium chloroaluminate [7784-16-9], $NaAlCl_4$, molten salt electrolyte. The positive electrode active material consists of a transition metal chloride such as iron(II) chloride [7758-94-3], $FeCl_2$, or nickel chloride [7791-20-0], $NiCl_2$, (286,287) in lieu of molten sulfur. This technology is in a younger state of development than the Na–S.

Lithium-Polymer Batteries. The lithium-polymer battery differs from other batteries in the type of electrolyte used. The polymer electrolyte replaces the traditional porous separator, which is soaked in electrolytes. The dry polymer design is rugged and has a thin profile. No liquid or gel is used, thus there is no danger of flammability.

The conductivity of the dry lithium-polymer is poor. The internal resistance is too high, and cannot deliver the current bursts needed for modern communication devices. Some dry lithium polymers are used in hot climates as standby batteries. High ambient temperatures do not degrade the service life of the battery. Research continues to develop a battery that performs at room temperature and this should come to pass in 2005 (287).

Most lithium-polymer batteries are a hybrid. The only functioning polymer battery in use today is this hybrid, more correctly know as lithium-ion polymer. The electrolyte in the lithium-ion polymer is solid and replaces the porous separator. Gelled electrolyte is added to enhance ion conductivity.

There have been technical difficulties manufacturing this battery. At present its only advantage is form. Wafer thin batteries are highly desirable in the mobile phone industry.

3.4. Economic Aspects. Almost all major battery manufacturers marketed some type of lithium battery. Research and development continued and innovative rechargeable battery configurations continue to be developed to meet the changing requirements of electronic equipment such as portable phones, computers, and video cameras. Lithium-ion batteries are of interest because they take advantage of the large power capacity available with fewer safety problems. Electric vehicles are considered a large potential market for lithium batteries, but general acceptance of these vehicles is slow. There is also the possibility that fuels cells will be the preferred source of power.

The consumption of lithium compounds in lithium batteries is one of the most rapidly expanding markets for lithium. Demand for lithium metal for batteries is expected to grow. Lithium-ion and lithium polymer batteries appear to posses the greatest potential for growth. First introduced in 1993, with minimal sales, the market for these rechargeable batteries grew to $\$3 \times 10^9$ in 1998 and is expected to top $\$6 \times 10^9$ by 2005 (288).

BIBLIOGRAPHY

The Alkaline Secondary Cells are treated in *ECT* 1st ed., under "Cells, Electric," Vol. 3, pp. 292–342, by W. J. Hamer, National Bureau of Standards, and "Cells, Electric," Suppl. 2, pp. 126–161, by C. K. Morehouse, R. Glicksman, and G. S. Lozier, Radio Corporation of America; "Batteries and Electric Cells, Secondary, Secondary Cells, Alkaline," in *ECT* 2nd ed., pp. 172–249, by W. W. Jakobi, Gould-National Batteries, Inc.; "Batteries and Electric Cells, Secondary, Alkaline Cells," in *ECT* 3rd ed., Vol. 3, pp. 592–639, by A. J. Salkind and E. Pearlman, ESB Technology Company; in *ECT* 4th ed., Vol. 3, pp. 1028–1083, by Alvin J. Salkind and Martin Klein, Rutgers University "Batteries, Electric (Lead-Acid Storage)" in *ECT* 1st ed., Vol. 2, pp. 340–360, by Joseph A. Orsino and Thomas C. Lynes, National Lead Company; "Secondary Cells, Lead–Acid" under "Batteries and Electric Cells, Secondary" in *ECT* 2nd ed., Vol. 3, pp. 249–271, by Joseph A. Orsino, National Lead Company; "Batteries and Electric Cells, Secondary (Lead–Acid)" in *ECT* 3rd ed., Vol. 3, pp. 640–663, by James B. Doe, ESB Technology Company; in *ECT* 4th ed., Vol. 3, pp. 1083–1107, by Kathryn R. Bullouk and John R. Pierson, Johnson Controls, Inc.; "Batteries and Electric Cells, Secondary (Other Cells)" in *ECT* 3rd ed., Vol. 3, pp. 663–670, by J. B. Doe, ESB Technology, Co.; in *ECT* 4th ed., Vol. 3, pp. 1101–1121, by Paul R. Gifford, Ovonic Battery Company.

CITED PUBLICATIONS

1. H. Takeshita, *Presentation at the 20th International Seminar and Exhibit on Primary and Secondary Batteries*, March 17, 2003.
2. Ger. Pat. 491,498 (July 6, 1928), K. Ackermann, P. Gomelin, G. Pfleiderer, and F. Spouna (to I. G. Farbenindustrie, A. G.); Brit. Pat. 331,540 (Jan. 4, 1929), 332,052 (July 8, 1929), 380,242 (1930), 339,645 (1930), to (I. G. Farbenindustrie, A. G.).
3. U.S. Pat. 2,571,927 (Oct. 16, 1951), U. Gottesman and G. Newmann (to Bureau Technique Gautrat Sarl); Brit. Pat. 784,851 (1952), (to Bureau Technique Gaurat).
4. Ger. Pat. 112,351 (1899); Brit. Pat. 15,370 (1899), T. De Michalowski.
5. Swed. Pat. 11,132 (1889), W. Jungner.
6. A. Fleischer, *J. Electrochem. Soc.* **94**, 289 (1948). A. Fleischer, *Proc. 10th Ann. Battery Res. Conf.* **73** (1956). U.S. Pat. 2,771,499 (1951), A. Fleischer.
7. G. W. Briggs, E. Jones, and W. F. K. Wynne-Jones, *Trans. Faraday Soc.* **51**, 1433 (1955); G. W. Briggs and W. F. K. Wynne-Jones, *Trans. Faraday Soc.* **52**, 1972 (1956).
8. A. J. Salkind and P. F. Bruins, *Nickel–Cadmium Sandia Project Reports*, Polytechnic University of Brooklyn, N.Y., 1956–1958; *J. Electrochem. Soc.* **108**, 356–360 (1962).
9. U.S. Pat. 2,819,962 (1958), (to SAFT).
10. J. A. McMillan, *Acta Cryst.* **7**, 640 (1954); *J. Inorg. Nucl. Chem.* **13**, 28 (1960).

11. V. Scatturin, P. Bellon, and A. J. Salkind, *J. Electrochem. Soc.* **108**, 819 (1961).
12. P. L. Bourgault and B. E. Conway, *Can. J. Chem.* **38**, 1557 (1960).
13. S. U. Falk, *J. Electrochem. Soc.* **107**, 661 (1960).
14. U.S. Pat. 3,003,015 and 3,121,029 (1961), J. C. Duddy.
15. A. J. Salkind and J. C. Duddy, *J. Electrochem. Soc.* **109**, 360 (1962).
16. D. Tuomi, *J. Electrochem. Soc.* **112**, 1 (1965).
17. H. Bode, K. Dehmelt, and J. Witte, *Crystal Structures of Nickel Hydroxides*, CITCE Meeting, Strasbourg, France, 1965.
18. Brit. Pat. 917,291 (1963), L. Kandler; U.S. Pat. 3,282,808 (1966), L. Kandler; E. Hausler, *5th Int. Power Sources Symp.* **287** (1966).
19. E. J. McHenry, *Electrochem. Tech.* **5**, 275–279 (1965).
20. U.S. Pat. 3,653,967 (1972), R. L. Beauchamp.
21. U.S. Pat. 3,873,368 (1972), D. F. Pickett.
22. M. A. Gutjahr, H. Buckner, K. D. Beccu, and H. Saufferer, in D. H. Collins, ed., *Power Sources*, Vol. 4, Oriel Press, UK, 1973, p. 79.
23. U.S. Pat. 3,898,099 (1975), B. Baker and M. Klein.
24. J. Edwards, T. Turner, and J. Whittle, *Proc. Int. Power Sources* **7**, (1970). U.S. Pat. 3,785,867 (1974), J. Edwards and J. Whittle.
25. U.S. Pat. 4,215,190 (1980), R. A. Ferrando and R. Satula.
26. U.S. Pat. 4,298,383 (1981); 4,312,670 (1981), J. F. Joyce and S. L. Colucci.
27. B. Bugnet and D. Doniat, *Proceedings of the 31st Power Sources Conference* 1984.
28. *DAUG Co. literature*, Germany, 1985.
29. K. Kordesch, J. Gsellmann, W. Harer, W. Taucher, and K. Tomantschger, *Prog. Batt. Solar Cells* **7**, 194–204 (1988); K. Kordesch and co-workers, *Electrochim. Acta* **26**, 1495 (1981).
30. U.S. Pat. 4,451,543 (1984), M. A. Dzieciuch, N. Gupta, H. Wroblowa, and J. T. Kummer; U.S. Pat. 4,520,005 (1985), Y. Y. Yao.
31. *Commercial literature*, Ovonic Battery Co., Troy, Mich, 1991; Matsushita Battery Co., Seattle, Wash., Oct. 1990; Toshiba Co., Seattle, Wash., Oct. 1990; Gates Battery Co., Gainsville, Fla., 1991; N. Furukawa, *JEC Battery Newsletter #2*, Sanyo Battery Co., JEC Press, Brunswick, Ohio, 1990.
32. Tayata, Honda commercial literature.
33. U.S. Pat. 6,596,436 (July 22, 2003), M. Maruta and co-workers (to Matsushita Electric Industrial Co., Ltd.).
34. U.S. Pat. 6,548,210 (April 15, 2003), K. Shinyama and co-workers (to Sanyo Electric Co., Ltd.).
35. U.S. Pat. 6,562,516 (May 13, 2003), K. Ohta and co-workers (to Matsushita Electric Industrial Co., Ltd.)
36. P. C. Milner and U. B. Thomas, P. Delahay and C. W. Tobias, eds., *Advances in Electrochemistry and Electrochemical Engineering*, Vol. 5, Interscience Publishers, New York, 1967.
37. Swed. Pat. 15,567 (1901), W. Jungner; Ger. Pat. 163,170 (1901), W. Jungner.
38. J. P. Harivel and co-workers, *Proceedings of the 5th International Power Sources Symposium*, Brighton, England, Sept. 1966.
39. B. C. Bradshaw, *Proceedings of the Annual Power Sources Conference* **12**, (1958).
40. F. Kornfeil, in Ref. 39.
41. B. V. Ershler, G. S. Tyvrikov, and A. S. Smirnova, *J. Phys. Chem. (USSR)* **14**, 985 (1940).
42. G. Halpert and L. May, *Extended Abstracts 169th Meeting of the Electrochemical Society*, Washington, D.C., Oct. 1983.
43. J. McBreen, W. E. O'Grady, K. I. Panda, R. W. Hoffman, and D. E. Sayers, *Langmuir* **3**, 428–433 (1987).

44. A. H. Zimmerman and P. K. Effa, *Extended Abstracts, 168th Meeting of the Electrochemical Society*, Oct. 1985.
45. D. T. Fritts, *Extended Abstracts, 164th Electrochemical Society*, Oct. 1983.
46. A. Estelle, *Tekn. Tidskizift* **39**, 105 (1909).
47. G. Halpert, *Proc. 176 Electrochem. Soc.* Oct. 1989.
48. "Cadmium," *Mineral Commodity Summaries*, U.S. Geological Survey, Reston, Va., Jan. 2003; *Minerals Yearbook*, 2001.
49. U.S. Pat. Appl. 20030160590 (Aug. 28, 2003), M. A. Schaefer and R. R. Reinhart (to Linvatec Corp.).
50. L. Ojefors, G. Kramer, and V. A. Olinpunom, *Proceedings of the 9th International Society for Electrochemistry*, Marcoussis, France, 1975; B. Andersson and L. Ojefors, *11th International Power Sources Symposium*, Brighton, England, 1978; *J. Electrochem. Soc.* **123**, 824 (1976).
51. A. Nilsson, private communication, 1991.
52. E. R. Bowerman, "Sintered Iron Electrode," *Proc. 22 Power Sources Conf.* (1968).
53. W. A.Bryant, *J. Electrochem. Soc.* **126**, 1899–1901 (1979).
54. Project reports, Eagle-Picher Co., Joplin, Miss., 1988–1991.
55. A. J. Salkind, J. J. Kelley, and J. B. Ockerman, *Proc. 176 Electrochem. Soc. Meet.* (Oct. 1989).
56. Reports on EPRI Nickel–Iron Electric Vehicle Project, Argonne National Labs, Argonne, Ill., 1988–1991.
57. R. Swaroop, *Reports on Electric Vehicle Batteries*, Electric Power Research Institute (EPRI), Palo Alto, Calif., 1989–1991.
58. T. Iwaki, T. Mitsumata, and H. Ogawa, *Prog. in Batt. Solar Cells* **4**, 255–259 (1982).
59. S. Hills and A. J. Salkind, "Alkaline Iron Electrode," *Proc. 22 Power Sources Conf.* (1968).
60. A. J. Salkind, C. J. Venuto, and S. U. Falk, *J. Electrochem. Soc.* **111**, 493–495 (1964).
61. P. Hersch, *Trans. Faraday Soc.* **51**, 1442–1448 (1955).
62. U.S. Pat. 2,644,022 (1953), J. Moulton and E. F. Schweitzer.
63. U.S. Pat. 3,483,291 (Dec. 16, 1969), M. J. Mackenzie and A. J. Salkind.
64. D. S. Poa, J. F. Miller, and N. P. Yao, *Argonne National Labs Report # ANL/OEPM-85-2*, Apr. 1985.
65. H. G. André, *Bull. Soc. Franc. Electriciens* **6**, 1, 132 (1941).
66. U.S. Pat. 2,317,711 (Apr. 27, 1943), H. G. André.
67. J. A. McMillan, *J. Inorg. Nucl. Chem.* **13**, 28 (1960).
68. V. Scatturin, P. Bellon, and A. J. Salkind, *J. Electrochem. Soc.* **108**, 819 (1961).
69. A. J. Salkind "Crystal Structures of the Silver Oxides," in A. Fleischer and J. J. Lander, eds., *Zinc–Silver Oxide Batteries*, John Wiley & Sons, Inc., New York, 1971.
70. *The Silver Institute Letter*, Vol. VII, No. 9, Oct. 1977.
71. N. A. Zhulidov and F. I. Yefrennov, *Vestn. Elektropromsti.* **2**, 74 (1963); M. C. Tisgankov, *Electrical Accumulators*, Moscow (1959).
72. V. N. Flerov, *Zh. Prikl. Khim.* **32**, 1306 (1959).
73. P. Goldberg, "Nickel–Zinc Cells Part 1," *Proceedings of the 21st Annual Power Sources Conference*, 1967.
74. P. V. Popat, E. J. Rubin, and R. B. Flanders, "Nickel–Zinc Cells Part 3," *Proceedings of the 21st Annual Power Sources Conference*, 1967.
75. M. J. Sulkes, "Nickel–Zinc Secondary Batteries," *Proceedings of the 23rd Annual Power Sources Conference*, 1969.
76. A. Charkey, "Sealed Nickel–Zinc Cells *Proceedings of the 25th Annual Power Sources Conference*, Atlantic City, N.J., 1972.
77. A. Charkey, "Nickel–Zinc Cells for Sustained High-Rate Discharge," *Proceedings of the 7th Intersociety Energy Confersion Engineering Conference*, 1972.

78. *Design and Cost Study Zinc–Nickel Oxide Battery for Electric Vehicle Propulsion in Final Report, ANL Contract No. 109-38-3543*, Yardney Elect. Corp., Oct. 1976.
79. Final Report, *Design and Cost Study of Nickel–Zinc Batteries for Electric Vehicles, ANL Contract No. 31-109-38-3541*, Energy Research Corp., Oct. 1976.
80. D. P. Boden and E. Pearlman, in D. H. Collins, ed., *Power Sources*, Vol. 4, Academic Press, New York, 1972.
81. J. M. Parry, C. S. Leung, and R. Wells, *Structure and Operating Mechanisms of Inorganic Separators, Report NASA CR-134692*, Mar. 1974.
82. Brit. Pat. 365,125 (1930), J. J. Drumm.
83. Ger. Pat. 2,150,005 (May 25, 1972), O. von Krusenstierna (to AGA Aktiebolaget); U.S. Pat. 3,923,550 (Dec. 2, 1975), O. von Krusenstierna (to AGA Aktiebolaget); O. von Krusenstierna, *SAE Meeting*, Mar. 4, 1977, paper 21.
84. J. Giner and J. D. Dunlop, *Electrochem. Soc.* **122**, 4 (1975).
85. M. Klein and M. George, *Proceedings of the 26th Power Sources Symposium*, Atlantic City, N.J., 1974, p. 18.
86. J. E. Clifford and E. W. Brooman, *Assessment of Nickel–Hydrogen Batteries for Terrestrial Solar Applications*, SAND80-7191, Sandia National Laboratories, 1981.
87. A. J. Salkind, *Samples of Metal Hydrides*, International Battery Materials Association.
88. H. Ogawa, M. Ikoma, H. Kawano, and I. Matsumoto, "Metal Hydride Electrode for High Energy Density Sealed Nickel–Metal Hydride Battery," *Proceedings of the 16th International Power Sources Conference*, UK, 1988.
89. "Nickel," *Mineral Commodity Summaries*, U.S. Geological Survey, Reston, Va., Jan. 2003; *Minerals Yearbook*, 2001.
90. M. Klein, in D. H. Collins, ed., *Power Sources*, Vol. 5, Academic Press, New York, 1974; P. Antoine and P. Fougtere, in J. Thompson, ed., *Power Sources*, Vol. 7, Academic Press, New York, 1979.
91. A. J. Appleby and J. M. Jacquier, *J. Power Sources* **1** (1976).
92. M. Klein and A. Charkey, *Zinc–Oxygen Battery Development*, Electrochemical Society, Atlanta, Ga., Oct. 1977.
93. L. Ojefors and L. Carlson, *J. Power Sources* **2** (1977–1978).
94. B. G. Demezyk, W. A. Bryant, C. T. Liu, and E. S. Buzzelli, "Performance and Structural Characteristics of the Iron–Air Battery System", 15th IECEC Conference, 1980.
95. E. Findl and M. Klein, "Electrolytic Hydrogen–Oxygen Fuel, Cell Battery", *Proceedings of the 20th Power Sources Conference*, Red Bank, N.J., 1966.
96. M. Klein and R. Costa, "Electrolytic Regenerative H2–O2 Secondary Fuel Cell", *Proceedings of Space Technology Conference, ASME*, June 1970.
97. A. L. Almerini and S. J. Bartosh, "Simulated Field Tests on Zinc–Air Batteries", *Proceedings of the 26th Power Sources Symposium*, Atlantic City, N.J., 1974.
98. W. R. Momyer and E. L. Litauer, "Development of a Lithium Water–Air Primary Battery", *Proceedings of the 15th Intersocietal Energy Conversion Engineering Conference*, Seattle, Wash., Aug. 1980.
99. J. F. Cooper, R. V. Homsy, and J. H. Landrum, "The Aluminum–Air Battery for Electric Vehicle Propulsion", in Ref. 98.
100. G. R. Smith, "Lead," *Minerals yearbook*, U.S. Geological Survey, Reston, Va., 2001.
101. *Storage Battery Technical Service Manual*, 10th ed., Battery Council International, Chicago, 1987.
102. K. Eberts and O. Jache, in *Lead 65, Proceedings of the 2nd International Conference on Lead-Arnheim, Belgium*, Pergamon Press, Inc., Elmsford, N.Y., 1967, p. 199.
103. D. H. McClelland, *Prog B&S* **3**, 194 (1980).

104. G. Planté, *Compt. Rend.* **49**, 402 (1859); *Recherches sur l'electricite'*, Gauthier-Villars, Paris, 1883, pp. 35, 36, 40.
105. R. H. Schallenberg, *Bottled Energy: Electrical Engineering and the Evolution of Chemical Energy Storage*, American Philosophical Society, Philadelphia, Pa., 1982.
106. T. A. Edison, *The Beginning of the Incandescent Lamp and Lighting System*, The Edison Institute, Dearborn, Mich., 1976.
107. Brit. Pat. 129 (Jan. 11, 1881), C. Fauré.
108. Brit. Pat. 3926 (Sept. 10, 1881), J. S. Sellon.
109. K. R. Bullock, "The Development and Applications of Storage Batteries—Historical Perspectives and Future Prospects," in *Proceedings, 7th Australian Electrochemistry Conference*, 1988.
110. J. H. Gladstone and A. Tribe, *Nature (London)* **27**, 583 (1883).
111. G. W. Vinal, *Storage Batteries*, 4th ed., John Wiley & Sons, Inc., New York, 1955.
112. W. H. Beck and W. F. K. Wynne-Jones, *Trans. Faraday Soc.* **50**, 136 (1954).
113. A. K. Covington, J. W. Dobson, and W. F. K. Wynne-Jones, *Trans. Faraday Soc.* **61**, 2050 (1965).
114. H. Bode, *Lead–Acid Batteries* (translated by R. J. Brodd and K. V. Kordesch), John Wiley & Sons, Inc., New York, 1977.
115. K. R. Bullock, *J. Power Sources* **35**, 197 (1991).
116. H. E. Wirth, *Electrochim. Acta* **50**, 1345 (1971).
117. W. L. Gardner, R. E. Mitchell, and J. W. Cobble, *J. Phys. Chem.* **73**, 2021 (1969).
118. T. H. Lilley and C. C. Briggs, *Electrochim. Acta* **20**, 257 (1975).
119. R. A. Robinson and R. H. Stokes, *Electrolyte Solutions*, 2nd ed., Butterworths, London, 1959, p. 477.
120. R. H. Gerke, *J. Am. Chem. Soc.* **44**, 1684 (1922); *Chem. Rev.* **1**, 377 (1925).
121. J. A. Duisman and W. F. Giauque, *J. Phys. Chem.* **72**, 562 (1968).
122. W. F. Giauque, E. W. Hornung, J. E. Kunzler, and T. R. Rubin, *J. Am. Chem. Soc.* **82**, 62 (1960).
123. W. H. Beck, K. P. Singh, and W. F. K. Wynne-Jones, *Trans. Faraday Soc.* **55**, 331 (1959).
124. W. H. Beck, J. V. Dobson, and W. F. K. Wynne-Jones, *Trans. Faraday Soc.* **56**, 1172 (1960).
125. K. R. Bullock, *J. Electrochem. Soc.* **127**, 662 (1980).
126. J. Burbank, A. C. Simon, and E. Willihnganz, in C. W. Tobias, ed., *Advances in Electrochemistry and Electrochemical Engineering*, Vol. 8, Wiley-Interscience, New York, 1971, p. 157.
127. J. L. Dawson, in A. T. Kuhn, ed., *The Electrochemistry of Lead*, Academic Press, London, 1979, p. 309.
128. A. T. Kuhn, in Ref. 127, p. 365.
129. D. Pavlov, in B. D. McNicol and D. A. J. Rand, eds., *Power Sources for Electric Vehicles*, Elsevier, Amsterdam, 1984, p. 111.
130. K. R. Bullock, *J. Electroanal. Chem.* **222**, 347 (1987).
131. K. R. Bullock and D. Pavlov, eds., *Proceedings of the Symposium on Advances in Lead Acid Batteries*, 84-14, The Electrochemical Society, Pennington, N.J., 1984.
132. D. A. J. Rand and D. Pavlov, eds., *Proceedings of LABAT-89*, Varna, 1989; *J. Power Sources*, Vols. 30 and 31, 1990.
133. D. A. J. Rand, *J. Power Sources* **15**, B1 (1985); **18**, B31 (1986); **21**, B1 (1987); **27**, B1 (1989).
134. D. Simonsson, *J. Appl. Electrochem.* **3**, 261 (1973); **4**, 109 (1974); *J. Electrochem. Soc.* **120**, 151 (1973).
135. K. Micka and I. Rousar, *Electrochim. Acta.* **18**, 629 (1973); **19**, 499 (1974); **21**, 599 (1976); *Colln. Czech. Chem. Commun.* **40**, 921 (1975).

136. J. Newman and W. Tiedemann, *J.A.I.Ch.E.* **21**, 25 (1975).
137. W. Tiedemann and J. Newman, *J. Electrochem. Soc.* **122**, 70 (1975); S. Gross, ed., *Proceedings of the Symposium on Battery Design and Optimization*, 79-1, The Electrochemical Society, Inc., Princeton, N.J., 1979, pp. 23, 39.
138. W. Tiedemann and J. Newman, in K. R. Bullock and D. Pavlov, eds., *Proceedings of the Symposium on Advances in Lead–Acid Batteries*, 84-14, The Electrochemical Society, Inc., Princeton, N.J., 1984, p. 336.
139. B. L. McKinney, W. Tiedemann, and J. Newman, in Ref. 138, p. 360.
140. A. Eklund, D. Simonsson, R. Karlsson, and F. N. Bark, "Theoretical and Experimental Studies of Free Convection and Stratification of Electrolyte in a Lead–Acid Cell," LABAT-89 Conference, Varna, Bulgaria, 1989.
141. S. Atlung and B. Fastrup, *J. Power Sources* **13**, 39 (1984).
142. D. M. Bernardi, *Extended Abstracts* 88-2, The Electrochemical Society, Inc., Princeton, N.J., 1988, p. 1.
143. N. E. Bagshaw, K. P. Bromelow, and J. Eaton, in D. H. Collins, ed., *Power Sources 6, Proceedings 10th International Power Sources Symposium*, Academic Press, Inc., New York, 1977, p. 1.
144. W. Tiedemann, J. Newman, and E. DeSua, in D. H. Collins, ed., *Power Sources 6*, 1977, p. 15.
145. J. H. Gladstone and A. Tribe, *Nature* **25**, 221 (1882).
146. P. Ruetschi and R. T. Angstadt, *J. Electrochem. Soc.* **105**, 555 (1958).
147. K. R. Bullock and D. H. McClelland, *J. Electrochem. Soc.* **123**, 327 (1976).
148. K. R. Bullock and E. C. Laird, *J. Electrochem. Soc.* **129**, 1393 (1982).
149. J. S. Symanski, B. K. Mahato, and K. R. Bullock, *J. Electrochem. Soc.* **138**, 548 (1988).
150. C. S. C. Bose and N. A. Hampson, *J. Power Sources* **19**, 261 (1987).
151. J. Mrha, K. Micka, J. Jindra, and M. Musilova, *J. Power Sources* **27**, 91 (1989).
152. R. F. Nelson and D. H. McClelland, in S. Gross, ed., *Battery Design and Optimization*, The Electrochemical Society, Princeton, N.J., 1979, p. 13.
153. U.S. Pat. 3,244,562 (Apr. 5, 1966), F. M. Coppersmith and G. J. Vahrenkamp (to National Lead Co.).
154. Ref. 114, pp. 162–176, 196–199, 207–216.
155. U.S. Pat. 4,900,643 (Feb. 13, 1990), M. D. Eskra, W. C. Delaney, G. K. Bowen.
156. V. M. Halsall and J. R. Pierson, "Plate Processing—The Heart of the Lead–Acid Battery," *BCI Proceedings*, June 1972.
157. U.S. Pat. 6,586,136 (July 1, 2003), R. Bkardway and co-workers (to Concorde Battery Corp.).
158. B. K. Mahato, *J. Electrochem. Soc.* **127**(8), 1679–1687 (1980).
159. B. K. Mahato, *J. Electrochem. Soc.* **128**(7), 1416–1422 (1981).
160. J. R. Pierson, P. Gurlusky, A. C. Simon, and S. M. Caulder, *J. Electrochem. Soc.* **117**(12), 1463–1469 (1970).
161. N. A. Hampson, J. B. Lakeman, and K. S. Sodhi, *Surface Technol.* **5**, 377–384 (1980).
162. N. A. Hampson and J. B. Lakeman, *J. Electroanal. Chem.* **119**, 3–15 (1981).
163. J. A. Orsino, "Mixing & Pasting—Part I," *The Battery Man*, Apr. 1982.
164. J. F. Dittmann and H. R. Harner, *Storage Battery Research*, Form No. A-391, Chemical Division, Eagle-Picher Co., Cincinnati, Ohio, 1956.
165. G. W. Vinal, *Storage Batteries*, 4th ed., John Wiley & Sons, Inc., New York, 1955, pp. 33 and 34.
166. S. Hattori and co-workers, *Final Report (ILZRO Project LE-197)*, International Lead–Zinc Research Organization, Inc., New York, 1976.
167. Ref. 114, 216–244.

168. J. Perkins, J. L. Pokorny, and M. T. Coyle, *Naval Postgraduate School (NPS) Report*, NPS-69PS76101, Monterrey, Calif., Oct. 1976, pp. 17–19, 23, 24.
169. J. R. Pierson and R. T. Johnson, *SAE Technical Paper Series 830277*, SAE International Congress & Exposition, Detroit, Mich., 1983.
170. Ref. 144, p. 15.
171. J. E. Puzey and W. M. Orriel, in D. H. Collins, ed., *Power Sources 2, Proceedings 6th International Power Sources Symposium*, Pergamon Press, Inc., Oxford, UK, 1968, p. 121.
172. H. Silverman, *Environmental Protection Agency Final Report*, Contract No. 68-04-0028, EPA, Washington, D.C., 1972.
173. *Prod. Eng.* **43** (1977).
174. U.S. Pat. 3,989,539 (Nov. 2, 1976), N. G. Grabb (to Varta Batteries, Ltd.).
175. U.S. Pat. 3,959,015 (May 25, 1976), J. Brinkmann, G. Trippe, and W. Heissman (to Varta Batterie AG).
176. Fr. Pat. 2,239,020 (Feb. 21, 1975), (to Société Fulmen et Compagnie Europeénne d Accumulateurs).
177. U.S. Pat. 3,956,012 (May 11, 1976), W. R. Scholle (to Scholle Corp.).
178. J. R. Pierson and C. E. Weinlein, "Development of Unique Lightweight, High Performance Lead–Acid Batteries," in J. Thompson, ed., *Power Sources 9*, Academic Press, London, 1983.
179. D. Marshall and W. Tiedemann, *J. Electrochem. Soc.* **123**(12), 1849–1855 (1976).
180. D. L. Douglas and G. W. Mao, in D. H. Collins, ed., *Power Sources 4, Proceedings 8th International Power Sources Symposium*, Academic Press, Inc., New York, 1973, p. 379.
181. R. T. Johnson and J. R. Pierson, "The Impact of Grid Composition on the Performance Attributes of Lead–Acid Batteries," in L. J. Pearce, ed., *Power Sources 11*, International Power Sources Symposium Committee, 1987.
182. D. Berndt and S. C. Nijhawan, *J. Power Sources* **1**, 3 (1976–1977).
183. D. E. Koontz and co-workers, *Bell Syst. Tech. J.* **49**, 1253 (1970).
184. Ref. 114, 251–255.
185. T. J. Hughel and R. H. Hammar, in D. H. Collins, ed., *Power Sources 3, Proceedings 7th International Power Sources Symposium*, Pergamon Press, Inc., Elmsford, N.Y., 1970, p. 209.
186. N. E. Bagshaw, *Lead 68, Proceedings 3rd International Conference on Lead*, Venice, Italy, Pergamon Press, Inc., Elmsford, N.Y., 1969, p. 209.
187. D. L. Douglas and G. W. Mao, in D. H. Collins, ed., *Power Sources 4, Proceedings 8th International Power Sources Symposium*, Academic Press, Inc., New York, 1973, p. 379.
188. M. Torralba, *J. Power Sources* **1**, 301 (1976–1977).
189. U.S. Pat. 4,275,130 (June 23, 1981), W. E. Rippel and B. Edwards.
190. Ger. Pat. 2,346,517 (Apr. 3, 1975), O. Metzler.
191. Ger. Pat. 2,315,984 (Oct. 17, 1974), (to Varta Batterie AG).
192. J. R. Pierson, *Power Sources*, Pergamon Press, New York, 1968, 103–118.
193. J. R. Pierson, *Electrochem. Tech.* **5**, 323–327 (1967).
194. U.S. Pat. 6,495,286 (Dec. 17, 2002), G. C. Zguris and F. C. Harman, Jr., (to Hollingworth and Vise Co.).
195. U.S. Pat. 6,511,775 (June 28, 2003), T. J. Clough (to Ensci Inc.).
196. K. Murata and S. Hattori, "Advantageous Features of Microporous Thin Embossed Waffle Shape Separator," *89th Battery Council International Meeting*, Washington, D.C., Apr. 1977.
197. N. I. Palmer, *Proceedings of the 87th Battery Council International Meeting*, Hollywood-by-the-sea, Fla., April 1975, p. 105.

198. *Battery Technical Manual*, 2nd ed., Battery Council International.
199. U.S. Pat. 3,716,412 (Feb. 13, 1973), K. Peters (to Electric Power Storage Ltd.).
200. U.S. Pat. 3,765,942 (Oct. 16, 1973), O. Jache.
201. U.S. Pat. 3,930,881 (Jan. 6, 1976), J. P. Cestaro and L. J. Crosby (to National Lead Industries, Inc.).
202. D. Pavlov, G. Papazov, and V. Iliev, *J. Electrochem. Soc.* **119**(1), 8–19 (1972).
203. D. Pavlov, V. Iliev, G. Papazov, and E. Bashtavelova, *J. Electrochem. Soc.* **121**(7), 854–860 (1974).
204. D. Pavlov and Papazov, *J. Electrochem. Soc.* **127**(10), (1980).
205. V. M. Halsall and R. R. Wiethaup, "A New Manufacturing Method for Lead–Acid Storage Batteries," SAE 720041, 1972.
206. J. R. Pierson, C. E. Weinlein, and C. E. Wright, "Determination of Acceptable Contaminant Ion Concentration Levels in a Truly Maintenance-Free Lead–Acid Battery," in D. H. Collins, ed., *Power Sources 5-1974*, Pergamon, London and New York, 1975.
207. "SAE Standard Test Procedure for Storage J537—Jun 86," *SAE Recommended Practices*, SAE, New York, June 1986.
208. "SAE J227, Electric Vehicle Test Procedure," *SAE Recommended Practices*, SAE, New York, Mar. 1971.
209. U.S. Pat. 6,392,413 (May 21, 2002), H. L. Huslebrock and co-workers (to VB Autobatteries GmbH).
210. R.L. Armistad, *14th Battery Council International Convention*, Orlando, Fla., April 17, 2002, presentation handout.
211. B. Cullen in Ref. 210.
212. *Advanced Battery Technology* **37**(12), 26 (2001).
213. M. Hughes, N. A. Hampson, and S. A. G. R. Karunathilaka, *J. Power Sources* **12**, 83–144 (1984).
214. E. Yeager, in E. Yeager and co-eds., *Proceedings of the Workshop on Lithium Nonaqueous Battery Electrochemistry*, Vol. 80–7, The Electrochemical Society, Inc., Cleveland, Ohio, 1980, 1–12.
215. V. R. Koch, *J. Power Sources* **6**, 357–370 (1981).
216. M. Garreau, *J. Power Sources* **20**, 9–17 (1987).
217. A. Dey, *Thin Solid Films* **43**, 131–171 (1977).
218. U.S. Pat. 6,569,573 (May 27, 2003), Y. V. Mikhaylik, T. A. Skotheim, and B. A. Trofimov (to Moltech Corp.).
219. U.S. Pat. 6,428,929 (Aug. 6, 2002), J. Kay and co-workers (to NBT GmbH).
220. U.S. Pat. Appl. 20030108793 (June 12, 2003), J. R. Davis and Z. Lu (to 3M Innovative Properties Co.).
221. S. B. Brummer, in Ref. 2, 130–142.
222. Y. Matsuda, *J. Power Sources* **20**, 19–26 (1987).
223. K. M. Abraham, *J. Power Sources* **14**, 179–191 (1985).
224. J. R. Stiles, *New Mater. New Processes* **3**, 89–91 (1985).
225. J. Gabano, *Prog. Batt. Solar Cells* **8**, 149–162 (1989).
226. M. Armand, *Solid State Ionics* **9**, **10**, 745–754 (1983).
227. A. Hooper, in K. M. Abraham and B. B. Owens, eds., *Materials and Processes for Lithium Batteries*, Vol. 89–4, The Electrochemical Society, Inc., Cleveland, Ohio, 1980, 15–32.
228. P. E. Harvey, *J. Power Sources* **26**, 23–32 (1989).
229. U.S. Pat. Appl. 20020192563 (Dec. 19, 2002), R. S. Morris and B. G. Dixon.
230. K. M. Abraham, *J. Power Sources* **7**, 1–43 (1981 and 1982).
231. A. D. Yoffe, *Solid State Ionics* **9**, **10**, 59–70 (1983).
232. B. Scosati, A. Selvaggi, and B. Owens, *Prog. Batt. Solar Cells* **8**, 135–137 (1989).

233. A. Hammou and A. Hammouche, *Electrochimica Acta* **33**, 1719, 1720 (1988).
234. F. Bonino, M. Ottaviani, and B. Scrosati, *J. Electrochem. Soc.* **135**, 12–15 (1988).
235. A. Hooper and J. North, *Solid State Ionics* **9**, **10**, 1161–1166 (1983).
236. D. Shackle, *4th International Seminar on Lithium Battery Technology and Applications*, Deerfield Beach, Fla., Mar. 1989.
237. U.S. Pat. 4,830,939 (May 1989), M. Lee, D. Shackle, and G. Schwab.
238. *Science News* **136**, 342 (1989).
239. M. Liu, S. Visco, and L. DeJonghe, in S. Subbarao and co-workers, eds., *Rechargeable Lithium Batteries*, Vol. 90–5, The Electrochemical Society, Inc., Cleveland, Ohio, 1980, 233–244.
240. N. Koshiba and K. Momose, in Y. Matsuda and C. Schlaikjer, eds., *Practical Lithium Batteries*, JEC Press, Inc., 1988, 79–81.
241. K. Momose, H. Hayakawa, N. Koshiba, and T. Ikehata, *Prog. Batt. Solar Cells* **6**, 56, 57 (1987).
242. *JEC Battery Newsletter*, (1), 7 (Jan./Feb. 1989).
243. *Japan Component News* **7**(2), 4–6 (Feb. 1990).
244. K. Inada and co-workers, in Ref. 26, 96–99.
245. M. Mohiri and co-workers, *J. Power Sources* **26**, 545–551 (1989).
246. U.S. Pat. 4,748,484 (July 19, 1988), N. Furukawa, T. Saito, and T. Nohma (to Sanyo Electric Co., Ltd.).
247. U.S. Pat. 4,904,552 (Feb. 27, 1990), N. Furukawa, T. Saito, and T. Nohma (to Sanyo Electric Co., Ltd.).
248. T. Nohma, T. Saito, and N. Furukawa, *J. Power Sources* **26**, 389–396 (1989).
249. J. Carcone, *3rd International Rechargeable Battery Seminar*, Deerfield Beach, Fla., Mar. 1990.
250. U.S. Pat. 6,465,129 (Oct. 15, 2002), J. Xu, B. B. Owens, and W. H. Smyryl (to the Regents of the University of Minnesota).
251. *Technical Brochure*, Moli Energy Ltd., Burnaby, British Columbia, Canada.
252. J. Stiles, in Ref. 26, 74–78.
253. F. C. Laman and K. Brandt, *J. Power Sources* **24**, 195–206 (1988).
254. E. J. Frazer and S. Phang, *J. Power Sources* **6**, 307–317 (1981).
255. D. H. Shen and co-workers, *Extended Abstract 49*, Vol. 87–2, *172nd Meeting of the Electrochemical Society*, Honolulu, Hawaii, Oct. 1987.
256. U.S. Pat. 4,084,046 (Apr. 1978), M. S. Whittingham (to Exxon Corp.).
257. U.S. Pat. 4,731,310 (Mar. 1988), M. Anderman and J. Lundquist (to W. R. Grace & Co.).
258. M. Anderman and J. Lundquist, *Extended Abstract 49*, Vol. 87–2, 172nd Meeting of the Electrochemical Society, Honolulu, Hawaii, Oct. 1987.
259. U.S. Pat. 3,864,167 (Feb. 4, 1975), J. Broadhead, F. J. DiSalvo, and F. A. Trumbore.
260. B. Vyas, *33rd International Power Sources Symposium*, Cherry Hill, N.J., June 1988.
261. F. Trumbore, *4th International Meeting on Lithium Batteries*, Vancouver, Canada, May 1988.
262. *JEC Battery Newsletter* (2), 26, 27 (1988).
263. U.S. Pat. 4,828,834 (May 1989), T. Nagaura and M. Yokokawa (to Sony Corp.).
264. U.S. Pat. 4,959,282 (Sept. 1990), J. Dahn and B. Way (to Moli Energy, Ltd.).
265. *Product Literature*, Moli Energy Ltd., Burnaby, British Columbia, Canada.
266. E. Plichta and co-workers, *J. Power Sources* **21**, 25–31 (1987).
267. K. Wiesener and co-workers, *J. Power Sources* **20**, 157–164 (1987).
268. K. West, B. Zachua-Christiansen, M. Ostergard, and T. Jacobsen, *J. Power Sources* **20**, 165–172 (1987).
269. A. N. Dey, K. C. Kuo, P. Piliero, and M. Kallianidis, *J. Electrochem. Soc.* **135**, 2115–2120 (1988).

270. C. Cecilio and co-workers, *4th International Seminar on Lithium Battery Technology and Applications*, Deerfield Beach, Fla., Mar. 1989.
271. W. Behl and D. Chin, *J. Electrochem. Soc.* **135**, 16–25 (1988).
272. U.S. Pat. 4,668,595 (May 1987), A. Yoshino, K. Sanechika, and T. Nakajima (to Sony Corp.).
273. Jpn. Pat. 01 122 562, (to Sony Corp.).
274. *JEC Battery Newsletter*, (2), 9–12 (1990).
275. E. J. Cairns, in J. Bockris and co-eds., *Comprehensive Treatise of Electrochemistry*, Vol. 3, Plenum Press, New York, 1981, Chapt. 11.
276. R. W. Glazebrood and M. J. Willars, *J. Power Sources* **8**, 327–339 (1982).
277. P. A. Nelson, *4th International Seminar on Lithium Battery Technology and Applications*, Deerfield Beach, Fla., Mar. 1989.
278. P. A. Nelson and H. Shimotake, *Prog. Batt. Solar Cells* **6**, 150–154 (1987).
279. T. D. Kaun, in Ref. 25, 294–306.
280. T. D. Kaun and co-workers, *Proc. of the 25th IECEC* **3**, 335–340 (1990).
281. J. L. Sudworth and A. R. Tilley, *The Sodium Sulfur Battery*, Chapman and Hall Ltd., 1985, and references therein.
282. D. Pletcher, *Industrial Electrochemistry*, Chapman and Hall Ltd., 1984, 272–274.
283. P. Bindin, *Proc. 20th IECEC Conf.* **2**, 1111–1114 (Aug. 1985).
284. S. Wolanczyk and S. Vukson, *Proc. 25th IECEC Conf.* **3**, 122–124 (Aug. 1990).
285. R. J. Bones, J. Coetzer, R. C. Galloway, and D. A. Teagle, *J. Electrochem. Soc.* **134**, 2379–2382 (1987).
286. R. C. Galloway, *J. Electrochem. Soc.* **134**, 256, 257 (1987).
287. "The Lithium-Polymer Battery, Substance or Hype?," *Powerpulse.net*, Aug. 7, 2003.
288. J. A. Ober, "Lithium," *Minerals Yearbook*, U.S. Geological Survey, Reston, Va., 2002.

ALVIN J. SALKIND
MARTIN KLEIN
Rutgers University
KATHRYN R. BULLOCK
JOHN R. PIERSON
Johnson Controls, Inc.
PAUL R. GIFFORD
Ovonic Battery Company